Selective Oxidation of Lignin Models and Extracts with Earth-Abundant Transition Metals and Hypervalent Iodine

by

Wei-Ching Chen

A Thesis Submitted to the
Faculty of Graduate and Postdoctoral Studies
in Partial Fulfillment of the Requirements for the Degree of

Master of Science
in Chemistry

Centre for Catalysis Research and Innovation
Ottawa-Carlton Chemistry Institute
University of Ottawa

Candidate
Wei-Ching Chen

Supervisor
R. Tom Baker

Table of Contents

Abstract

As a significant component of lignocellulosic biomass, lignin represents a potential source of value-added aromatic chemicals. In this thesis, catalytic systems with earth-abundant metal catalysts such as molybdenum(VI) and hypervalent iodine complexes were developed to selectively break down lignin models into lower molecular weight chemicals under mild conditions. Due to the complexity of lignin, simple lignin model substrates (**A** to **E**), representing common linkages in lignin, were used to investigate the catalytic activity/selectivity of these catalysts. With the molybdenum catalysts [**7**–**11**]/SPC/Adogen®464 system (SPC = sodium percarbonate), oxidation of simple β-1 model compound **A** in acetonitrile showed primarily C-H bond cleavage to form the ketone product, benzoin methyl ether, whereas the C_α-C_β bond cleavage product, methyl benzoate, was obtained by switching the reaction solvent to benzonitrile. Preference for generating the C_α-C_β bond cleavage product, i.e. benzaldehyde, can also be achieved with other early to middle transition metal catalysts using $H_2O_{2(aq)}$ as the terminal oxidant. Stoichiometric amounts of hypervalent iodine/Lewis acid systems [**20a-c**] were able to selectively cleave C_α-C_β bonds to aldehydes with both simple β-1 model compound **A** and β-O-4 model compound **C**. In contrast, other lignin model compounds with different linkages were unable to be oxidized to a great extent using these Mo- or iodine-based complexes.

The catalytic activity and selectivity of the reported vanadium complexes, copper salts and non-metal system **1**-**5** on non-volatile organosolv (NVO) lignin was investigated under basic condition. Details of the depolymerisation of lignin were determined by using Gel Permeation Chromatography (GPC) and the two-dimensional NMR technique, quantitative HSQC (q-HSQC) spectroscopy. Vanadium [**2**] and copper systems were found to be the most active for depolymerization of NVO lignin.

List of Symbols and Abbreviations

Å	Angström
acac	acetylacetonato
atm	Atmosphere
bz	Benzene
^{o}C	Degrees centigrade
cm^{-1}	Wavenumbers
CAN	Ceric ammonium nitrate
$CDCl_3$	Deuterated chloroform
CD_3CN	Deuterated acetonitrile
Cp	Cyclopentadienyl
Cp*	Pentamethylcyclopentadienyl
FTIR	Fourrier-transform infrared spectroscopy
GC-MS or GC-FID	Gas chromatography-mass spectrometry or flame ionization detector
GPC	Gel permeation chromatography
h	Hour
HQ	Hydroxyquinolinato
Hz	Hertz
mesnacnac	$[2,6\text{-}(2,4,6\text{-}Me_3\text{-}C_6H_2)N(Me)C)]_2CH$
mL	mililitre
NMR	Nuclear magnetic resonance
NVO lignin	Non-volatile organosolv lignin
ORTEP	Oak Ridge thermal ellipsoid program
Ph	Phenyl
q-HSQC	Quantitative heteronuclear single quantum coherence
TEMPO	(2,2,6,6-Tetramethyl-1-piperidinyl)oxyl
TBHP	Tert-butyl hydroperoxide

List of Complexes

#	Complex	#	Complex
1	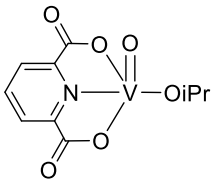	**2**	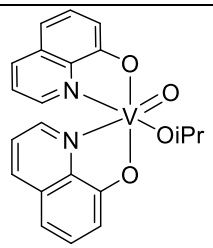
3	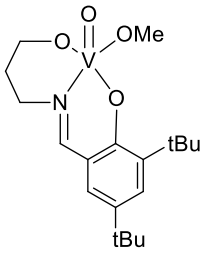	**4**	**4a** CuCl/TEMPO **4b** Cu(OTf)/TEMPO/2,6-lutidine
5	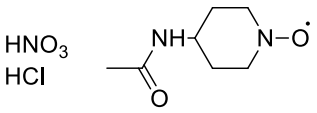	**6**	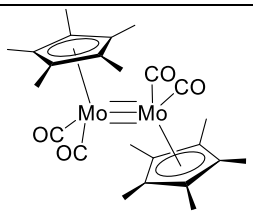
7	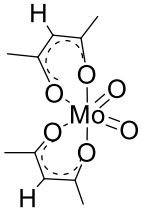	**8**	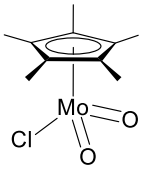
9	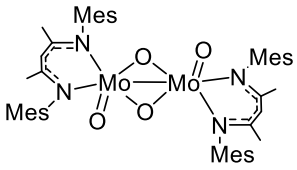	**10**	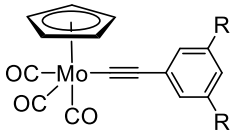 **10a** R = H **10b** R = CF_3
11	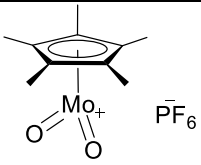	**12**	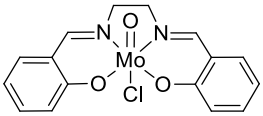

13	**13a** 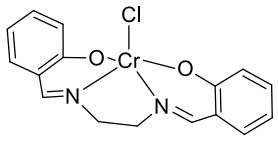 **13b** 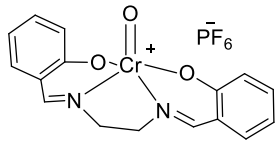	**14**	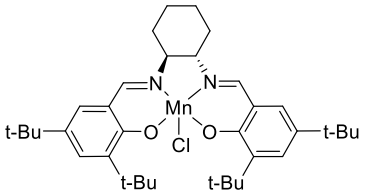
15	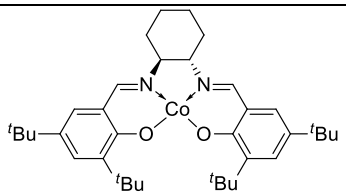	**16**	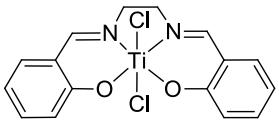
17	$Ti(O^iPr)_4$	**18**	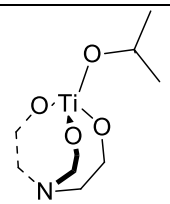
19	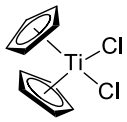	**20**	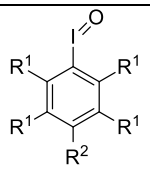 **20a**: R^1, R^2 = H **20b**: R^1, R^2 = F **20c**: R^1= H; R^2 = NO_2

List of Tables

Chapter 2:

Chapter 3:

List of Figures

List of Schemes

Chapter 1:

Chapter 2:

Chapter 3:

Publications and Presentations

1. Diaz-Urrutia, C.; Chen, W.-C.; Crites, C.-O.; Baker, R. T. Towards Lignin Valorization: Selective Aerobic Oxidation of Organosolv Lignin by Oxovanadium(V) Complexes. *Energy Environ. Sci.* **2014, Submitted**.
2. Chen, W.-C.; Díaz-Urrutia, C.; Baker, R. T. Oxidation of Lignin Models using Dioxomolybdenum Complexes. Presented at Fibre Network and Lignoworks. Cornwall, ON. May 2013.
3. Chen, W.-C.; Díaz-Urrutia, C.; Baker, R. T. Oxidation of Lignin Models using Dioxomolybdenum Complexes. Presented at 2013 Sustainable Chemistry Summit. Montreal, QC. June 5-7, 2013.
4. Chen, W.-C.; Baker, R. T. Oxidation of Lignin Models using Molybdenum Complexes. Presented at 97th Canadian Chemistry Conference and Exhibition and Lignoworks.Vancouver, BC. June 1-7, 2014.

Acknowledgements

I would like to thank my research supervisor Prof. Baker for giving me the opportunity to work as a graduate student for the Lignin project. Thanks to NSERC and Lignoworks, our research network, for funding the lignin project. Without Prof. Baker's continuous support, guidance and funding to the project, this thesis would not have been able to be accomplished.

I would also like to thank all my lab mates for helping me throughout my entire stay in the Baker group. Notably, I would like to thank Christian Díaz-Urrutia from the lignin team for helping and assisting me to get familiar with different laboratory techniques since the start of my degree. Working in the lab would not have been the same without the heated discussions and help from my friend and lab mate Alexandre Sicard.

A special thanks to Dr. Gang Ye, our NMR technician, for teaching and assisting me with the 2D-NMR experiments, to Dr. Ilia Korobov for the X-ray diffraction studies and to Roxanne Clément for GC training.

Finally, I would like to thank my family for supporting me throughout my degree.

Chapter 1. Introduction to Lignin and Delignification Methods

1.1 Introduction:

Lignin is one of the three main components of lignocellulosic biomass and is the second most abundant biopolymer on Earth, after cellulose.[1] This irregular and complex biopolymer constructed from three main building blocks, coniferyl, sinapyl and *p*-coumaryl alcohol[1], and are assembled by way of enzymatic radical condensation that gives rise to different linkages: β-O-4, β-1, β-β, β-5, 5-5', 4-O-5 and dibenzodioxocin. The amount of each type of linkage is dependent on the wood species (Figures 1.1 and 1.2), although β-O-4 is always the most abundant (>40% in lignin content).[1]

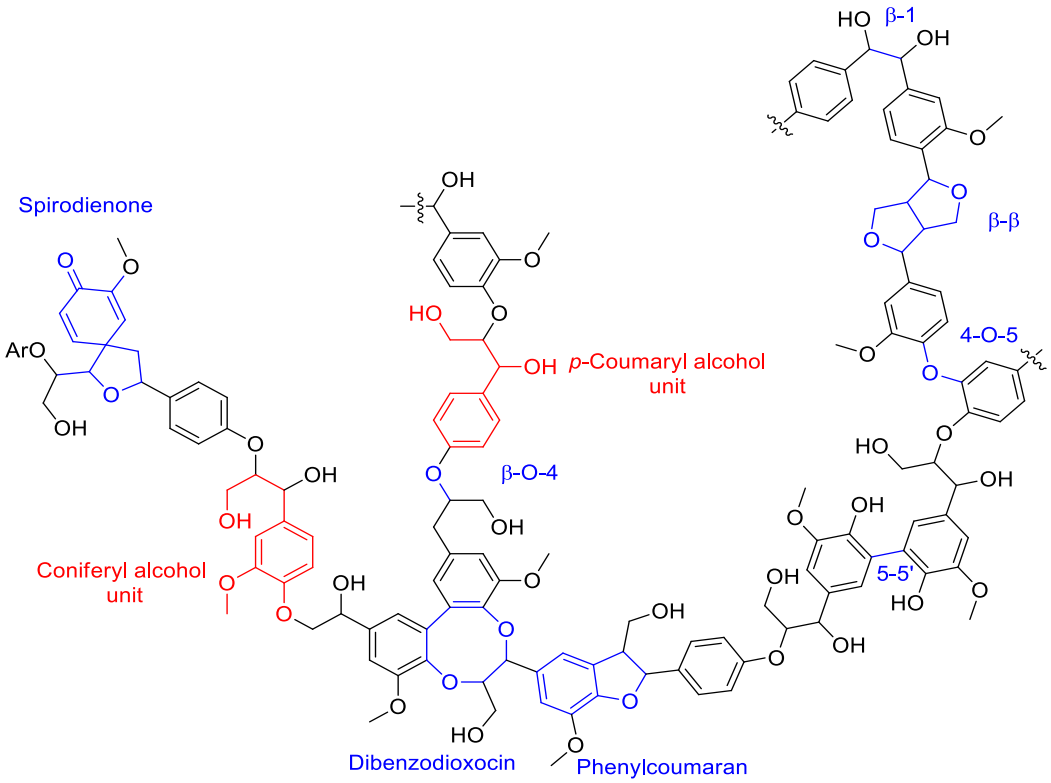

Figure 1.1 Schematic representation of softwood lignin (blue represents the linkages and red represents the building units).

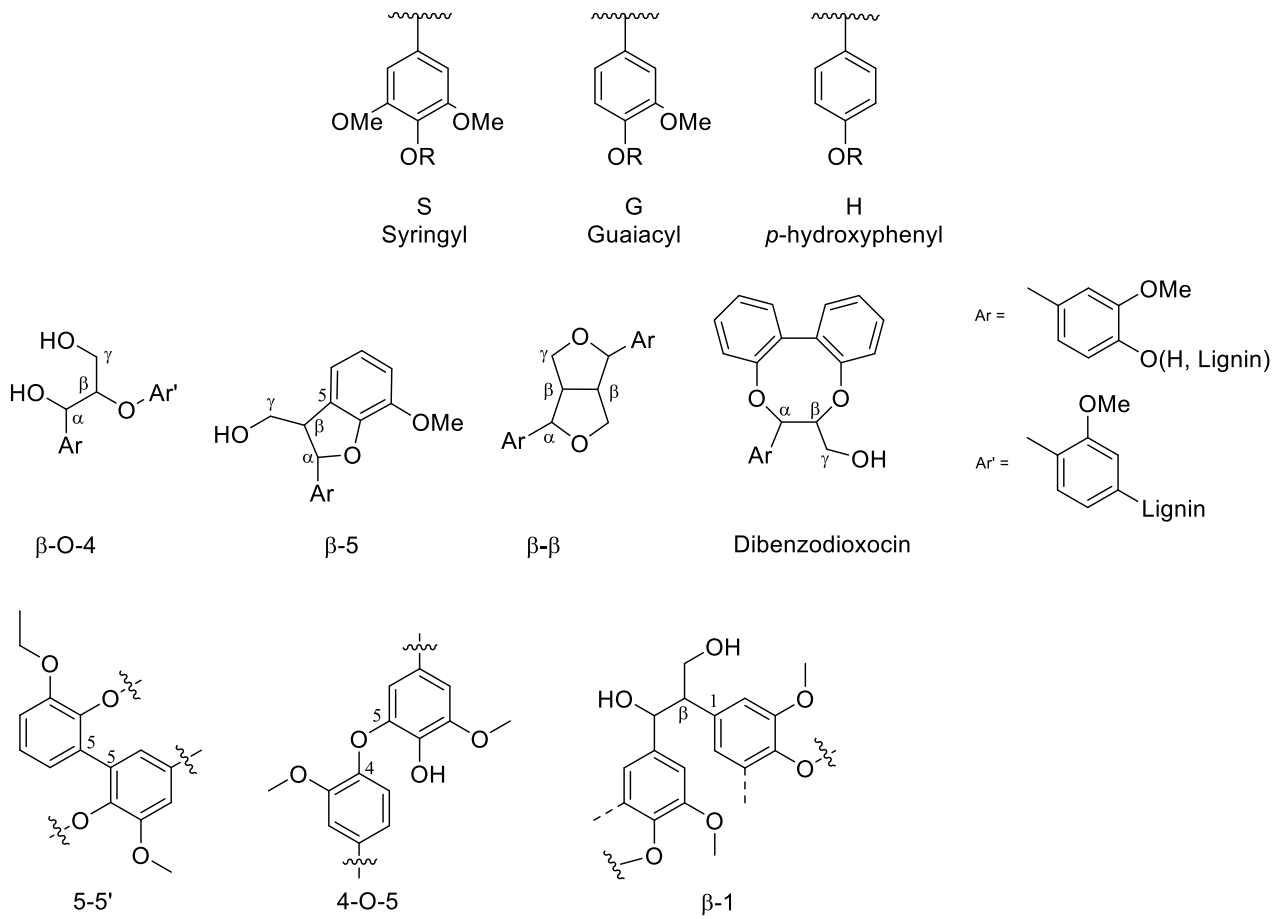

Figure 1.2 Major building blocks and common linkages of lignin.

Much of the research on valorization of lignocellulosic biomass has been focused on cellulose due to its relatively simple and repetitive nature. The existing applications of lignin are mainly focused on low-valued products such as adhesives, resins and binders or fuels to be burned for process heat.[2,3] However, over the past few years, lignin's renewability and unique chemical structure have attracted great attention for generation of value-added, low molecular-weight aromatic chemicals. To this end, two lignin depolymerization methods have been employed: oxidative and reductive. The main advantage of the oxidative approach (over reductive) is the preservation of the highly oxygenated functionalities inherent to lignin, the specificity of which adds value to the products. By comparison, the hydrogenation of lignin or its models (e.g. with Raney Ni) tends to give more highly reduced oxygenates such as cyclohexanol.[4] For example, oxidation of the phenolic subunit of lignin can lead to useful products such as quinones.

Alternatively, oxidation of benzylic alcohol subunits can lead to aldehydes which are of industrial relevance for flavourings, fragrances (e.g. vanillin), pharmaceuticals or reaction intermediates/platform chemicals (e.g. cinnamaldehyde).[5,6]

Conventional technologies to directly yield value-added chemicals from lignin involve energy-intensive processes and harsh reaction conditions (high temperatures and pressures and/or alkaline conditions).[1,6] For example, alkaline oxidation of lignin requires copper/iron metal salts in conjunction with caustic soda at 170 ^{o}C and 1.4 MPa.[7] Despite the demanding reaction conditions, the process is not high-yielding (e.g. 14 wt. % of aldehydes).[7] Another existing degradation method makes use of actinomycetes bacteria and a lignin-peroxidase enzyme under aerobic conditions to give aryl-ether and biphenyl derivatives; isolation of these products and separation from other bacterial metabolites, however, present a challenge and has yet to be optimized.[8]

In search of a more environmentally-friendly and efficient transformation of lignin into value-added products, both heterogeneous and homogeneous catalytic approaches have been explored. Most current methods give rise primarily to hydrolytic C-O bond cleavage.[9,10] Hereto is a brief summary of the current state of the art in catalytic oxidation of lignin.

This thesis centers on the selective oxidation of lignin extracts into valuable aromatics using homogeneous earth-abundant transition metal complexes/catalysts Ti^{IV}, V^{V}, $Cr^{III}/^{V}$, $Mo^{V}/^{VI}$ and Mn^{III} and, will be compared to a main-group element (hypervalent iodine).

1.2 Aerobic Oxidation of Lignin Model Compounds with Transition Metal Complexes

Due to the amorphous and complex nature of lignin, various lignin model compounds mimicking the major linkages of lignin are commonly used to investigate the reactivity and selectivity of catalysts and reaction conditions (Figure 1.3). By using these model compounds, characterization and analysis of the catalytic transformation can be simplified, and the results can be extended/correlated to the real lignin. The model compounds also allow for insight into the products derived from the breakage of *specific* linkages within the polymer.

The homogeneous catalytic approach with earth-abundant transition metals is industrially attractive due to the vast tunability of the catalyst's molecular structure and the possibility of modifying its selectivity by varying the ligand scaffolds. Metalloporphyrin complexes (based on Mn^{III}[11], Fe^{III}[11,12], Co^{II}[13], Rh^{II}[14]), metallosalen complexes (in particular, Co^{III})[15-20], polyoxometalates (polyoxotungstate/molybdate)[21] and simple metal salts ($Cu^{II/I}$, Fe^{III}, $Co^{III/II}$, $Mn^{III/II}$) have been reported to oxidatively cleave lignin model compounds and extracts.[1] Approaches with porphyrins and phthalocyanines of Fe, Co and Mn have been investigated heavily since they mimic biologically active monooxygenase enzymes using molecular oxygen as the terminal oxidant[13,22] or peroxidase enzymes using peroxide as the oxidant.[12] Systems involving Mn^{III} and Brønsted acids in an ionic liquid medium have also been used with some success.[23,24]

For the focus of our project, early and middle transition metals (Ti^{IV}, V^{V}, $Cr^{III}/^{V}$, $Mo^{V}/^{Vi}$ and Mn^{III}) were investigated with economical and easily prepared ligand sets, as well as several commercially-available complexes.

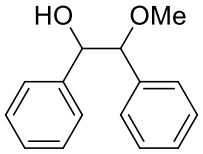

1,2-diphenyl-
2-methoxyethanol
(DPME)
β-1 model
[**A**]

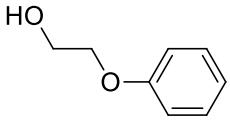

2-phenoxyethanol
β-O-4 model
[**B**]

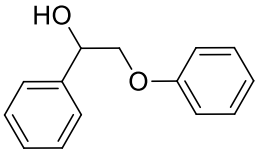

1-phenyl-2-
phenoxyethanol
β-O-4 model
[**C**]

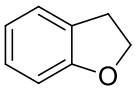

2,3-dihydrobenzofuran
β-5 model
[**D**]

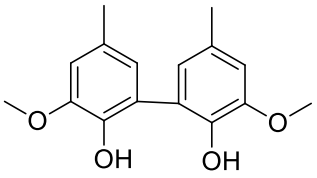

3,3'-dimethoxy-5,5'-diethyl-biphenyl-2,2'-diol
5-5' model
[**E**]

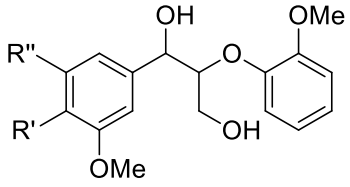

1-(4-ethoxy-3-methoxyphenyl)-
2-(2,6-dimethoxyphenoxy)propane-1,3-diol
β-O-4 model
[**F$_1$**] R' = H; R'' = OMe
[**F$_2$**] R' = OMe; R''= H
[**F$_3$**] R' = OEt; R'' = H
[**F$_4$**] R' = OH; R'' = OMe

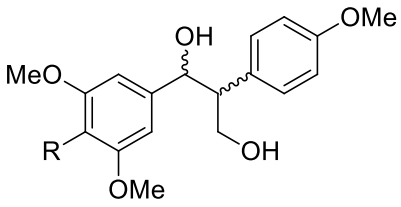

1-(4-hydroxy-3,5-dimethoxyphenyl)-
2-(4-methoxyphenyl)-propane-1,3-diol
β-1 model
[**G$_1$**] R = H
[**G$_2$**] R = OH

Figure 1.3 Some examples of common lignin model compounds.

1.2.1 Oxovanadium (V) Complexes and Copper Salts for Selective Oxidation of Lignin Model Compounds and Non-organosolv Lignin

Several oxovanadium (V) complexes were reported to exhibit oxidaitive or non-oxidative cleavage of lignin model compounds. Oxovanadium (V) complexes from our group (catalysts [**1**] and [**2**]) and the Toste group (catalyst [**3**]) are depicted in Figure 1.4. It has been shown that different ligand environments and reaction conditions (e.g. solvent, temperature) can alter the selectivity and reactivity of the oxovanadium catalyst for oxidative cleavage of the model compounds tested.

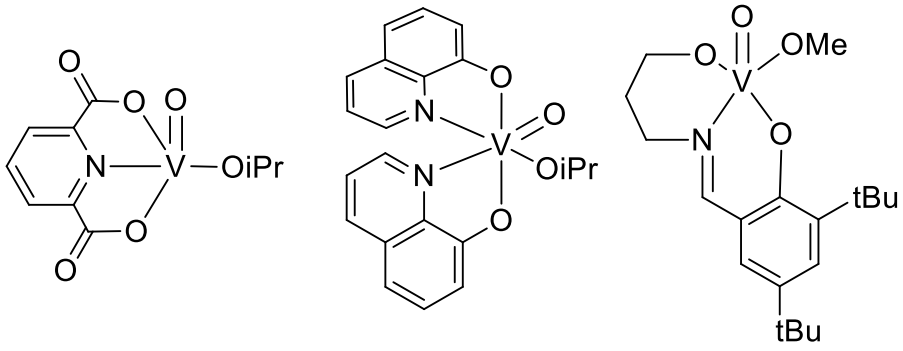

1 **2** **3**

CuCl/TEMPO **4a**

Cu(OTf)/TEMPO/2,6-lutidine **4b**

Figure 1.4 Selective oxovanadium complexes/copper salts for oxidative lignin depolymerization.

Oxidation of Simple Monomeric Lignin Model Compounds:

Vanadium Systems

Dipicolinate vanadium catalyst [**1**] and 8-hydroxyquinolinate vanadium catalyst [**2**] have been reported to effect aerobic oxidative cleavage of C_α-C_β or C-H bond of simple β-1 model compound **A** depending on the reaction solvent.[25] A two-electron base-assisted redox dehydrogenation mechanism was shown to proceed for catalyst [**1**] and [**2**] using triethylamine or pyridine as a base (Scheme 1.1).[26,27] As a result, the C-C bond being cleaved is that of the ketone intermediate, leading primarily to the carboxylic acid and ester. In contrast, in DMSO solvent, a proposed one-electron pathway leads to C-O and C-C bond cleavage, affording methanol and benzaldehyde as the major products (Scheme 1.2, entry 1 *vs.* 2).

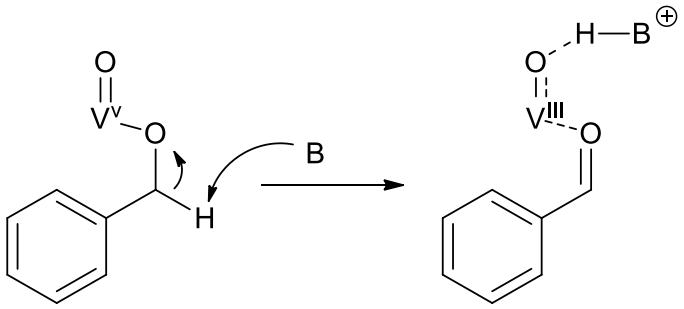

Scheme 1.1 General schematic of the base-assisted redox dehydrogenation mechanism (B = base).

Dipicolinate vanadium catalyst [**1**] with β-O-4 model susbtrate **B** afforded a low conversion (20%) with phenol (18%) and formic acid (6%) as major products (Scheme 1.3, entry 1). Improved catalytic performance was obtained with vanadium-HQ catalyst [**2**] (69% conversion *vs.* 20% conversion), whereby the major products obtained were 2-phenoxyethylformate (18%), phenol (55%), formic acid (3%) and CO_2 (Scheme 1.3, entry 2).

In previous reports, vanadium-dipic [**1**] was reported to afford 95% conversion for the more activated and bulky substrate **C** to benzoic acid (81%), phenol (77%), formic acid (46%) and 1-phenyl-2-phenoxyethanone (9%) after heating at 100 ^oC for 1 week in

DMSO-d_6 (Scheme 1.4, entry 1).[25] Catalyst [**2**] was only able to consume 58% of **C** after heating to 100 ^oC for 48h in pyr-d_5. The major products of the reaction were comparable to the earlier report: benzoic acid (46%), phenol (45%), 1-phenyl-2-phenoxyethanone (16%) and a smaller amount of formic acid (2% vs. 46%) (Scheme 1.4, entry 2). The ketone, 1-phenyl-2-phenoxyethanone, was shown to be the intermediate for the formation of benzoic acid and phenol for this reaction as the same products were observed starting from the ketone reacted under the same reaction conditions.

Copper Systems

Simple copper (I) salts (CuCl [**4a**] or Cu(OTf) [**4b**]) used in conjunction with TEMPO and organic base (2,4-lutidine or pyridine), which generate *in-situ* the active species Cu^{II}, have been shown to be more selective for oxidative C_α-C_β bond cleavage of β-1 model compound **A** than vanadium complexes as they yielded primarily benzaldehyde (84% with [**4a**]) (Scheme 1.2, entry 3).[28]

For β-O-4 substrate **B**, copper catalyst [**4a**] was as unreactive as vanadium catalysts [**1**] and [**2**] (Scheme 1.3, entry 3).

Unlike the vanadium catalysts, oxidation of substrate **C** using the copper system [**4a**] gave benzoic acid, phenol and 1-phenyl-2-phenoxyethanone as minor products, 2-phenoxy-1-phenylformate (18%) and TEMPO adduct (14%) as the primary products (Scheme 1.4, entry 3).

$CuSO_4$/1,10-phenanthroline(phen)/base system was able to selectively oxidize veratryl alcohol to veratryl aldehyde (~20% in 1 hour and 93% in 23 h with O_2) in alkaline water.[29]

In short, the formation of the more stable 1-phenyl-2-phenoxyethanone from substrate **C** may suppress the formation of formylation products, as observed for substrate **B**.

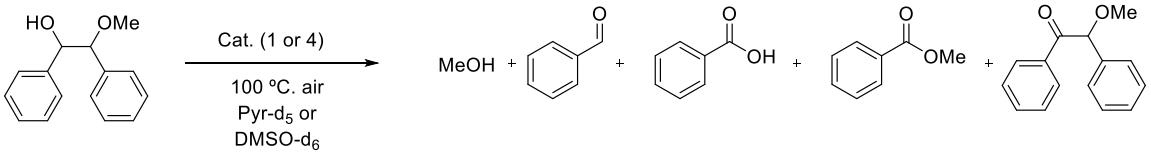

Entry	Cat.	Solvent	Time	Yield					Conversion
1	**1** (10 mol%)	Pyr-d_5	6 days	6%	9%	85%	84%	9%	99%
2	**1** (5 mol%)	DMSO-d_6	20 h	69%	73%	5%	5%	13%	94% (96%)*
3	**4a** (20 mol% CuCl, 30 mol% TEMPO	Pyr-d_5	48 h	-	84%	-	88%	-	92%

*96% with 48 h reaction time

Scheme 1.2 Vanadium and copper-catalyzed oxidation of simple β-1 model compound **A** (yield based on theoretical maximum yield from the initial substrate amount).

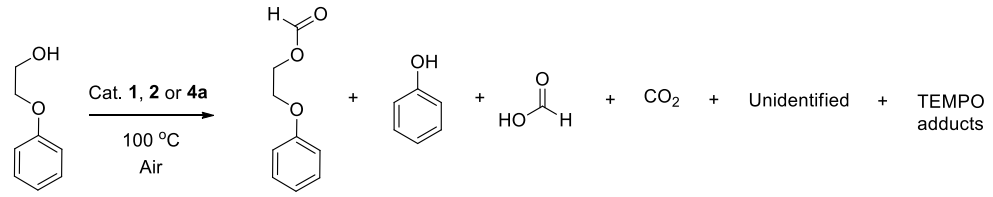

Entry	Cat.	Solvent	Time	Yield						Conversion
1	**1** (10 mol%)	DMSO-d_6	7 days	-	18%	6%	-	2-5%	-	**20%**
2	**2** (10 mol %)	Pyr-d_5	48 h	18%	55%	3%	-	-	-	**69%**
3	**4a** (20 mol%)	Toluene	40 h	12%	-	-	-	-	12%	**40%**

Scheme 1.3 Oxidation of model compound **B** with vanadium catalyst [**1**], [**2**] and, copper catalyst [**4a**] (yield based on theoretical maximum yield from the initial substrate amount).

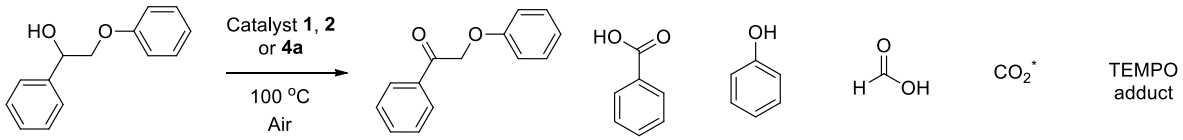

Entry	Cat.	Solvent	Time	Yield						Conversion
1	**1** (10 mol%)	DMSO-d_6	7 days	9%	81%	77%	46%	-	-	**95%**
2	**2** (10 mol%)	Pyr-d_5	48 h	16%	46%	45%	2%	-	-	**58%**
3	**4a** (20 mol%)	Toluene	40 h	1%	1%	2%	-	-	14%	**67%**

*Not quantified

Scheme 1.4 Oxidation of model compound **C** with vanadium catalyst [**1**], [**2**] and copper catalyst [**4a**] (yield based on theoretical maximum yield from the initial substrate amount).

Oxidation of Dimeric Lignin Model Compounds

*Oxidation of Dimeric β-O-4 Compounds **F**:*

Vanadium Systems:

For dimeric phenolic β-O-4 model compound **F4**, Schiff base-type vanadium catalyst [**3**] yielded primarily non-oxidative C-O bond cleavage products while (HQ) vanadium catalyst [**2**] mainly afforded C_{aryl}-Cα bond cleavage products (Scheme 1.5). The reaction with catalyst [**2**] also worked in ethyl acetate, THF and 2-MeTHF, where ethyl acetate and 2-MeTHF gave slightly more C_{aryl}-Cα bond cleavage product than pyr-d_5.[30] The difference in selectivity between catalyst [**2**] and [**3**] further suggested that catalyst [**3**] goes through an one-electron aryloxy radical mechanism and catalyst [**2**] follows the two-electron base-assisted redox dehydrogenation pathway.[27,31]

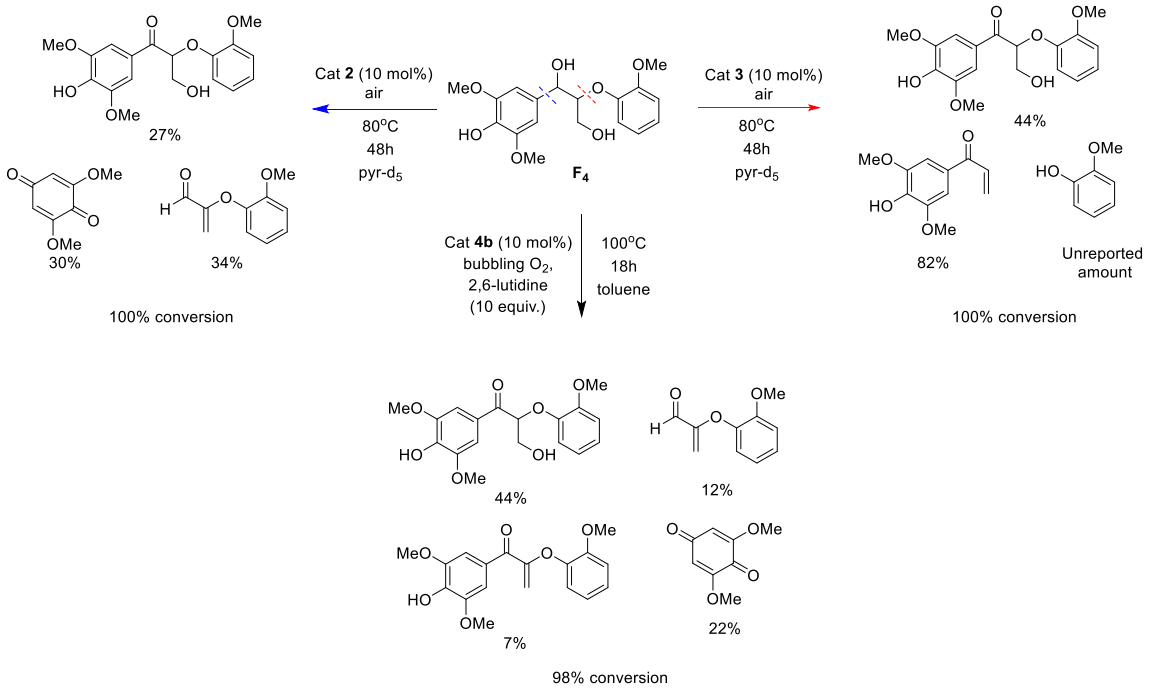

Scheme 1.5 Selective oxidative/non-oxidative C-O or C_{aryl}-Cα bond cleavage products of phenolic β-O-4 model compound **F4** (yield based on theoretical maximum yield from the initial substrate amount).

For non-phenolic dimer **F₁**, the vanadium-HQ catalyst [**2**] only managed partial conversion (65%) and no C-C bond cleavage product was observed (Scheme 1.6, entry 3) while the vanadium-dipic catalyst [**1**] was able to get at most a trace amount of 3,5-dimethoxybenzaldehyde and some ene-one (up to 29%) and the ketone (27%) in pyr-d_5 (Scheme 1.6, entry 1). More ketone (up to 65%) and less ene-one (14%) were obtained from the reaction in DMSO-d_6 (Scheme 1.6, entry 2). These results indicated that the phenolic group on the lignin model compound can have an impact on the selectivity and provide a different product distribution for the reaction.[30]

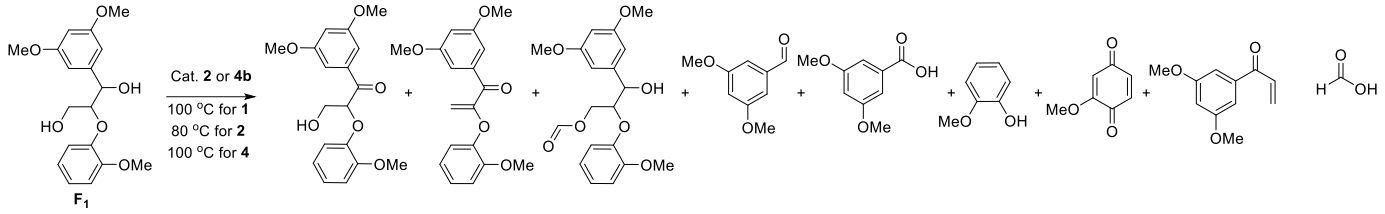

Entry	Cat.	Solvent	Time	Conversion	Yield							
1	**1** (10 mol%)	Pyr-d_5	48 h	**~85%**	27%	14%	-	4%	6%	-	-	29%	<1%
2	**1** (10 mol%)	DMSO-d_6	48 h	**>95%**	65%	5%	-	2%	11%	-	-	14%	4%
3	**2** (10 mol%)	Pyr-d_5	48 h	**65%**	55%	10%	-	-	-	-	-	-	-
4	**4a** (10 mol%)	Pyr-d_5	40 h	**~89%**	1%	2%	-	43%	13%	7%	-	-	7%
5	**4b** (20 mol %)	Toluene	40 h	**95%**	7%	5%	18%	54%	-	10%	5%	-	-

Scheme 1.6 Oxidation of non-phenolic model substrate **F₁** with vanadium [**2**] and copper [**4b**] catalysts (yield based on theoretical maximum yield from the initial substrate amount).

For a similar non-phenolic dimeric β-O-4 model compound **F₃**, vanadium-Schiff base catalyst [**3**] was also selective for non-oxidative C-O bond affording ene-one (82 %) and 2-methoxyphenol (57 %) as major products (Scheme 1.7).[30]

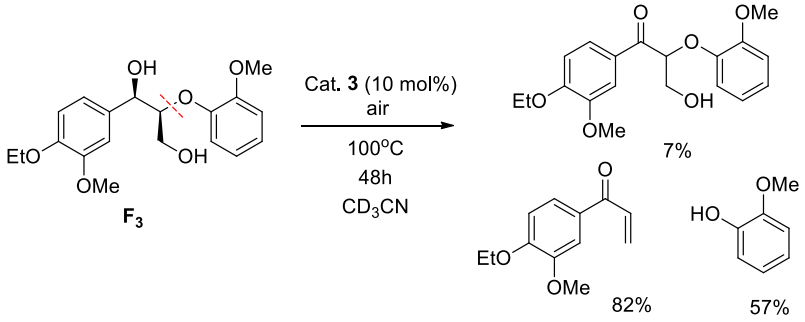

Scheme 1.7 Non-oxidative C-O bond cleavage of non-phenolic β-O-4 model compound **F₃** with catalyst [**3**] (yield based on theoretical maximum yield from the initial substrate amount).

Copper Systems:

The copper system Cu(OTf)/TEMPO/2,6-lutidine [**4b**] provided close to full conversion (95%) of non-phenolic substrate **F_1** with 54% of 3,5-dimethoxybenzaldehyde (Scheme 1.6, entry 5) and CuCl/TEMPO [**4a**] system was slightly less efficient for 3,5-dimethoxybenzaldehyde formation (43%) (Scheme 1.6, entry 4).[32]

Another copper system, Cu(OTf)/bpy/TEMPO/N-methylimidazole, yielded mainly veratryl aldehyde from another non-phenolic dimeric β-O-4 model compound **F_2**.[33] The mechanism of this system was proposed to go through a binuclear Cu_2O_2 intermediate where Cu^{I} precursors are oxidized by O_2 and, the alcohol substrate is oxidized by forming a Cu^{II} alkoxide intermediate.[34]

On the other hand, the copper(I) triflate catalytic system [**4b**] was inefficient at generating aldehyde products from phenolic β-O-4 model compound **F_4** (Scheme 1.5).[32]

*Oxidation of β-1 Model Compounds **G***

Vanadium Systems:

Positive results from oxidative cleavage of simple β-1 model compound **A** led to further studies on catalytic activity of dimeric non-phenolic and phenolic β-1 model compounds **G**. Catalyst [**2**] showed preferential oxidation of the non-phenolic threo isomer **G_1** (100% conversion) to the erythro isomer (76% conversion) in pyr-d_5. Similar product distribution with ketone and dehydrated ketone as major products for both isomers and, negligible amounts of C_α-C_β bond cleavage products (<10%) were observed (Scheme 1.8, entries 1 and 2).[35] When the reaction was carried out in toluene using catalyst [**2**], the erythro isomer of **G_1** mostly converted to the corresponding ketone (72%) (Scheme 1.8, entry 3).

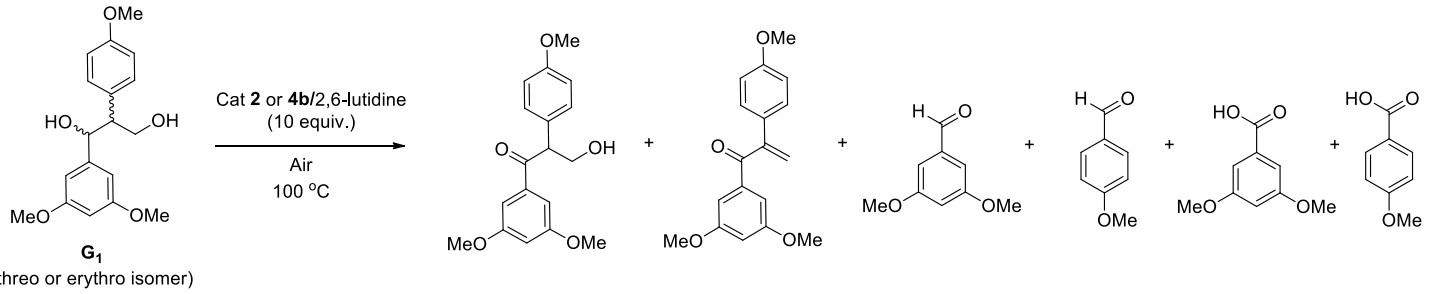

G_1
(threo or erythro isomer)

Entry	Cat.	Solvent	Time	Conversion	Yield					
1	**2** (10 mol%)	Pyr-d_5	48 h	**100%**	34%	57%	3%	3%	3%	4%
2*	**2** (10 mol%)	Pyr-d_5	48 h	**76%**	29%	38%	4%	4%	8%	6%
3*	**2** (10 mol%)/ NEt_3 (15 mol%)	Toluene	48 h	**100%**	72%	-	7%	2%	-	-
4	**4b** (20 mol %)	Toluene	48 h	**100%**	-	-	81%	69%	1%	1%
5*	**4b** (20 mol %)	Toluene	48 h	**100%**	-	-	78%	60%	1%	1%

*Reaction done using the erythro isomer of starting substrate. No star means threo isomer.

Scheme 1.8 Product distribution from vanadium [**2**] and copper-catalyzed [**4b**] oxidation of non-phenolic β-1 model compound **G_1** (yield based on theoretical maximum yield from the initial substrate amount).

For phenolic β-1 compound **G_2**, a different selectivity was obtained for oxidation with catalyst [**2**]**,** where C_{aryl}-C_α bond cleavage dominated with 2,6-dimethoxybenzoquinone (60%) as the major product, which was also seen with β-O-4 model compound **F**. Thus, phenolic and non-phenolic model compound led to a distinct reaction pathway for catalyst [**2**]. On the other hand, the dipicolinate vanadium catalyst [**1**] mainly generated a new non-C-C bond cleaved aldehyde product (44%). The mechanism for the formation of this new aldehyde product is still under investigation (Scheme 1.9, entries 1-3).

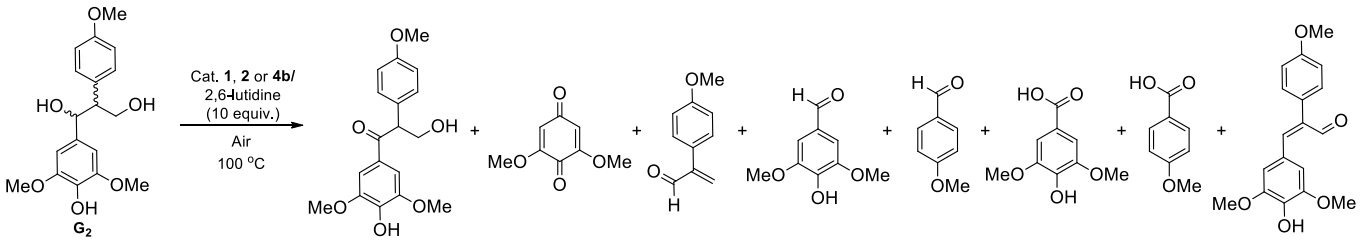

Entry	Cat.	Solvent	Time	Conversion	Yield						
1	**2** (10 mol%)	Pyr-d_5	24 h	**100%**	23%	60%	-	1%	1%	10%	12%	-
2*	**2** (10 mol%)	Pyr-d_5	24 h	**100%**	7%	43%	-	3%	6%	7%	14%	-
3*	**1** (10 mol%)	Pyr-d_5	48 h	**100%**	7%	-	-	5%	3%	9%	9%	44%
4	**4b** (1 equiv.)	Toluene	18 h	**100%**	-	82%	9%	6%	25%	-	1%	-
5	**4b** (20 mol %)	Toluene	18 h	**100%**	78%	8%	5%	2%	4%	-	1%	-
6*	**4b** (20 mol %)	Toluene	18 h	**100%**	82%	7%	3%	1%	5%	-	1%	-

*Reaction done using the erythro isomer of starting substrate. No star means threo isomer.

Scheme 1.9 Product distribution from vanadium [**1**] and [**2**] and copper-catalyzed [**4b**] oxidation of non-phenolic β-1 model compound **G_2** (yield based on theoretical maximum yield from the initial substrate amount).

Copper system:

Copper-based catalytic system [**4b**] for non-phenolic model compound **G_1** favoured the formation of aldehydes (for the threo isomer, 3,5-dimethoxybenzaldehyde (81%) and 4-methoxybenzaldehyde (69%)) from C_α-C_β bond cleavage, which was analogous to the selectivity observed for oxidation of non-phenolic β-O-4 model compound **F**. Also, no major difference in reactivity for the two **G_1** isomers was noted for copper catalytic systems (Scheme 1.8, entries 4 and 5).

With regards to the phenolic model **G_2**, for copper-based catalyst [**4b**]**,** the reaction selectivity favours the ketone product with insignificant C-C bond cleavage, which suggested a mechanism change from the previously proposed mechanism for β-O-4 model **F** (Scheme 1.9, entries 5 and 6). The opposite prevailed when using stoichiometric amount of catalyst [**4b**], where the C_{aryl}-C_α bond cleavage pathway dominated yielding 2,6-dimethoxybenzoquinone (82%) and 4-methoxybenzaldehyde (25%) as the major products (Scheme 1.9, entry 4).[28]

Finally, the C_α-C_β bond cleavage pathway was not predominant for either vanadium nor copper systems for phenolic model **G_2**, contrasting with observations for the non-phenolic β-1 substrate **G_1,** specifically when using the copper system [**4b**].[28] This discrepancy could be explained by the more electron-rich substrate **G_1** (bearing methoxy groups), which can facilitate the single-electron transfer C-C bond cleavage by stabilizing the possible radical intermediate formed during the reaction.[36]

Oxidation of Lignin Extract with Oxovanadium (V) or Metal-Free Systems

Toste and coworkers reported the oxidation of several types of lignin (organosolv lignin, dioxasolv lignin, acetosolv lignin and ethanosolv) with catalytic system [**3**]. With advanced characterization techniques, 2D-NMR and GPC (gas permeation chromatography), a reduction in major linkages β-O-4 and β-β' of lignin was detected, which was in accordance with previous studies on β-O-4 lignin model compounds with predominant C-O bond cleavage. A few aldehyde products (vanillin, syringaldehyde and 4-hydroxybenzaldehyde) were detected by GC-MS.[37]

Very recently, our group has also extended the vanadium catalytic system [**1-3**] and copper salts [**4b**] towards oxidation of organosolv lignin. Detailed discussion of these catalytic systems will be covered in chapter 4.[38] Interestingly, Stahl and coworkers have described preliminary studies into the oxidation of Aspen lignin to benzylic ketone and vanillate units using 4-acetamido-TEMPO [**5**] and a catalytic amount of strong acid (10 mol% of HNO_3 and 10 mol% HCl) under O_2 atmosphere (1 atm). β-O-4 linkages were mostly converted to their ketone derivatives.[33]

Chapter 2. Dioxo/Oxo-Peroxo Molybdenum Complexes and Early-Transition Metallosalen Complexes for Oxidation of Lignin Model Compounds

2.1 Introduction

Oxidation of alcohols to aldehydes and ketones ranks amongst one of the most important organic transformations. Conventionally, stoichiometric chromate and permanganate reagents were used for this purpose but environmental issues have limited their use. Many of the current methods in metal-catalyzed alcohol oxidation aim to use environmentally friendly oxidants, such as molecular oxygen or peroxides. For fine chemicals production, hydrogen peroxide, even at a higher cost, can be favoured over molecular oxygen due to the ease of handling.[39] Early transition metals tend to work efficiently with peroxides and late transition metals with molecular oxygen.[40]

Metal-catalyzed oxidation of alcohols with peroxides generally employs metal-oxo, -peroxo/peroxy complexes as active species. The early transition metals with d^0 configuration (e.g. Ti^{IV}, V^{V}) preferentially proceed through a peroxy-metal species (Scheme 2.1, centre) and, early middle metals (eg. Mo^{VI}, W^{VI}, Re^{VII}) tend to go through a metal-oxo or -peroxo active species (Scheme 2.1, left and right). Late and first row transition metals (e.g. Cr^{VI}, Mn^{V}, Os^{VIII}, Ru^{VI} and Ru^{VIII} prefer the metal-oxo active species (Scheme 2.1, left). However some metals can have ambiguous preference between oxo or peroxo as the active oxidant depending on the substrate[40,41,42] Generally, if oxidation occurs with a stoichiometric amount of metal complex and substrate without peroxide as oxidant, then the metal-oxo pathway occurs, lowering the oxidation state of the metal by two electrons. If stoichiometric oxidation does not occur in the absence of peroxide, the peroxo-/peroxy-metal pathway occurs.[40]

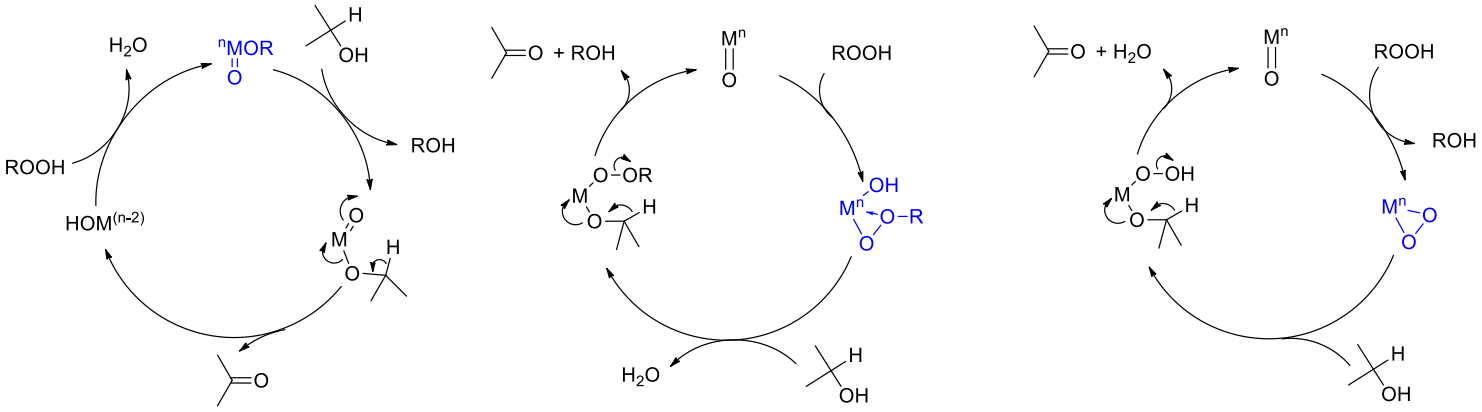

Scheme 2.1. Pathways for oxo- (left), peroxy- (centre) and peroxo- (right) metal-catalyzed oxidation of alcohol[40]

Many biological enzymes for oxidative metabolism of carbon-, nitrogen- and sulfur-containing molecules have mononuclear molybdenum (VI) as the active site (e.g. oxotransferases such as xanthine oxidase, nitrate reductase and sulfite oxidase) (Figure 2.1)[43], Mimicking the nature of said enzymes, dioxo/peroxo-oxo molybdenum (VI) complexes have been employed in oxidation reactions such as epoxidation of olefins, oxidation of phosphines and thiols, *etc*. *via* oxygen-atom/oxo transfer (OAT) mechanism.[44] Typically, these complexes cycle between oxidation state (VI) and (IV) through a two-electron transfer mechanism. In the dioxomolybdenum complexes, the role of the second oxo group can be crucial in OAT reaction as it provides a "spectator oxo" effect, where the formation of strong metal-oxo bond with formal triple bond (one σ and two π interactions from two d-orbitals) of the newly formed mono-oxo complex, compensates for the enthalpic cost of cleaving the other metal-oxo bond for OAT to the substrate.[43,45]

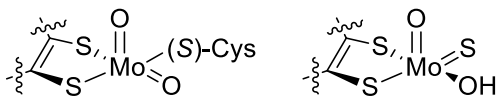

Sulfite oxidase family Xanthine oxidase family

Figure 2.1 Active site of some oxo-tranferase enzymes

Being the species most studied for OAT reactions, dioxo/peroxo molybdenum (VI) complexes were first investigated with different oxidants for oxidation of lignin model compounds. Additionally, due to the natural abundance of these molybdenum species, they are also economically viable. The details on oxidation of lignin model compounds will be discussed in the following sections.

2.2 Experimental Methods

Unless otherwise indicated, all syntheses of molybdenum complexes were done under an inert N_2 atmosphere using glove box and Schlenk line techniques. Common solvents such as hexanes, toluene, tetrahydrofuran (THF), glyme and diethyl ether were dried using an MBraun solvent purification system that was modified by JCMeyer. Deuterated solvents were purchased from Cambridge Isotope Laboratories. Regular and deuterated acetonitrile, dichloromethane and chloroform were dried by refluxing with CaH_2 and distilled. Alcohols, isopropanol and ethanol, were dried with Mg and I_2 and distilled. All dried solvents were stored under an inert N_2 atmosphere and activated molecular sieves (4Å).

Most commercially available reagents were purchased from Sigma-Aldrich and used without further purification. $MoO_2(acac)_2$ [**7**] was purchased from Alfa Aesar and $[Cp^*Mo(CO)_2]_2$ [**6**] was purchased from Strem or $[Cp^*Mo(CO)_2]_x$ (x = 2 and 3) can be made from a reported literature by decarbonylation of $Mo(CO)_6$.[46] Triethylamine was purchased from Aldrich and further purified by distillation.

^1H (300 MHz) and $^{13}C[^1H]$ (75 MHz) NMR experiments were carried out with Bruker AVANCE 300 and 300 II instruments with a QNP probe with Z gradient and autotuning broadband probe with Z gradient respectively. ^1H (400 MHz) and $^{13}C[^1H]$ (100 MHz) NMR experiments were carried out with Bruker AVANCE 400 instrument with an auto-tuning broadband probe with Z gradient. All samples were prepared in the glove box and sealed with Parafilm/Teflon tape for NMR experiments. All NMR spectra were referenced to residual solvent peaks. The spectral width was set from 15 to -2 ppm and 150 to 0 ppm for ^1H and ^{13}C dimensions respectively.

A Varian 640-IR FT-IR spectrometre was used for sample acquisition from 4000 to 700 cm^{-1}. For air sensitive samples, Nujol mull was prepared. Other air-stable samples were collected with the ATR setup.

Single crystal X-ray diffraction (XRD) measurements of molybdenum complexes ([**9**] and [**10b**]) were performed by Dr. Ilia Korobkov. The structures were collected at 202 K on Bruker Kappa X8 APEX CCD single-crystal diffractometer equipped with a sealed Mo tube and graphite monochromator (λ = 0.71073 Å). The SADABS program was applied for empirical absorption correction and the SHELXTL program was used to solve and refine the crystal structures.

All GC-MS analyses were performed using a Hewlett Packard Agilent 6890 GC system equipped with a Hewlett Packard 5873 mass selective detector. Selective quantification of products was performed with GC-FID using an Agilent 6850 series II GC system equipped with a flame ionization detector.

2.3 General Procedures

2.3.1 General Oxidation of Lignin Model Compound with Metal Complex

Lignin model compound (1 equiv.), oxidant (≥1 equiv.) and metal complex (10 mol%) were stirred in deuterated or regular solvent (0.7 mL) in a sealed vial or Schlenk tube at 60 or 70 or 100 ^{o}C for 17 hours depending on the solvent used. Insoluble precipitate (if any) was isolated after centrifugation or filtration through a Celite-padded pipette. The filtrate was then analyzed by ^{1}H-, ^{13}C-NMR and/or GC.

2.3.2 General Oxidation of Lignin Model Compound with Metal Complex and Lewis Acid Additive

The procedure is the same as above except Lewis acid (10 mol% of substrate) was added to the reaction mixture.

2.3.3 Example of Attempted Oxidation of Lignin Model Compound with *In-situ* Generation of Cationic Molybdenum Complex [Cp*MoO_2]PF_6 [11]

Part A: To a solution of Cp*MoO_2Cl (3 mg, 0.01 mmol; 0.1 equiv.) in THF (1 mL) was added $TlPF_6$ (0.1 equiv.). The reaction afforded a yellow cloudy mixture just after 15 mins of stirring and then turned to dark purple in colour. The reaction mixture was stirred for 1 hour and filtered through Celite-padded pipette. The volatiles were removed under reduced pressure leaving a dark orange solid.

Part B: To the above dried solid, lignin model compound (1 equiv.) and oxidant (stoichiometric amount) were added and the reaction was stirred and heated at 70 or 100 ^oC depending on the solvent (1 mL) for 17 hours. The reaction mixture was then analyzed using ^1H-, ^{13}C-NMR spectroscopy and/or GC.

2.4 Synthesis of Dioxomolybdenum (VI) Complexes or Oxo-peroxo Molybdenum (VI) Complexes

2.4.1 Synthesis of Pentamethylcyclopentadienyl Dioxomolybdenum (VI) Chloride [8]

Cp*MoO_2Cl [**8**] was prepared similarly to a published method with small variations.[47] A solution of [Cp*$Mo(CO)_2]_2$ (2.0 g, 0.004 mol) in $CHCl_3$ (100 mL) was vigorously stirred. 27% aq. solution of H_2O_2 (10 mL, 0.04 mol) and the concentrated HCl (3.1 mL, 0.0375 mol) were added via syringe to the above solution. The temperature of the reaction mixture was maintained at room temperature with a cold water bath. The reaction mixture was stirred for 1 hour with colour change from dark (black) red/brown to citrus orange. The stirring was continued in air for 4 hours. Another portion of H_2O_2 and HCl was added into the reaction mixture and stirring was continued overnight (16 hours). During this time, the solution turned mostly from bright orange/yellow to bright transparent yellow. The aqueous layer was separated and extracted with $CHCl_3$ (3x20 mL). All chloroform extracts were combined, washed with water (3x100 mL), then treated with an aqueous solution of $FeSO_4$ (7.5 g in 150 mL) to remove residual H_2O_2. The chloroform layer was extracted again. The organic extract was then extracted from brine (150 mL) and dried over Na_2SO_4

for 1 h, which was filtered off. The solvent was removed under reduced pressure to yield an orange/yellow solid. The orange/yellow solid was dissolved in THF for recrystallization overnight in the freezer at -20 ^{o}C in the glove box. After 14 hours, some yellow powder was formed (643 mg, 46 % yield). The product was found to be moderately thermo- and light sensitive. The ^{1}H-NMR spectrum taken matched with the reported data.
^{1}H-NMR (300 MHz, $CDCl_3$): δ 2.0 (s, 15 H, Cp-(C*H*$_3$)$_5$,).

2.4.2 Synthesis of $CpMo(CO)_3$(phenylacetylide) [10a]

This complex was made from the precursor $CpMo(CO)_3Cl$[48,49], which was in turn synthesized from $Na[CpMo(CO)_3]$, followed by $CpMo(CO)_3H$.[50] The preparation closely followed the published synthesis.[48]

2.4.3 Synthesis of $CpMo(CO)_3$(1-ethynyl-3,5 bis-(CF_3)bz) [10b]

In a vial, $CpMo(CO)_3Cl$ (200 mg, 0.58 mmol), 1-ethynyl-3,5-bis(trifluoromethyl)benzene (196 mg, 0.82 mmol), a catalytic amount of CuI (1.0 mg, $5.85x10^{-6}$ mmol) and triethylamine (5.55 mL, 0.040 mol; as a solvent) were added. The reaction mixture was stirred at 30 ^{o}C for 22 hours and 30 minutes. Triethylamine was then removed under reduced pressure. The residue was dissolved in a minimum amount of DCM and loaded onto a silica gel column with 80:20 v/v of hexanes:DCM as eluent to separate from some dark orange-brown residue. The product was then eluted with DCM and the solvent was removed under reduced pressure to afford a light yellow solid. Yield 60 mg (21 %). Yellow crystals suitable for X-ray diffraction (XRD) were grown from hexanes in a NMR tube in the glovebox freezer for two weeks. See appendix A for more details.
^{1}H-NMR (300 MHz, $CDCl_3$): δ 7.69 (br, 2H, *o*-Ph-*H*); 7.59 (br, 1H, *p*-Ph-H); 5.59 (s, 15H, Cp). ^{19}F-NMR (282 MHz, $CDCl_3$): δ -63.09 (s, 6F, Ph-C*F*$_3$).

2.4.4 Synthesis of MoO(*u*-O)(nacnac) Dimer [9]

The precursor MoO_2Cl_2(dme) was prepared from a reported preparation from Chiu *et al*.[51] To a solution of MesnacnacH (74 mg, 0.21 mmol) in THF (2 mL) was added triethylamine (29 uL, 0.21 mmol) and the mixture was stirred for 15 minutes. This solution was then added to a solution of MoO_2Cl_2(dme) (60 mg, 0.21 mmol) in THF (2 mL). The

solution turned from orange to dark brown immediately upon addition and some white precipitate formed. After stirring for 27 hours the dark brown mixture was filtered through a silica column and a golden yellow band was eluted with DCM. The solvent was removed under reduced pressure affording a golden yellow solid (40% yield). X-ray quality crystals were grown from DCM:hexanes using the vapour diffusion technique.
^{1}H-NMR (300 MHz, $CDCl_3$): δ 6.66 (2H, s, Ar*H*), 6.54 (2H, s, Ar*H*), 5.55 (1H, s, backbone-*CH*), 2.40 (6H, s, Ar-*p*-*CH3*), 2.04 (6H, s, Ar-*o*-CH_3), 1.65 (6H, s, Ar-*o*-CH_3), 1.17 (6H, s, -NCH_3).

2.5 Synthesis of Metallosalen Complexes

2.5.1 Synthesis of Ti(salen)Cl_2 [16]

According to a modified preparation from Gagné *et al*.[52], Ti(IV)-salen complex [**16**] was prepared by slow addition of titanium tetrachloride (347 mg, 1.83 mmol) solution in anhydrous THF (8 mL) to a solution of H_2salen ligand (486 mg) in anhydrous THF (7 mL) with stirring (inert atmosphere). Dissolution of titanium tetrachloride produced a yellow suspension immediately, with some heat. A red-orange precipitate immediately formed after adding the salen ligand solution. The resulting suspension was refluxed for 1 hour, cooled to ambient temperature, and dried under reduced pressure to give an orange-brown solid. The solids were slurried in anhydrous diethyl ether (20 mL), filtered, washed with additional ether, and dried under reduced pressure to give the title compound as a tangerine-colored amorphous powder (600 mg, 85% yield). The ^{1}H NMR spectrum matches that reported in $CDCl_3$.[53]

2.5.2 Synthesis of Cr(salen)Cl [13a] and cationic [Cr(salen)(O)]PF_6 [13b]

The cationic complex was made first by synthesizing the Cr(salen)Cl [**13a**] as described below. Similar to the preparation from Jacobsen *et al.*[54], the salen-chromic chloride complex was prepared by adding anhydrous chromous chloride (309 mg) to a THF solution (20 mL) containing H_2salen ligand (614 mg) with stirring under N_2 atmosphere, producing an initially pale yellow-green suspension. After three hours of stirring at room temperature under N_2, the solution (having darkened to hazel-brown) was stirred for another three hours under air. Methyl tert-butyl ether was added, and the solution

extracted thrice each with aqueous ammonium chloride and brine. The organic phase was then dried with magnesium sulfate, and the solvents removed under reduced pressure, affording a brown powder.

(Salen)oxochromium(V) hexafluorophosphate cationic complex [**13b**]

According to Gilheany *et al*.[55], the salen-chromic hexafluorophosphate complex was prepared by first dissolving Cr(salen)Cl (150 mg, 424 µmol) in methanol (25 mL), and then adding potassium hexafluorophosphate (85 mg, 462 µmol) in water (5 mL). The mixture was stirred overnight at room temperature and dried in vacuo. The resulting brown powder was re-dissolved in acetonitrile, and 93 mg of iodosobenzene added with stirring. Within 5 minutes the solution had turned to a very dark opaque green. After 20 minutes of stirring, the solvent was removed in vacuo and the resulting dark green solids extracted into acetone (10 mL). The extracts were filtered (to remove any excess iodosobenzene) and the filtrate dried at 80ºC under reduced pressure for 30 minutes to give the title compound as a green-black powder (101 mg, 50% yield - verified by IR as reported).[55]

2.5.3 Synthesis of MoO(salen)Cl [12]

Disodium-salen salt (Na_2Salen)

H_2Salen (250 mg, 932 µmol) was dissolved in anhydrous THF (10 mL). With vigorous stirring was added sodium hydride (48 mg, 2.0 mmol ; 2.2 equivalents) portion-wise over 10 minutes, maintaining gentle bubbling. After the bubbling ceased, the solution changed from yellow to colorless, with some remaining unreacted NaH suspended. The suspension was filtered through Celite and the solvent removed from the filtrate under reduced pressure to give a white amorphous powder (isolated 261 mg, 90% yield).

Molybdenum oxytrichloride

According to Gibson *et al*.[56], the Mo(V) complex was prepared by combining (under inert atmosphere) a dichloromethane solution (3 mL) containing hexamethyldisiloxane (594 mg, 3.66 mmol) with a dichloromethane solution (4 mL) containing anhydrous molybdenum(V) chloride (1.00 gram, 3.66 mmol). The resulting mixture was stirred at room temperature for 2 hours, producing a brown precipitate and a clear supernatant, which was decanted off. The solids were collected, washed (hexanes), and dried under reduced pressure to give a medium-brown solid (750 mg, 94% yield).

(Salen)molybdenum(V) oxychloride [**12**][57]

A solution of molybdenum(V) oxytrichloride (100 mg, 458 µmol) in anhydrous ethanol was added dropwise to a suspension of salen disodium (143 mg, 1 equivalent) in the same solvent. Immediately the solution darkened and a red-brown precipitate resulted. The mixture was stirred continuously at room temperature for 2 hours and filtered. The product was isolated as a medium red-brown powder and dried under high-vacuum ($1x10^{-6}$ torr), (93 mg, 49% yield) - verified by IR as reported.

2.6 Synthesis of lignin model compounds

All lignin model compounds were prepared by the reported procedures except for 1,2-diphenyl-2-methoxyethanol (DPME) and benzofuran (β-5 model) which were purchased from Sigma-Aldrich (AldrichCPR).

2.6.1 Synthesis of 1-Phenyl-2-phenoxyethanol (simple phenolic β-O-4 model) [C]

The compound was prepared according to a reported procedure[58,59] and was reduced from the corresponding ketone - 2-phenoxyacetophenone. 2-bromoacetophenone (10 g, 50 mmol) and phenol (4.7 g, 50 mmol) in the presence of potassium carbonate (8.3 g, 60 mmol) in acetone (250 mL) were stirred for 18 hours (8 g, 75 % Yield).

^{1}H-NMR (300 MHz, $CDCl_3$): δ 5.26 (s, 2H), 6.90-7.01 (m, 3H), 7.25-7.31 (m, 2H), 7.47-7.51 (m, 2H), 7.58-7.61 (m, 1H), 7.98-8.01 (m, 2H).

The ketone (2.0 g, 9.4 mmo)l was reduced with $NaBH_4$ (356 mg, 9.4 mmol) in MeOH (50 mL). The solvent was then removed under reduced pressure. The crude off-white solid was recrystallized from a minimum of hot 95% EtOH. Yield = 700 mg (35%).
^{1}H-NMR (300 MHz, $CDCl_3$): δ 2.82 (s, 1H), 3.96-4.12 (m, 2H), 5.09-5.12 (d, 1H, J) 8.7 Hz), 6.80-7.00 (m, 3H), 7.10-7.47 (m, 7H).

2.6.2 Synthesis of 3,3'-dimethoxy-5,5'-diethyl-biphenyl-2,2'-diol (5-5' model compound) [E]

The synthesis followed closely to the published preparation.[60] A solution of $K_3Fe(CN)_6$ (36 g, 0.28 mol) in distilled water (250 mL) was added drop-wise to a vigorously stirring mixture of creosol (7.5 g, 54.3 mmol) and sodium acetate (15.25 g, 0.19 mol) in distilled water (400 mL) using an addition funnel at room temperature.
After 3 hours, a cream-colored solid formed. The reaction mixture was acidified to pH 2 with concentrated HCl and turned to a grassy green colour. It was then extracted with $CHCl_3$ (3x250 ml), where the aqueous layer was grassy green and the organic layer was yellow. The extracts were dried over anhydrous $MgSO_4$ and the solvent was removed under reduced pressure to give a crude yellow-white solid, which was recrystallized from ether/petroleum ether (1:10, v/v) to give pure 3,3'-dimethoxy-5,5'-diethyl-biphenyl-2,2'-diol (off-white/very pale yellow-white; 1.01 g, 7% yield unoptimized).
^{1}H-NMR (MHz, acetone-d_6): δ 2.27(6H, s, -*CH3*), 3.85 (6H, s, ArO*CH3*), 6.67(2H, d, *J*= 2.0, Ar*H*), 6.78(2H, d, *J*=2.0, Ar*H*), 7.29(1H, s, Ar*OH*);

2.7 Results and Discussion

2.7.1 Oxidation of β-1 Model Compound A with Molybdenum Complexes and Various Oxidants

At first, commercially available molybdenum complexes/cluster were screened for their catalytic reactivity on the relatively activated β-1 lignin model compound **A**. A somewhat positive result from the only reported molybdenum-based catalyst PMA/MeOH/H_2O (80:20 vol%) for lignin oxidation led to the first test reaction with oxidation of model compound **A** with PMA and O_2 bubbling (2 min) into the reaction

system. However, this system did not give any oxidation product, probably due to the lack of thermal energy and pressure in the reaction system as the reported literature requires 170 ^{o}C and 5 bar[61]

Aiming for milder reaction conditions to achieve selective oxidative cleavage, other commercially-available molybdenum catalyst [**6**] was investigated. Since early/middle metal complexes with d^0 configuration tend to work effectively with peroxide as oxidant[40], complex [**6**] was tested with hydrogen peroxide. Fairly poor reactivity other than a slight enhancement in selectivity for aldehyde was observed by adding catalyst [**6**] into the reaction system (Table 2.1). Further characterization of complex [**6**] in the presence of H_2O_2 was not studied in detail but the carbonyls were indeed eliminated from the dimer [**6**] as confirmed by FT-IR (v(CO) = 1850-1940 cm^{-1} absent)[62] (Appendix B). The dimer [**6**] was likely first oxidized by the peroxide to form some oxo or peroxo active species.

Table 2.1 Attempted optimization of catalytic system with $[Cp^*Mo(CO)_2]_2$ **[6]**[a]

Mol % of Catalyst [6]	Oxidant	Solvent	Conversion %[a]	Yield %			
				Benzaldehyde	Methyl benzoate	Benzoin methyl ether	MeOH
-	30 % H_2O_2	$CDCl_3$	26[b]	-	-	-	-
-	30% H_2O_2	CD_3CN	52	25	26	49	-
-	30% H_2O_2 (4 equiv.)	CD_3CN	65[e]	3	32	49	-
1	30% H_2O_2	CD_3CN	30[c]	45	22	11	22
	30% H_2O_2	Pyr-d_5	0	-	-	-	-
3	**30% H_2O_2**	**$CDCl_3$**	**28**	**78**	**-**	**22**	**-**
	O_2[d]	$CDCl_3$	0	-	-	-	-
		CD_3OD	0	-	-	-	-
10	**30 % H_2O_2 (4 equiv.)**	**CD_3CN**	**30**	**51**	**8**	**18**	**23**

[a]The conversions/yields % are based on NMR internal standard (1,3,5-tri-*tert*-butylbenzene (TTB) or dimethylsulfone (DMS)). All reactions heated at 10 ^{o}C less than the boiling point of the solvent for 17 hours unless otherwise noted; 30% H_2O_2 to substrate 2:1 equiv. The bold text in the table represents the best system for selectivity and/or reactivity for the reaction.
[b]Trace amount of benzoic acid was observed in GC.
[c]32 h reaction time.
[d]O_2 purging for 2 minutes into the reaction flask and then the flask was sealed.
[e]Some formic acid was observed (16%).

Attempted oxidation of lignin model compound A with dioxo/oxo-peroxo molybdenum complexes and SPC/Adogen®464 system

In search of a more potent catalytic system for oxidative cleavage of model compound **A**, a different stoichiometric oxidant, sodium percarbonate (SPC), was employed in various solvents (Scheme 2.2) using several Mo complexes (Table 2.2). SPC is a dry carrier of hydrogen peroxide with inorganic base Na_2CO_3. SPC/Adogen464® catalytic system was previously reported by Muzart *et al*. for oxidation of various primary and secondary alcohol substrates. With their catalytic system, benzoin was able to undergo C-C bond cleavage to yield benzoic acid and benzil.[63] Solvents containing nitrile group (acetonitrile and benzonitrile) provide the most active catalytic systems for oxidizing substrate **A** with C_α-C_β bond cleavage products (benzaldehyde, methyl benzoate, benzoic acid). It was first assumed that peroxy acid could be formed from the oxidation of nitrile group of the solvent with basic hydrogen peroxide (SPC) (scheme 3).[64] However, peroxy acid was not observed when stoichiometric amount of both SPC and acetonitrile were mixed for 17 hours at 70 ^oC. Therefore, the nitrile-containing solvent may simply stabilize/solvate more the activated complex or the metal catalyst, thereby decreasing the activation energy for this organic transformation.

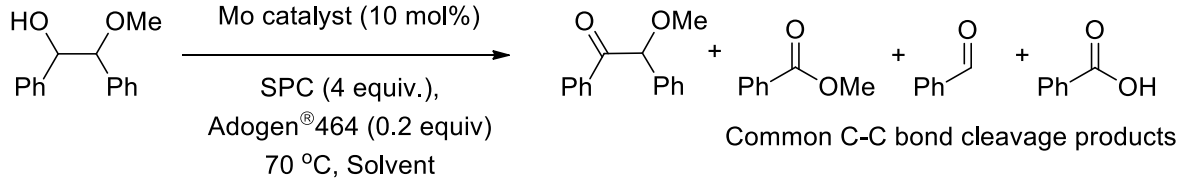

Scheme 2.2 Typical catalytic oxidation of model compound **A** with molybdenum catalyst and SPC/Adogen®464 system.

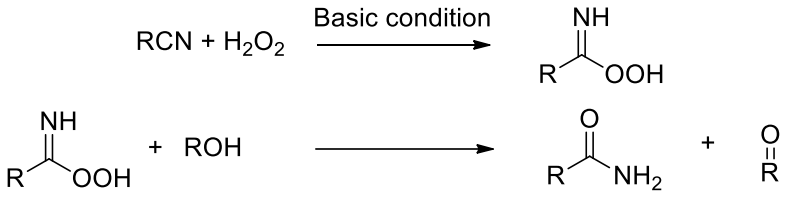

Scheme 2.3 Initial hypothesis for peroxy acid formation from nitrile functionality under basic condition.

Table 2.2 Summary of various molybdenum complexes with SPC/Adogen® 464 for their catalytic activity on lignin model compound **A**[a]

Complex	**Conversion %**	**Yield %**				
		Benzoin methyl ether	Benzil	Methyl benzoate	Benzaldehyde	MeOH
*	50	40	-	40	20	-
**	26	-	-	-	-	-
***	64[b]	100	-	-	-	-
$MoO_2(acac)_2$ [**7**]	94[b]	78	-	22	-	-
	100[c]	27	11	31	<1	31
[Mo(O)(μ-O)(Mesnacnac)]$_2$ [**9**]	100[c]	50	-	50	<1	-
CpMo(CO)$_3$(Phacetylide) [**10a**]	**93[b]**	**30**	**-**	**70**	**-**	**-**
	97[c]	57	5	19	<1	18
CpMo(CO)$_3$(1-ethynyl-3,5 bis-(CF_3)bz) [**10b**]	99[b]	70	-	30	-	-
	100[c]	53	9	37	<1	-
Cp*MoO_2Cl [**8**]	**97[b]**	**32**	**-**	**68**	**-**	**-**
	100[c]	27	13	22	<1	37
	81[d]	**93**	**-**	**7**	**-**	**-**

[a]All reactions employed 10 mol% catalyst, 4: 0.2: 1 equiv. of SPC to Adogen464® to substrate. The conversions were calculated based on internal standard TMSE or TTB from NMR; The yield % represents the product distribution of all the observed products in the organic filtrate observed by NMR; benzoic acid was observed in all reactions and can be extracted from the white salt formed with the Na_2CO_3 from SPC. Its isolated yield was calculated from the theoretical maximum yield from the amount of starting substrate (~ 18%).

[b]The reaction was heated to 100 ^oC in benzonitrile. An aliquot of the reaction was used to determine conversion/yield of products; non-observation of MeOH may be due to the high reaction temperature.

[c]The reaction was heated to 70 ^oC in CD_3CN.

[d]The reaction was performed in 27% H_2O_2 (6 equiv.), Na_2CO_3 (4 equiv.), Adogen464® (0.2 equiv.) in CD_3CN at 70 ^oC.

*Control reaction with SPC/adogen464® in CD_3CN heated to 70 ^oC.

**Control reaction with SPC only in CD_3CN heated to 70 ^oC. Negligible amount of ketone and aldehyde were formed.

*** Control reaction with SPC/adogen464® in benzonitrile heated to 100 ^oC.

Dioxomolybdenum (VI) bis(acetylacetonate) [**7**] with the SPC/Adogen®464 system achieved 100% conversion when heated at 70 ^{o}C for 17 hours in CD_3CN with methyl benzoate (31%) and benzoin methyl ether (27%). When a higher boiling point reaction solvent, benzonitrile, was used, less C_α-C_β bond cleavage was obtained (benzoin methyl ether (78%) and methyl benzoate (22%). This may be due to the catalyst decomposition as some blue precipitate was observed after 17 h of heating to 100 ^{o}C.

Next, a bulkier nacnac-derived dioxomolybdenum (VI) chloride complex was also synthesized by simple salt methathesis. Unexpectedly, a bridging oxo-Mo dimer was formed (Scheme 2.4), which was confirmed and characterized by X-ray diffraction (See section 2.7 for crystal structure and Appendix A). Nevertheless, the Mo(mesnacnac) dimer [**9**] was tested for its reactivity for oxidation of model compound **A** with SPC system. The same amount of methyl benzoate and benzoin methyl ether was obtained (both 50%).

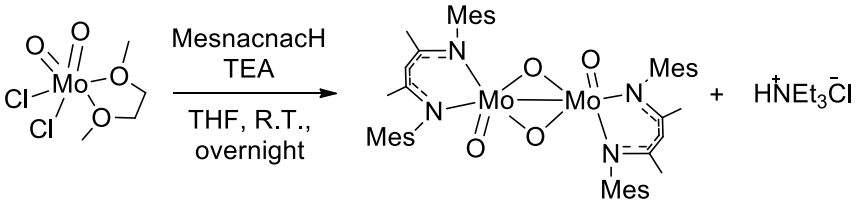

Scheme 2.4 Synthesis of Mo(mesnacnac) dimer [**9**]

A previously reported catalyst for oxidation of various alcohols to aldehydes, Mo(II) acetylide complex precursor [**10a**], which generated *in-situ* the active species Mo(VI) oxo-peroxo acetylide in the presence of 30% H_2O_2 (Scheme 2.5)[49], was also examined. A more Lewis acidic fluoro-substituted complex, $CpMo(CO)_3$(1-ethynyl-3,5 bis-(CF_3)bz) [**10b**], was also prepared and compared to the non-fluoro substituted complex [**10a**] for their catalytic activity on lignin model compound **A**. Both complex [**10a**] and [**10b**] yielded somewhat similar product distribution under identical catalytic reaction conditions in deuterated acetonitrile. Interestingly, in benzonitrile, the non-fluoro-substituted complex [**10a**] yielded more C_α-C_β bond cleavage product than the fluoro-substituted [**10b**]. This may be due to the “triply” bonded character of M-O bond originated from the more electron-deficient metal centre of complex [**10b**], thereby rendering the cleavage of the M-O bond more difficult for the redox transformation (refer to Scheme 2.1).

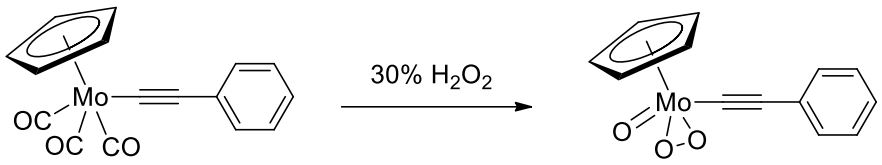

Scheme 2.5 Generation of active species CpMo(VI) oxo-peroxo acetylide from CpMo(II) acetylide.

Cp*MoO_2Cl complex [**8**]**,** also being an olefin epoxidation catalyst[65], was tested for its reactivity towards model compound **A**. Similarly, in benzonitrile, more C_α-C_β bond cleavage was obtained in similar distribution as for catalyst [**10a**].

To summarize the results obtained in Table 2.2, SPC/Adogen® catalytic system has the tendency of forming methyl benzoate and the over-oxidized product benzoic acid. This could be explained by the possible formation of hydrate from the aldehyde with water byproduct from the reaction. Surprisingly, when simulating the SPC catalytic system with the same equivalent of H_2O_2 from aqueous 27% H_2O_2, Na_2CO_3 and Adogen®464 using catalyst [**8**], the reaction for oxidation of substrate **A** did not afford full conversion and almost no C_α-C_β bond cleavage products were detectable other than the C-H bond cleavage product benzoin methyl ether (Table 2.2). This demonstrated that a dry carrier of H_2O_2 was required to obtain more C_α-C_β bond cleavage product and that the presence of water (from aqueous H_2O_2) may be detrimental to the selectivity/reactivity of this reaction.

*Dioxo/oxo-peroxo molybdenum complexes/H_2O_2 or TBHP or Oxone® system for oxidation of lignin model compound **A***

In an attempt to improve the selectivity of the oxidation of substrate **A** to the more valuable aldehyde with the dioxo/peroxo-oxo molybdenum complexes, other common oxidants such as hydrogen peroxide, tert-butyl hydroperoxide (TBHP) and Oxone® ($KHSO_5$) were tested (Table 2.3). Generally, in the presence of *tert*-butyl hydroperoxide (TBHP) as stoichiometric oxidant with molybdenum catalyst, the C-H bond cleavage pathway predominates by forming the ketone (benzoin methyl ether) regardless of the molybdenum catalyst used (Table 2.3). The catalytic system with Oxone® was selective for the ketone formation as well (Table 2.3, entry 7). More C_α-C_β bond cleavage products, benzaldehyde and methyl benzoate, were achieved with hydrogen peroxide as the stoichiometric oxidant. In addition, formic acid was formed in most of the reactions containing H_2O_2, which most likely arose from the oxidation of MeOH produced from C-O bond cleavage of substrate **A**.

In brief, Cp*MoO_2Cl [**8**]/H_2O_2 system outperformed other molybdenum catalytic systems (Table 2.3 in bold) in selectivity with benzaldehyde as the major product (41%), although the percent conversion did not improve drastically with the presence of molybdenum catalyst compared to control experiment with only H_2O_2 (Table 2.3, entry 1 *vs.* 11).

*Preliminary studies on the mechanism for catalytic oxidation of substrate **A** with complex [**8**] and H_2O_2*

Complex [**8**] in stoichiometric amount with model compound **A** *without peroxide* yielded C-H bond cleavage product, benzoin methyl ether (18%), and some C_α-C_β bond cleavage products, methyl benzoate (24%), benzaldehyde (7%), and benzoic acid (51%) (Table 2.3, entry 10). However, stoichiometric amounts of catalyst [**8**] and benzoin methyl ether afforded 77% conversion with no C-C bond cleavage products, although some C-O and C-H bond cleavage products were observed (MeOH (40%) and benzil (60%)). Only in the presence of peroxide (e.g. H_2O_2) was complex [**8**] (catalytic amount tested in this

case) able to convert benzoin methyl ether (73% conversion) to benzaldehyde (21%), methyl benzoate (30%), methanol (42%) and benzil (7%).

The above mentioned results suggest two hypotheses: **1)** the presence of peroxide must be responsible for generating the active species which can produce the C-C/C-O bond cleavage products benzaldehyde, methyl benzoate and MeOH in significant amount from the alcoholic substrate or the ketone. This is in accordance with a previous report where a molybdenum oxo-peroxo complex was generated from peroxide, H_2O_2 or TBHP, and complex [**8**] (Scheme 2.6)[65,66]; **2)** benzoin methyl ether *may be* the intermediate for the generation of C-C bond cleavage products. To test hypothesis **1)**, a catalytic amount of Cp*Mo(oxo-peroxo) complex[66] was reacted with substrate **A** under the same reaction conditions as the dioxomolybdenum system. A similar product distribution was obtained with less formic acid formed (15%) and more MeOH (27%) produced. This is unlike the alkene epoxidation where the oxo-peroxo complex was found to be the inactive species/poison to the catalytic system.[65]

*Brief discussion on complex [**10b**]/peroxide system with substrate **A***

For complex **10,** the system with H_2O_2 was more selective for aldehyde production (47% yield) than that with TBHP. This may be due to the slight difference in active species produced *in-situ* with these two different peroxides as H_2O_2 would generate the oxo-peroxo species (Scheme 2.5)[49] and TBHP would generate the peroxy species (Scheme 2.7)[67].

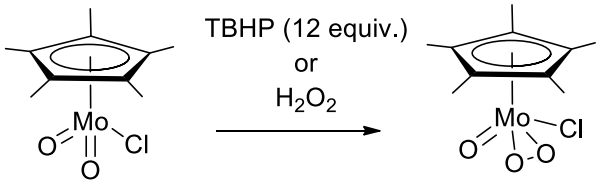

Scheme 2.6 Mono-oxo-peroxo molybdenum chloride from dioxomolybdenum complex [**8**].

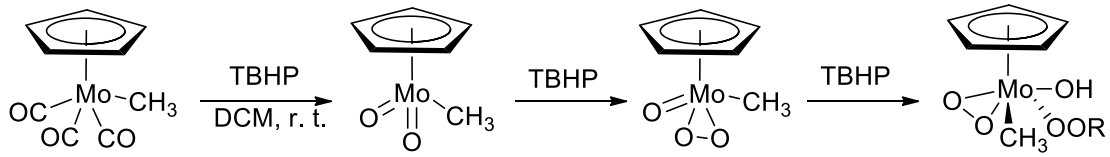

Scheme 2.7 *In-situ* formation of peroxomolybdenum alkyl peroxide complex from oxidative decarbonylation.[67]

Table 2.3 Attempted optimization with different oxidants/solvents and various molybdenum complexes for oxidation of β-1 model compound **A**[a]

Entry	Catalyst	Oxidant	Solvent	Conversion%	Yield %			
					Benzoin methyl ether	Benzaldehyde	Methyl benzoate	Methanol
1	**-**	**H_2O_2**	**CD_3CN**	**65[c]**	**49**	**3**	**32**	**-**
2	-	TBHP	CD_3CN	62	67	-	33	-
3	-	Oxone®	CD_3CN	71	34	-	19	47
4	$MoO_2(acac)_2$ [**7**]	H_2O_2	Pyr-d_5	0	-	-	-	-
5		H_2O_2	CD_3CN	60[c]	8	34	2	23
6		TBHP	CD_3CN	87	79	<<1	21	-
7		Oxone®	CD_3CN	70	~100	-	-	-
8	**MoO_2Cl_2**	**H_2O_2**	**CD_3CN**	**88**	**41**	**25**	**25**	**9**
9		TBHP	CD_3CN	55[c]	51	12	7	19
10	**Cp*MoO_2Cl [8]**	-[b]	CD_3CN	82	18	7	24	-
11		**H_2O_2**	**CD_3CN**	**66[c]**	**16**	**41**	**5**	**19**
12		TBHP	CD_3CN	26	48	15	7	30
13	[Mo(O)(μ-O)(mesnacnac)]$_2$ [**9**]	H_2O_2	CD_3CN	74	93	7	-	-
14	$CpMo(CO)_3$ (1-ethynyl-3,5 bis-(CF_3)bz) [**10b**]	H_2O_2	CD_3CN	32[c]	30	26	5	-
15		TBHP	CD_3CN	73	~100	-	-	-
16		H_2O_2	C_6D_6	0	-	-	-	-
17	[Cp*MoO_2][PF_6] [**11**]	H_2O_2	CD_3CN	52[c]	8	46	7	17
18		TBHP	CD_3CN	81	64	25	11	-

[a]The conversions were calculated with the internal standard trimethylsilylethanol (TMSE) or 1,3,5-*tert*-butylbenzene (TTB). All H_2O_2 reactions used 1:4 equiv. of substrate to H_2O_2 and all TBHP reactions used 1:2 equiv. of substrate to TBHP. All Oxone® reactions used 1:1 equiv. of substrate to Oxone®. All reactions were heated to 70 °C. The bold texts in the table represent the systems with the best selectivity and/or reactivity for the reaction.

[b]Stoichiometric amount of Mo catalyst (1 equiv.) was used in the absence of other oxidant. Benzoic acid was detected and quantified by GC-FID (51%).

[c]Formic acid was observed for most reactions with H_2O_2. For reaction with: entry 17 **=** 22%; entry 14 = 39%; entry 11 = 19%; entry 5 = 32%; entry 1 = 16% of formic acid obtained.

In brief, the slight difference in steric/electronic properties of the molybdenum catalyst with TBHP or H_2O_2 directs the selectivity of the oxidation pathway, where the C-H bond cleavage pathway becomes more favourable for more electron rich/bulky alkyl peroxide TBHP and C-C bond cleavage was preferred with hydrogen peroxide.

2.7.2 Oxidation of Lignin Model Compounds with Metal Salen Complexes

As mentioned in Chapter 1, metallosalen complexes, especially cobalt-based ones, were reported as very efficient catalyst for oxidation of a few lignin model compounds. Thus, a variety of other metallosalen complexes such as $Ti^{iv}(salen)Cl_2$ [**16**], $Cr^{III}(salen)Cl$ [**13a**], $[Cr^{V}(salen)(O)][PF_6]$ [**13b**], $Mo^{V}(salen)(O)Cl$ [**12**] and Jacobsen's catalyst ($Mn^{III}(salen)Cl$) [**14**] were screened for oxidation of simple lignin model **A** (Table 2.4). All in all, titanium and molybdenum-based complexes were not very efficient at making C-C bond cleavage products from substrate **A**. It is worth noting that when H_2O_2 was used as an oxidant with metallosalens, formic acid can be generated from the reaction, most likely from the oxidation of methanol produced from C-O bond cleavage of the substrate **A** (as observed in the previous section). Also, TBHP oxidant tends to preferentially generate the C-H bond cleavage product, benzoin methyl ether, over C-C bond cleavage products. When $[Cr(salen)O]PF_6$ [**13b**] was used with H_2O_2, both formic acid (30%) and formylated product from the starting substrate **A**, benzoin formate (9%), were formed as detected by GC-MS and NMR (Table 2.4, entry 14 and 15). Amongst the tested metallosalen complexes for oxidation of model compound **A**, Jacobsen's catalyst [**14**] was the most selective catalyst for benzaldehyde (63-69%)**,** which unexpectedly worked the best with TBHP as the oxidant (Table 2.4, entry 10).

Table 2.4 Oxidation of model **A** with simple titanium complexes and metallosalens[a]

Entry	Catalyst	Oxidant	Conversion%	Yield %			
				Benzoin methyl ether	Benzaldehyde	Methyl benzoate	Methanol
1	$Ti(OiPr)_4$ [**17**]	TBHP	73	100	-	-	-
2		H_2O_2	41	85	15	-	-
3	$Ti(O^iPr)(O_4(CH_2)_2)_3N)$ [**18**]	TBHP	80	100	-	-	-
4		H_2O_2	64[e]	-	-	-	-
5	Cp_2TiCl_2 [**19**]	TBHP	43	~100	-	-	-
6		H_2O_2	63[e]	22	7	12	-*
7	$Ti(salen)Cl_2$ [**16**]	TBHP	68	77	-	23	-*
8		H_2O_2	72[e,g]	16	4	12	-*
9	**Jacobsen's catalyst** [**14**]	H_2O_2	47[b]	-	55	45	-
10		**TBHP**	**63[b]**	**12**	**63**	**25**	-
11		TBHP	61[b,d]	26	65	9	-
12		TBHP	96[b,c]	9	69	22	-
13	Cr(salen)Cl [**13a**]	H_2O_2	77[f]	27	43	22	-
14	$[Cr(O)(salen)][PF_6]$ [**13b**]	H_2O_2	75[e,f]	17	14	14	17
15		TBHP	72[f,f2]	48	4	12	36
16	Mo(O)(salen)Cl [**12**]	H_2O_2	35[e]	19	22	8	21
17		TBHP	64	~100	-	-	-

[a]All reactions were done in CD_3CN heated to 70 ^oC and the conversions/yields were determined by NMR with internal standard unless otherwise mentioned. Catalyst (0.1 equiv.), TBHP (2 equiv.), H_2O_2 (4 equiv.) of substrate (1 equiv.). The bold text in the table represents the best system for this transformation.
[b]The yield/conversion was calculated from GC-FID due to paramagnetism of the metal complex. MeOH/formic acid and other possible low boiling-point products were not detectable from this quantification method due to high injection temperature.
[c]The conversion/yield was determined 14 days leaving at room temperature after the reaction date.
[d]The reaction was done in $CDCl_3$ heated to 60 ^oC
[e]Some formic acid was observed by ^1H-NMR. For reaction with H_2O_2, entry 16 (30%), entry 14 (29%), entry 8 (11%), entry 4 (100%), entry 6 (59%) of formic acid was observed.
[f]Benzoin formate from the formylation of substrate **A** was observed in GC-MS and NMR: 9% with H_2O_2 and negligible amount with TBHP. [f2]Diphenyl ether was observed (negligible amount).
[g]Benzoic acid (57%) and diphenyl ether (trace amount) were observed by GC.
*****MeOH may be covered by broad peak in the NMR.

2.7.3 Lewis acid-assisted Catalytic Oxidation of Simple β-1 Model Compound A with Molybdenum Complexes

Many organic transformations employ Lewis acids to catalyze and assist the reaction by rendering it more selective and by activating the substrate which would otherwise not occur.[68] In the case of oxidation, Lewis acids can help to activate the metal oxo- group or the stoichiometric oxidants, thereby facilitating the oxygen atom transfer process to the substrate.[69,70] Due to the more water resistant properties of lanthanides (III) salts compare to conventional Lewis acids (e.g. $AlCl_3$), they are frequently used to enhance the reactivity/selectivity of reactions. Owing to the lanthanide contraction effect, $Yb(OTf)_3$ is amongst the strongest Lewis acid with the highest charge to radius ratio (Z/r) in the lanthanide series.[71] Thus, a few lanthanide (III) triflates and some conventional Lewis acidic salts were used in conjunction with molybdenum catalysts to test for the reactivity of the model compound **A** oxidation.

Since a bromate salt/Lewis acid system was reported to oxidize various organic substrates (e.g. alcohols, acyloins, hydroquinones) to their corresponding carbonyl compounds,[72] $NaBrO_3/AlCl_3$ system was investigated for oxidation of substrate **A**. However, C_α-C_β bond cleavage products were not predominant (Table 2.5, entry 3). With commercially available $MoO_2(acac)_2$ [**7**] in the absence of Lewis acid, no conversion of substrate **A** was observed. Only when Lewis acid was present, (for example $AlCl_3$), the ketone product, benzoin methyl ether, was formed as the only product (Table 2.5, entry 4 *vs.* 5) with no improvement in selectivity to C_α-C_β bond cleavage product. When testing the best performing catalytic system of complex [**8**] with Lewis acid additive $Yb(OTf)_3$, no to little improvement on selectivity and conversion was observed compared to the reaction without Lewis acid (Table 2.5, entry 9 *vs.* 10). Therefore, Lewis-acid additives do not assist the molybdenum/peroxide catalytic systems for oxidation of substrate **A**.

An interesting point worth noting was when reacting substrate **A** with Lewis acid alone, α-phenyl-benzeneacetaldehyde and 1-methoxy-2,2-diphenylethene were formed as major products (Table 2.5, entry 2 and 7), which were detected by GC-MS and NMR (Appendix C). The α-phenyl-benzeneacetaldehyde is most likely formed from a Meinwald rearrangement[73], where an epoxide (probably a short-lived intermediate) undergoes a phenyl shift forming α-phenyl-benzeneacetaldehyde. This rearrangement was previously

observed with erbium triflate and stilbene oxide in DCM at room temperature in less than an hour reaction time. Additionally, when trans-stilbene oxide was used, only α-phenyl-benzeneacetaldehyde was obtained.[74] This hypothesis was then tested by reacting trans-stilbene oxide with catalytic amount of $Yb(OTf)_3$ and $AlCl_3$ (10 mol %) in CD_3CN. Indeed, the Meinwald rearrangement product α-phenyl-benzeneacetaldehyde was observed. Particularly, the reaction with $AlCl_3$ converted 100% of trans-stilbene oxide to α-phenyl-benzeneacetaldehyde (Appendix C). Therefore, stilbene-oxide may be the intermediate for forming the Meinwald rearrangement product from substrate **A** in the presence of Lewis-acid additives. Furthermore, the ethene compound, 1-methoxy-2,2-diphenylethene, was formed from the α-phenyl-benzeneacetaldehyde and methanol with Lewis acid, which was demonstrated by reacting the epoxide with methanol and a catalytic amount of Lewis acid ($AlCl_3$) (heated for 17 hours (Appendix C)). This transformation was also previously reported by using Zeolite and trimethyl orthoformate (TMOF) with α-phenyl-benzeneacetaldehyde.[75] The exact mechanism for the formation of these two products is still under investigation. Additionally, these two rearrangement products were observed in lesser amount or became absent when stoichiometric oxidant (e.g. H_2O_2 or $NaBrO_3$) were added in conjunction with Lewis acid $Yb(OTf)_3$ or $AlCl_3$ (Table 2.5, entry 3, 4). Other Lewis acid-assisted oxidations with hypervalent iodine will be discussed in chapter **3**.

Table 2.5 Selective Lewis acid-assisted oxidation of lignin model compound **A**[a]

Entry	Complex	Lewis Acid	Oxidant	Conversion %[a]	Yield %					
					Benzoin methyl ether	Methyl benzoate	Benz-aldehyde	Methanol	α-phenyl-benzene acetaldehyde	1-methoxy-2,2-diphenyl ethene
1	-	-	$NaBrO_3$	0	-	-	-	-	-	-
2	-	**$AlCl_3$**	**-**	**96**	**-**	**-**	**-**	**28**	**34**	**38**
3	-	$AlCl_3$	$NaBrO_3$	91	68	-	8	24	trace	-
4	[**7**]	-	$NaBrO_3$	0	-	-	-	-	-	-
5		**$AlCl_3$**	**$NaBrO_3$**	**99**	**100**	**-**	**-**	**-**	**-**	**-**
6		$La(OTf)_3$	$NaBrO_3$	0	-	-	-	-	-	-
7	**-**	**$Yb(OTf)_3$**	**-**	**77**	-	-	-	**-**	**85**	**15**
8	-	$Yb(OTf)_3$	H_2O_2[b]	79[d,e]	16	11	16	-	5	3
9	[**8**]	**-**	**H_2O_2[b]**	**66[c]**	**16**	**5**	**41**	**19**	**-**	**-**
10		**$Yb(OTf)_3$**	**H_2O_2[b]**	**72[c]**	**20**	**3**	**35**	**22**	trace	trace
11		$AlCl_3$	H_2O_2[b]	66	18	13	19	50	-	-

[a]All reactions were heated to 70 °C in CD_3CN. Catalyst:Lewis acid:oxidant:substrate (0.1:0.1:1:1 equiv.).
[b]H_2O_2:substrate (4:1 equiv.). The bold text represent the best systems in reactivity and/or selectivity for this reaction.
[c]Formic acid was observed: 20% with $Yb(OTf)_3$; 19% without $Yb(OTf)_3$.
[d]The conversion/yield was quantified by GC-FID.
[e]Benzoic acid (48%) and benzil (<1%) were detected by GC.

2.7.4 Attempted Oxidation of Lignin Model Compounds B (2-phenoxyethanol), C (1-phenyl-2-phenoxyethanol), D (2,3-dihydrobenzofuran) and E (3,3'-dimethoxy-5,5'-diethyl-biphenyl-2,2'-diol)

According to the result obtained in Table 2.6, the above mentioned catalytic systems were unable to oxidize β-O-4 **B**, β-5 **D** and 5-5' **E** model compound with the SPC/Adogen®464. Nonetheless, the catalyst [**8**] with SPC/Adogen®464 was capable of oxidizing the β-O-4 model **C** to the corresponding ketone, 2-phenoxyacetophenone in 94% conversion, similar to what was observed with substrate **A**. On the contrary, catalyst [**8**]/H_2O_2 system poorly converted substrate **C** to some 2-phenoxyacetophenone and formic acid, with small amount of benzaldehyde (10%). Jacobsen's catalyst [**14**]/H_2O_2 was completely unreactive toward substrate **C**. In brief, the above developed catalysts were not effective catalysts for oxidation of β -O-4 **B** and **C**, β-5 **D** and 5-5' **E**.

Table 2.6 Oxidation of simple β-O-4 model compound **C** (1-phenyl-2-phenoxyethanol)

Complex	Oxidant System	Solvent	Conversion %	Yield %	
				Benzaldehyde	2-Phenoxy acetophenone
MoO_2Cl_2	H_2O_2[a]	$CDCl_3$	0	-	-
Cp*MoO_2Cl [**8**]	SPC/Adogen® 464[b]	CD_3CN	94	-	100
Cp*MoO_2Cl [**8**]	H_2O_2[b,c]	CD_3CN	14	10	44
Jacobsen's catalyst [**14**]	H_2O_2[b]	CD_3CN	0	-	-

[a]H_2O_2:catalyst: substrate = 2:0.1:1 equiv. The reaction was heated to 60 °C.
[b]H_2O_2:catalyst: substrate = 4:0.1:1 equiv. The reaction was heated to 70 °C.
[c]Formic acid was observed (46%).

2.8 Conclusion

Dioxo/oxo-peroxo molybdenum/SPC/Adogen®464 system prefers the formation of over-oxidized product benzoic acid and not the desired benzaldehyde from model substrate **A**. On the other hand, Cp*MoO_2Cl [**8**]/H_2O_2 system was found to be the most active system for the oxidation of model compound **A** for benzaldehyde formation amongst all the dioxo/oxo-peroxomolybdenum complexes studied herein. The presence of peroxide is crucial for obtaining C_α-C_β bond cleavage products, benzaldehyde and methyl benzoate. Amongst all the metallosalen complexes studied herein, Jacobsen's reagent/TBHP was the most effective catalyst for the oxidation of substrate **A.** The addition of catalytic amount of Lewis acids into molybdenum-based catalytic system had little or no effect on improving the catalytic efficiency/selectivity of oxidaiton of lignin model compounds. If anything, it encouraged the formation of Meinwald rearrangement products on its own.

Moreover, the above developed catalytic systems were generally inactive for other linkage model compounds, such as β-O-4 **B**, β-5 **D** and 5-5' **E**, except for β-O-4 **C**. Substrate **C** can be easily transformed to the ketone 2-phenoxyacetophenone with the SPC/Adogen®464 system. The peroxide-based systems performed poorly for the other models, except for substrate **A**.

2.9 Crystal Structures Data

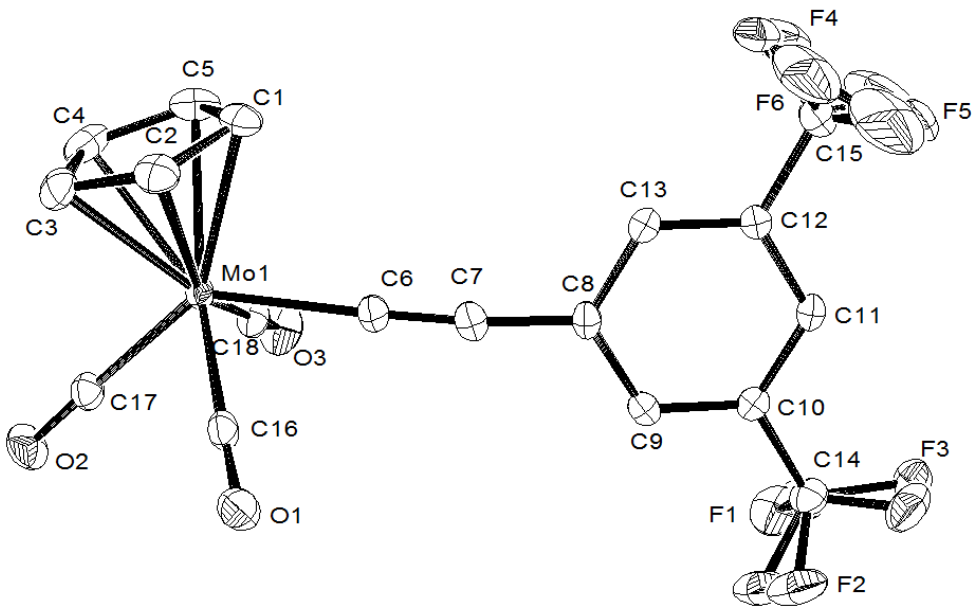

Figure 2.2 X-ray crystal structure of $CpMo(CO)_3$(1-ethynyl-3,5 bis-(CF_3)bz) [**10b**]. Thermal elipsoids are drawn at 30% probability level. Selected bond lengths (Å) and angles (º): Mo(1)-C(18) = 2.001(2), Mo(1)-C(16) = 2.001(2), Mo(1)-C(17) = 2.003(2), Mo(1)-C(6) = 2.1382(19), Mo(1)-C(4) = 2.296(2), Mo(1)-C(3) = 2.298(2), Mo(1)-C(5) = 2.335(2), Mo(1)-C(2) = 2.3442(19), Mo(1)-C(1) = 2.365(2), C(6)-C(7) = 1.206(3), C(7)-C(6)-Mo(1) = 177.71(18), C(18)-Mo(1)-C(16) =110.41(9), C(18)-Mo(1)-C(17) = 77.91(9), C(16)-Mo(1)-C(17) = 79.38(8), C(18)-Mo(1)-C(6) = 73.90(8), C(16)-Mo(1)-C(6) = 73.65(8), C(17)-Mo(1)-C(6) = 130.50(8).

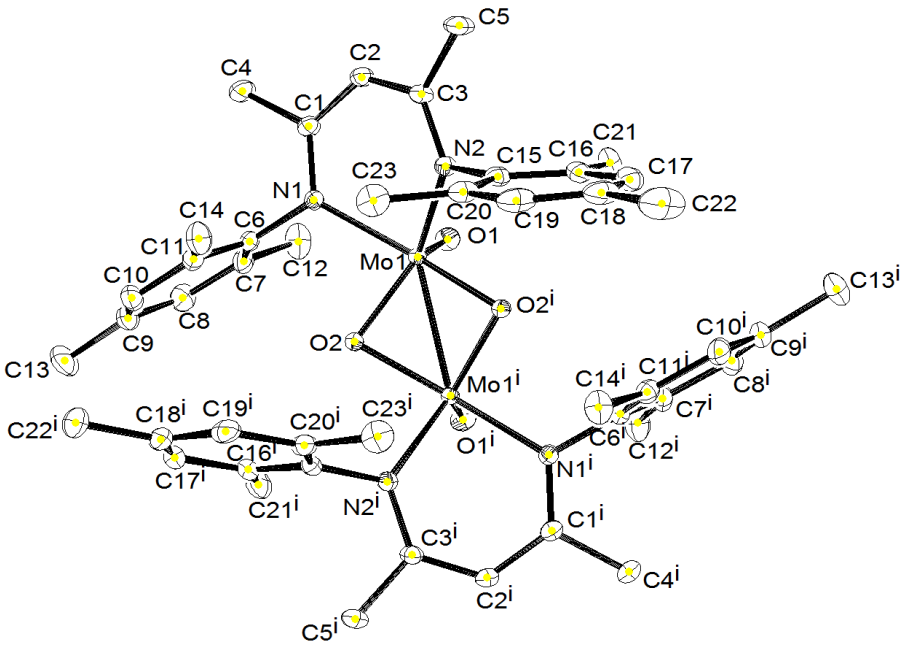

Figure 2.3 X-ray crystal structure of [Mo(O)(μ-O)(Mesnacnac)]$_2$ [**9**]. Thermal elipsoids are drawn at 30% probability level. Selected bond lengths (Å) and angles (°): Mo(1)-O(1) = 1.686(2), Mo(1)-O(2) =1.9066(17), Mo(1)-O(2i) = 1.9647(18), Mo(1)-N(2) = 2.100(2), Mo(1)-N(1) = 2.142(2), Mo(1)-Mo(1i) = 2.5620(3), O(1)-Mo(1)-O(2)= 119.51(9), O(1)-Mo(1)-O(2i)= 106.14(9), O(2)-Mo(1)-O(2i) = 90.25(8), O(1)-Mo(1)-N(2) =110.15(9), O(2)-Mo(1)-N(2)=129.74(8), O(2i)-Mo(1)-N(2) = 82.98(8), O(1)-Mo(1)-N(1) = 95.25(8), O(2)-Mo(1)-N(1) = 83.20(7), O(2i)-Mo(1)-N(1) = 158.07(8), N(2)-Mo(1)-N(1) = 85.21(8), O(1)-Mo(1)-Mo(1i) = 102.92(7), O(2)-Mo(1)-Mo(1i)= 49.54(5), O(2i)-Mo(1)-Mo(1i) = 47.60(5), N(2)-Mo(1)-Mo(1i) =126.69(6), N(1)-Mo(1)-Mo(1i) =132.40(6), Mo(1)-O(2)-Mo(1i) = 82.86(7).

Chapter 3. Oxidation of Lignin Model Compounds with Hypervalent Iodine

3.1 Introduction

The movement towards environmentally benign and efficient oxidative transformations of organic substrates has led to an increase in research on metal-free and enzymatic oxidation methods.[76] Hypervalent iodine complexes have been applied to the oxidation of a wide scope of organic substrates.[77] Some notable hypervalent iodine oxidants such as Dess-Martin periodinane,[78] 2-iodoxybenzoic acid (IBX), and iodosobenzene have been used for selective oxidative transformations.[77,79,80]

Iodosobenzene is commonly accepted to have a polymeric structure connecting intermolecularly monomeric units of PhIO with a network of I---O---I (Scheme 3.1).[81] It is therefore insoluble in most non-reactive organic solvents. In the presence of a catalytic amount of Lewis acid (e.g. BF_3-Et_2O[82], lanthanoid salts[83,84]), bromide salts (e.g. KBr (Scheme 3.2)[85]) or hydroxylic solvent (e.g. water, alcohol[86]), it can generate the activated monomeric species for oxidation reaction by helping to depolymerize and coordinate to iodine's oxygen atom to enhance the positive charge on iodine (III) (Scheme 3.1)[77].

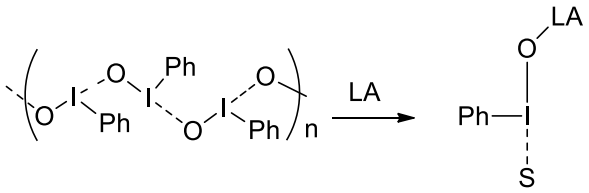

Scheme 3.1 Activation of zigzag polymeric structure of iodosobenzene with Lewis acid (S = solvent).[82]

For example, a catalytic amount of Lewis acid $Yb(OTf)_3$ with iodosobenzene as stoichiometric oxidant and some additives such as TEMPO was reported to oxidize efficiently different alcohol derivatives.[83] $Yb(NO_3)_3$ and other lanthanoid nitrate were also able to catalyze oxidation of primary alcohol and secondary alcohol to the corresponding aldehyde and ketone with iodosobenzene in 1,2-dichloroethane.[84] In addition, transition metal complexes have been employed as catalysts to effect said transformations.

Manganese(III) porphyrin, for example, in conjunction with stoichiometric iodosobenzene was able to oxidize hydrocarbons in moderate yield by generating two types of oxidizing moieties from the dimeric Mn(IV): Mn-O-Mn from the bridging *u*-oxo, and Mn-O-I from iodosylbenzene.[87]

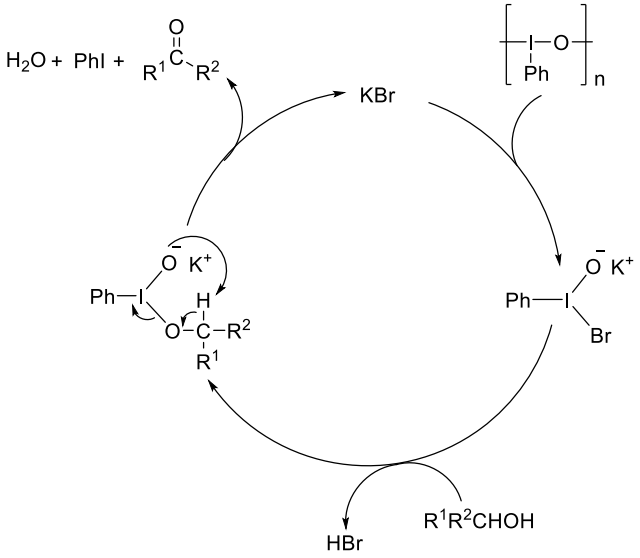

Scheme 3.2 Catalytic activation of iodosobenzene with KBr.[85]

A wide application of 2-iodoxybenzoic acid (IBX) and its derivatives have been used for selective oxidation of alcohols to the corresponding ketone, aldehydes or carboxylic acids.[88] Due to the potential explosiveness of IBX and its poor solubility in most organic solvents, Vinod and other groups have demonstrated that 2-iodobenzoic acid (catalytic amount) with Oxone® (stoichiometric amount) can *in-situ* generate IBX to yield the corresponding ketones and carboxylic acids from secondary and primary alcohols respectively in a biphasic (water/acetonitrile) system (Scheme 3.3).[89,90] Interestingly, when Oxone® is substituted with the more organic-soluble and bulky tetraphenylphosphonium monoperoxysulfate (TPPP), aldehydes were obtained from primary alcohols.[91] Another example included the use of a more Lewis acidic IBX derivative, 2-iodoxybenzenesulfonic acid, either generated *in-situ* with 2-iodobenzenesulfonate or used directly with Oxone®. This system was superior to

modified IBX (with electron-donating groups) at transforming a wide scope of alcoholic substrates to the corresponding ketones, aldehydes or carboxylic acids.[89]

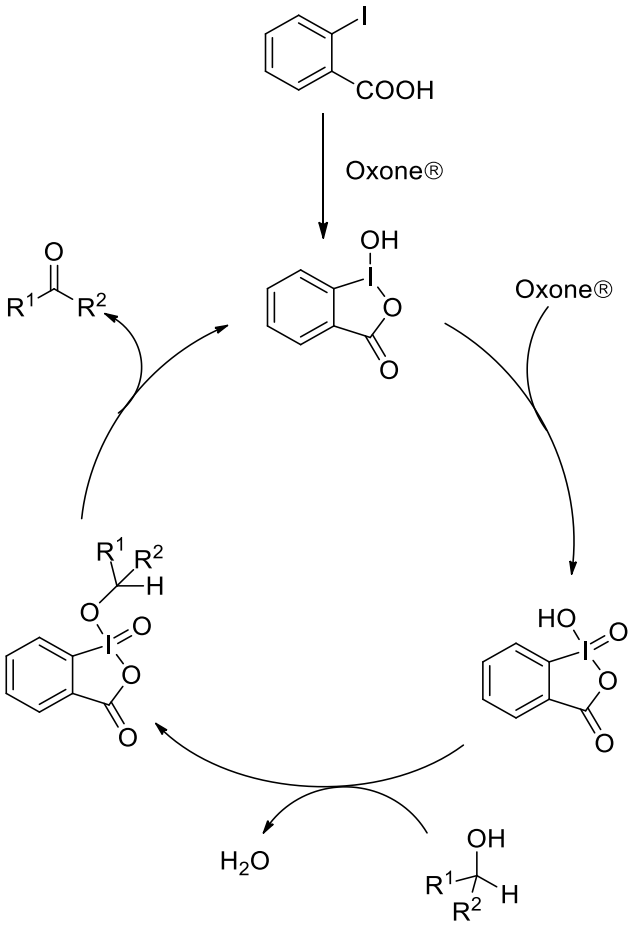

Scheme 3.3 Catalytic oxidation of alcohols with *in-situ* generation of IBX with Oxone®.

In the goal of finding a more selective and potent oxidation system for lignin model substrates, hypervalent iodine complexes, iodine(III) (iodosobenzene derivatives), iodine(V) (2-iodoxybenzoic acid (IBX)) and iodine (VII) (periodate), were investigated either as stoichiometric or catalytic reagents for oxidation of lignin model compounds.

3.2 Synthesis of Hypervalent Iodine Complexes

The starting material iodopentafluorobenzene was synthesized from I_2, pentafluorobenzene and K_3PO_4 in DMF according to a literature preparation (56% yield).[92]

3.2.1 Synthesis of Iodosobenzene [20a]

Iodosobenzene was prepared according to a reported preparation in which bis(acetoxy)iodobenzene was hydrolyzed by aqueous NaOH.[93]

3.2.2 Synthesis of Iodosopentafluorobenzene [20b]

This complex was synthesized first from the precursor [Bis(trifluoroacetoxy)iodo] benzene, which was prepared from Oxone® and trifluoroacetic acid from iodopentafluorobenzene.[94] The precursor [Bis(trifluoroacetoxy)iodo] benzene was then treated with saturated aqueous $NaHCO_3$ and stirred for one hour to yield the iodosopentafluorobenzene (37% yield).[95]

3.2.3 Synthesis of *p*-iodosonitrobenzene [20c]

A similar preparation to iodosopentafluorobenzene was performed to synthesize *p*-iodosonitrobenzene, except the starting material used was iodonitrobenzene. 4-nitroiodobenzene (2.0 g (8.0 mmol)) and Oxone® (5.0 grams (1 equiv.)) were suspended in trifluoroacetic acid (7 mL) and stirred with vigor for 3 hours. The solvent was removed in vacuo to give a crude product which was extracted into acetonitrile, with the insoluble matter filtered off using a medium frit. The filtrate was dried in vacuo to give a pale yellow solid as the product – 4-nitroiodobenzene diacetate. The diacetate (500 mg) was hydrolyzed in saturated aqueous sodium bicarbonate (20 mL) over 3 hours, filtered, washed with water, and dried in vacuo to give the iodosonitrobenzene (86 mg – 31% yield with respect to the acetoxy precursor). The IR spectrum matched with the reported data.[96]

3.3 Results and Discussion

3.3.1 Oxidation of Lignin Model Compound A with Hypervalent Iodine

As a starting point, a simple salt such as sodium periodate, $NaIO_4$, which has the capability of oxidatively cleaving vicinal diols to aldehydes,[8] was examined. However, for the lignin model compounds, the periodate failed to do any oxidative conversion of substrate **A**. The lack of second alcoholic functional group on the model substrate for the formation of cyclic periodate ester (iodine VII) may be the reason for the negative result (Scheme 3.4).

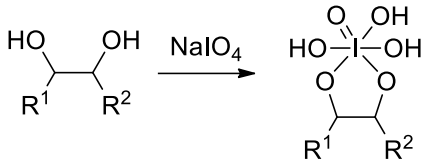

Scheme 3.4 Formation of five-membered cyclic periodate ester from vicinal diol.[8]

Then, iodosobenzene derivatives in conjunction with various lanthanide (III) salts (e.g. $La(OTf)_3$, $Yb(OTf)_3$ and $Sc(OTf)_3$) and other common Lewis acids (e.g. $Cu(OTf)_2$ and $AlCl_3$) were screened for their effect on the catalytic oxidation of lignin model compound **A**. In most cases, the product distribution shifted mainly towards benzaldehyde with the system Lewis acid/iodosobenzene. No significant catalytic reactivity with different lanthanide salts was observed for oxidation of model compound **A** (Table 3.1, entry 4-6, 8 and 9), where $Yb(OTf)_3$ and $Cu(OTf)_2$ afforded the most benzaldehyde in respect to the total conversion (Table 3.1, entry 4 and 8).

In general, molybdenum complex [**7**] with iodosobenzene and Lewis acid additive yielded worse or similar conversion and selectivity to benzaldehyde (Table 3.1, entry 12-14) than without molybdenum complex. With complex [**8**], the selectivity remains identical or with very slight improvement (Table 3.1, entry 17 and18) compared to the system without the presence of complex [**8**].

A similar complex to cationic chromium complex **13**, Cr^{V}(salen)(O)Cl, was previously noted as a chemoselective C-H oxidation catalyst for various alcohols using iodosobenzene in a reasonable yield (50 to ~90%)[97]. Complex [**13**] was able to afford 85% conversion and 76% of benzaldehyde (Table 3.1, entry 21). Nevertheless, $Yb(OTf)_3$ or

$Cu(OTf)_2$/iodosobenzene system was still the most selective catalytic system for benzaldehyde production (Table 3.1, entry 4 and 8).

As noted, some reactions yielded diphenyl ether (Table 3.1, entry 10, 11, 14, 21), which probably originated from nucleophilic attack of phenol on the by-product iodobenzene.

Encouraged by these positive results with iodosobenzene, more electron-withdrawing derivatives of iodosobenzene plus the most efficient Lewis acid for this oxidation transformation, $Yb(OTf)_3$, were investigated. As expected, iodosoperfluorobenzene [**20b**] also showed preferential selectivity for benzaldehyde with $Yb(OTf)_3$ from oxidation of substrate **A** (Table 3.2, entry 1-4, especially for the reaction in CD_3CN (Table 3.2, entry 3). When the reaction was performed in $CDCl_3$, the effect of Lewis acid additive is minimal as both the conversion and selectivity were similar, especially with iodosonitrobenzene (Table 3.2, entry 2 *vs.* 4, 5 *vs.* 6). The selectivity to aldehyde was much enhanced for the reaction in CD_3CN with $Yb(OTf)_3$ (Table 3.2, entry 3 *vs.* 1) compared to the same reaction in $CDCl_3$ where not much difference was observed. Moreover, the most electron-withdrawing nitro-substituted iodine complex [**20c**] in this case provided less conversion than the fluorinated iodosobenzene [**20b**] (Table 3.2, entry 6). When using catalytic amount of [**20b**]/$Yb(OTf)_3$ with stoichiometric oxidant Oxone®, conversion of 74% was achieved. Nevertheless, the selectivity for benzaldehyde was not as high as with stoichiometric amount of [**20b**] (Table 3.2, entry 7).

In brief, these substituted iodosobenzene derivatives [**20b** and **20c**] are not dramatically better than iodosobenzene for oxidation of substrate **A**, other than their increased solubility in polar organic solvents (Table 3.1 *vs.* Table 3.2). This may be caused by the inductive stabilization of the electrons on the oxygen of the oxo ligand of the iodine complex from these electron-withdrawing groups (perfluoro- or nitro-).

Table 3.1 Lewis acid-assisted oxidation of lignin model compound **A** with iodosobenzene as oxidant.[a]

Entry	Complex (10 mol%)	Lewis Acid (10 mol%)	Conversion %	Yield %			
				Benzoin methyl ether	Methyl benzoate	Benzaldehyde	Methanol
1	-	**-**	**32**	**3**	**4**	**70**	**23**
2		-	31[c]	38	24	38	-
3		$AlCl_3$	83	22	-	64	14
4		**$Cu(OTf)_2$**	**94**	**-**	**-**	**83**	**17**
5		$La(OTf)_3$	87	8	-	85	7
6		**$Yb(OTf)_3$**	**77**	**5**	**1**	**70**	**24**
7		$Yb(OTf)_3$	0[b]	-	-	-	-
8		**$Yb(OTf)_3$**	**95[c]**	**-**	**-**	**79**	**21**
9		$Sc(OTf)_3$	87	3	-	82	15
10	$MoO_2(acac)_2$ [**7**]	-	50[d]	63	-	37	-
11		-	85[c,d]	43	-	57	-
12		$AlCl_3$	84	32	-	68	-
13		$La(OTf)_3$	90	-	-	74	26
14		$Yb(OTf)_3$	88[d]	61	-	39	-
15	Cp^*MoO_2Cl [**8**]	-	72	81	-	19	-
16		$AlCl_3$	98	28	-	60	12
17		$Cu(OTf)_2$	71	7	-	85	8
18		**$Yb(OTf)_3$**	**88**	**3**	**-**	**78**	**19**
19		$Sc(OTf)_3$	89	9	-	70	21
20	$[Cp^*MoO_2]^+[PF_6]$ [**11**]	-	49[d]	47	10	27	16
21	$[Cr(salen)(O)]^+[PF_6]$ [**13**]	-	85[c-e]	5	-	76	-

[a]All reactions were heated to 60 °C in $CDCl_3$ for 17 hours. Substrate:PhIO = 1:1 unless otherwise noted. For most reactions, the yield is based on the product distribution determined by ^{1}H-NMR with internal standard TTB. The bold texts in the table represent the systems for the best reactivity and/or selectivity for this reaction.

[b]*t*-butyl hydroperoxide as stoichiometric oxidant (2 equiv.) and heated for 24 hours.

[c]Reaction in CD_3CN heated at 70 °C with same reaction conditions as note a.

[d]Diphenyl ether was observed by GC-MS.

[e]The conversion/yield was determined by GC-FID.

Table 3.2 Oxidation of lignin model compound **A** with iodosoperfluorobenzene and iodosonitrobenzene.[a]

Entry	Oxidant	Lewis Acid (10 mol%)	Solvent	Conversion %	Yield %					
					Benzoin methyl ether	Methyl benzoate	Benz-aldehyde	MeOH	α-phenyl benzene-acetaldehyde	1-methoxy-2,2-diphenyl ethene
1	$IO(C_6F_5)$ (**20b**)	-	CD_3CN	82[d]	20	2	55	20	-	-
2			$CDCl_3$	57	3	-	85	12	-	-
3	**$IO(C_6F_5)$ (20b)**	**$Yb(OTf)_3$**	**CD_3CN**	**90[c,e,f]**	**<1**	**-**	**82**	**-**	**13**	**-**
4			$CDCl_3$	73	<1	-	88	12	-	-
5	*p*-$IO(C_6H_4)(NO_2)$ (**20C**)	-	**$CDCl_3$**	**72**	**13**		**73**	**14**	**-**	**-**
6		**$Yb(OTf)_3$**	**$CDCl_3$**	**69**	**8**	**-**	**74**	**18**	**-**	**-**
7	$IO(C_6F_5)$ / Oxone®[b]	$Yb(OTf)_3$	CD_3CN	74[c-e]	2	2	25	35	6	8

[a]All reactions contained 1:1 $IO(C_6F_5)$:substrate. The yields/conversions were determined by ^{1}H-NMR of identifiable products with internal standard unless otherwise noted. The bold texts in the table represent the systems with the best reactivity and/or selectivity for this reaction.
[b]$IO(C_6F_5)$ (10 mol%), Oxone® (1 equiv.).
[c]Trace amount of benzil was determined by GC-FID/MS.
[d]Formic acid was observed in ^{1}H-NMR: entry 1 = 3%; entry 7 = 8% of formic acid.
[e]Unknown (2%), phenol (12%) were determined by NMR.
[f]The yield/conversion was calculated from GC-FID (so MeOH not observable) due to broadness of NMR spectrum. Benzil was detected (5%).

3.3.2 Oxidation of 1-Phenyl-2-Phenoxyethanol (β-O-4 model)

With β-O-4 model substrate **C**, the most electrophilic iodosonitrobenzene [**20c**] system yielded the most selective oxidation to aldehyde (Table 3.3, entry **5**), which can be explained by its more electrophilic nature. It is still not understood why the fluorinated derivative [**20b**] was worse at selectivity/reactivity than the unsubstituted iodosobenzene [**20a**]. Additionally, there is no dramatic difference in reactivity with or without the Lewis acid additives (Table 3.3, entry 1 *vs.* 2; entry 3 *vs.* 4). Overall, moderate reactivity and selectivity were observed for these hypervalent iodine systems (Table 3.3, entry 1-5).

Table 3.3 Oxidation of 1-phenyl-2-phenoxyethanol **C** with various oxidants.

Entry	**Lewis Acid (0.1 equiv.)**	**Oxidation System**	**Conversion %**	**Yield %**		
				Benzaldehyde	2-Phenoxy acetophenone	Unknown
1	-	Iodoso-benzene[b,c]	73	47	36	17
2	$Yb(OTf)_3$	Iodoso-benzene[b,c]	74	36	43	21
3	**-**	Iodosoperfluoro-benzene[a]	68	9	91	-
4	$Yb(OTf)_3$	Iodosoperfluoro-benzene[a]	63	-	100	-
5	**$Yb(OTf)_3$**	**Iodosonitro-benzene[a]**	**77**	**69**	**31**	**-**

All reactions with hypervalent iodine were heated to 60 °C in $CDCl_3$. All yields/conversions were calculated based on the identifiable products. The bold text represents the system with the best selectivity and reactivity for this reaction.

[a]1:1:0.1:0.1 equiv. of substrate:oxidant:Lewis acid:catalyst.

[b]1.5 equiv. of iodosobenzene to substrate

[c]Diphenyl ether was observed.

3.4 Comparison of Molybdenum and Hypervalent Iodine Catalytic Systems with Reported Catalytic Systems for Oxidation of Lignin Model Compounds

The reported catalytic systems for substrate **A** oxidation with vanadium, copper and typical oxidation systems (IBX and CAN systems) were compared with the best molybdenum-based and hypervalent iodine catalytic systems herein.

Ceric ammonium nitrate (CAN)/$NaBrO_3$ catalytic system (Table 3.4, entry 4) gave 100% conversion with ketones, benzoin methyl ether and benzil, as the major products and no C-C bond cleavage product. The IBX system, which is generated *in-situ* from 2-iodobenzoic acid, also gave benzoin methyl ether as the major product (Table 3.4, entry 6).

Both molybdenum-based and hypervalent iodine catalytic systems (Table 3.4, entry 4-7) required less reaction time for full (or close to 100%) conversion of the substrate **A** as compared to vanadium or copper-based catalysts (17 h *vs.* >20 h). The molybdenum system is selective for methyl benzoate production (Table 3.4, entry 5) while the iodosobenzene/Lewis acid system was found to be the most selective system for benzaldehyde production from oxidation of substrate **A** (Table 3.4, entry 7), beating the catalytic reactivity/selectivity of the copper/TEMPO system (Table 3.4, entry 3 (48%) *vs.* 7 (79%)).

When comparing the catalytic system for oxidation of β-O-4 model compound **C**, hypervalent iodine systems again outperformed all the existing vanadium and copper systems, with 77% conversion and 69% benzaldehyde produced (Table 3.5, entry 3).

Table 3.4 Comparison of catalytic reactivity with reported oxidation catalytic systems herein and developed catalytic systems herein for β-1 model compound **A**.[a]

Entry	Catalytic System	Reaction time	Conversion %	Yield %					
				Benzoin methyl ether	Methyl benzoate	Benzoic acid	Benz-aldehyde	MeOH	Benzil
1	(dipic)V(O)(O^iPr) (10 mol%)/air/ pyr-d_5	6 days	99	5	43	44	5	3	-
2	(dipic)V(O)(O^iPr) (5 mol%)/air/ DMSO-d_6	20 h	94	8	3	3	44	42	-
3	**CuCl (20 mol%) /TEMPO (30 mol%)/O_2/pyr-d_5**	**48 h**	**92**	**2**	**50**	**-**	**48**	**-**	**-**
4	CAN/$NaBrO_3$[b] CD_3CN	17h	96	62	3	-	<<1	-[d]	35
5	**Cp*MoO_2Cl [8], SPC, Adogen®464, PhCN**	**17 h**	**97[b]**	**32**	**68**	**18[c]**	**-**	**-**	**-**
6	2-iodobenzoic acid/Oxone®/ *n*-Bu_4NHSO_4, CD_3CN/H_2O	16 h	100	92	4	3	<1	-[d]	-
7	**Iodosobenzene/ Yb(OTf)$_3$, CD_3CN**	**17 h**	**95**	**-**	**-**	**-**	**79**	**21**	**-**

[a]All vanadium and copper catalytic reactions were carried out at 100 °C. For entries 1-3, the percent yield was converted to out of 100% instead of basing on the theoretical maximum of each individual product calculated from the initial amount of the substrate as reported by Hanson *et al*.[25,98]

[b]CAN:substrate:oxidant (0.01:1:1 equiv.). The reaction solvent was a mixture of CD_3CN:H_2O (7:3 v/v). The reaction mixture was then extracted with water/benzene, where the organic layer was isolated and dried under vacuum for NMR analysis.

[c]Isolated yield of benzoic acid to the theoretical maximum of substrate introduced.

[d]MeOH may not be observed since the reaction mixture was extracted and dried under reduced pressure.

Table 3.5 Comparison of catalytic reactivity with existing reported oxidation systems for β-O-4 model compound 1-phenyl-2-phenoxyethanol [**C**].[a]

Entry	Catalytic system	Reaction time	Conversion %	Yield %					
				Phenol	2-phenoxy-acetophenone	Benzoic acid	Formic acid	Benz-aldehyde	2-phenoxy-1-phenyl formate
1	$(HQ)_2V(O)(O^iPr)$ (10 mol%)/air/ pyr-d_5[35]	48 h	58	41	15	42	2	-	-
2	CuCl (0.2 equiv.)/TEMPO (0.2 equiv.)/2,6-lutidine (10 equiv.)/ O_2 in pyr-d_5[35]	40 h	67	9	5	5	-	-	81
3	**Iodoso-nitrobenzene [20c]/$Yb(OTf)_3$ in $CDCl_3$**	**17 h**	**77**	**-**	**31**	**-**	**-**	**69**	**-**

[a]The bold text represents the system with the best selectivity and reactivity for the reaction.

3.5 Conclusion

Overall, hypervalent iodine systems were found to be effective terminal oxidants for the lignin model compounds tested. The effect of Lewis acid auxiliaries was found to be mostly positive in enhancing selectivity for aldehyde products. Furthermore, the effect of electron-withdrawing substituents on the iodosylbenzene predictably enhanced the reactivity of said oxidants in some cases. Rather noteworthy was the performance of said systems when compared to the copper and vanadium catalysts discussed earlier. For oxidation of β-1 model compound **A**, both molybdenum and hypervalent iodine based systems outperformed the aforementioned vanadium and copper catalytic systems in both reaction time and selectivity. Thus the conclusion can be made that hypervalent iodine reagents (being effective agents of oxo-atom transfer) are more effective terminal oxidants than those used in earlier systems. Furthermore, simple

trifluoromethanesulfonate salts of metals bearing a “hard” Lewis-acidity can act as effective catalysts without the need for complex ligand frameworks. Moreover, the Cp^*MoO_2Cl [**8**]/SPC/Adogen®464 system in benzonitrile was able to generate methyl benzoate as the major product in almost full conversion. The greatest performance was attained with the p-nitroiodosobenzene/$Yb(OTf)_3$ system, which yielded benzaldehyde as the major (90%) product with ~70% conversion.

For oxidation of β-O-4 model compound **C**, the hypervalent iodine catalytic systems once again surpassed the existing copper and vanadium systems in selectivity and reactivity. Conversions as high as 77% with yields as high as 70% of benzaldehyde could be achieved.

Chapter 4. Quantitative Heteronuclear Single Quantum Coherence Spectroscopy (q-HSQC) - Characterization Technique for Lignin Depolymerization with Vanadium/Copper/Cobalt Complexes[38]

4.1 Introduction

Quantitative Heteronuclear Single Quantum Coherence Spectroscopy (q-HSQC) is a very powerful technique to characterize and quantify the main structural linkages of lignin (Figure 4.1 and 4.2), which would be difficult to characterize with one-dimensional NMR techniques.[99] Selectivity/reactivity of catalysts for lignin depolymerization can be easily deciphered by quantifying the main structural linkages before and after the catalytic transformation with q-HSQC.

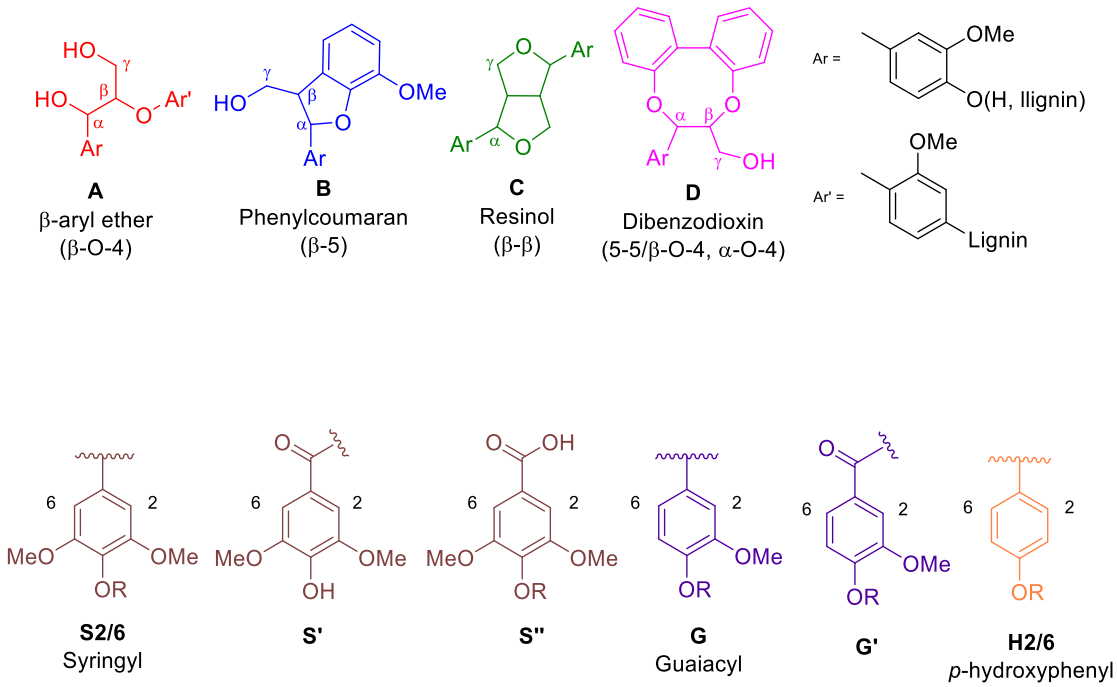

Figure 4.1 Lignin linkages observed by q-HSQC NMR.

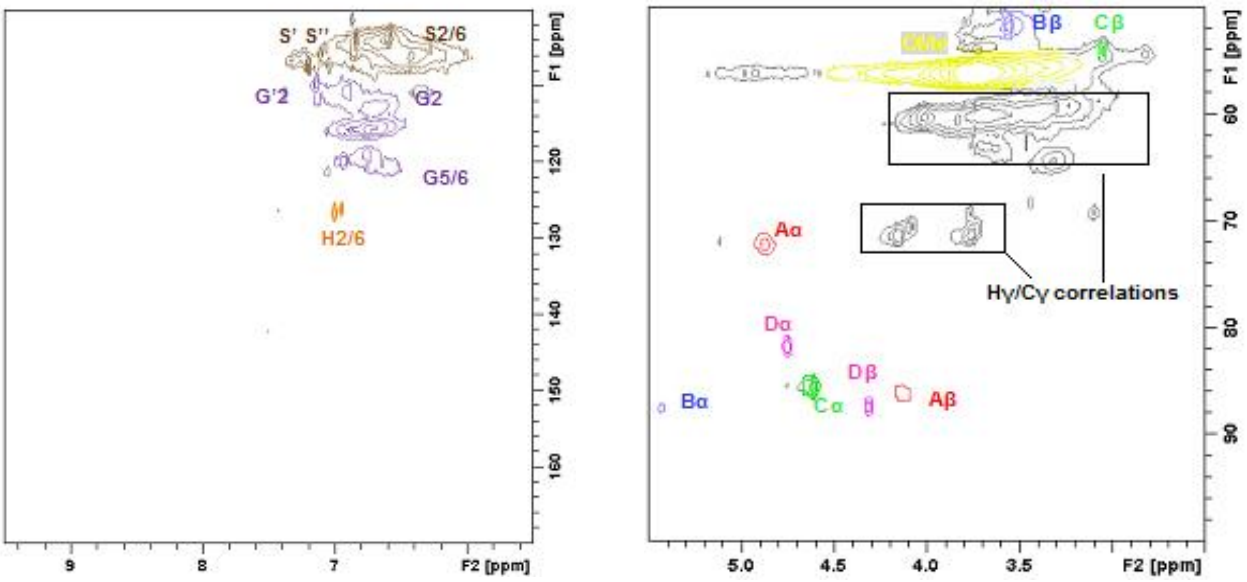

Figure 4.2 q-HSQC spectra of non-volatile organosolv (NVO) lignin.

Very recently, catalytic non-oxidative lignin depolymerisation was analyzed with quantitative-Heteronuclear Single Quantum Correlation (q-HSQC) for vanadium catalyst system.[37] In our submitted paper, catalytic systems with vanadium [**1**-**3**], copper [**4b**], cobalt [**15**] catalysts and a metal-free catalytic system [**5**] were investigated with the q-HSQC technique.

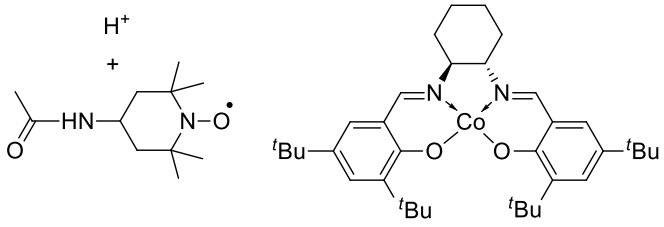

5 **15**

Figure 4.3 4-acetamido-TEMPO/acid [**5**] and cobalt^{II}(salen) [**15**] catalysts for the oxidation of lignin models/extracts.

4.2 Experimental Methods

4.2.1 NMR Spectroscopy

For q-HSQC, the pulse program was obtained from the reported method.[25] The spectral width was set to 12-0 ppm and 170-0 ppm for ^{1}H and ^{13}C dimensions respectively. For quantitative data, the recycle delay was set to 5 s. The number of collected points was 2048 for ^{1}H dimension. The number of scans was 88 with 256 increments for a total time of approximately 33 hours. The squared sine, QSINE, function with a sine bell shift of 2 was applied in both dimensions. All spectra were processed with TopSpin 3.0.

4.2.2 q-HSQC NMR Analysis

In order to validate the performance of the catalysts employed**,** q-HSQC was used as the analytical tool (Figure 4.2). For the catalytic oxidation of NVO lignin using catalyst [**2**] (EtOAc, 10 wt. % [**2**] and 10 wt. % Et_3N), all of the syringyl units **S2/6** and most of the guaiacyl units **G** were oxidized to the corresponding **S'**, **S''** and **G'**; the ratio of **G'2** to **G2** increased to 0.74 from 0.16 in the control (no catalyst) (Figure 4.4). q-HSQC also revealed that all the *p*-hydroxyphenyl units **H2/6** of NVO lignin completely disappeared using this catalyst. On the other hand, catalyst [**1**] (EtOAc, 10 wt. % [**1**] and 10 wt. % Et_3N) also resulted in an increase in oxidized **S** – the ratio of (**S''** + **S'**) to **S** increasing to 1.4 from 0.16 in the control (no catalyst) – and oxidized **G** units – the ratio of **G'2** to **G2** increasing to 0.69 from 0.16 in the control (no catalyst) – with the disappearance of **H2/6** unit.

We then examined the performance of catalyst [**2**] using *n*-butyl acetate (10 wt. % [**2**] and 10 wt. % Et_3N). Under these conditions some **S2/6** still remained but the major structural units in the oxygenated aliphatic region were cleaved. The ratio of (**S''** + **S'**) to **S2/6** increased to 1.8 and the ratio of **G'2** to **G2** increased to 0.50.

The data shows that catalyst [**2**] (in EtOAc) is more active than catalyst [**1**] for the oxidation of NVO lignin. The lower activity showed by [**1**], might be explained by the decomposition of this catalyst in the presence of water to form dioxo- anionic species.[26] At the end of the catalytic oxidation of NVO lignin using catalyst [**1**], ^{51}V NMR spectroscopy revealed a strong signal at -522 ppm corresponding to the anionic dioxovanadium(V) complex.[100]

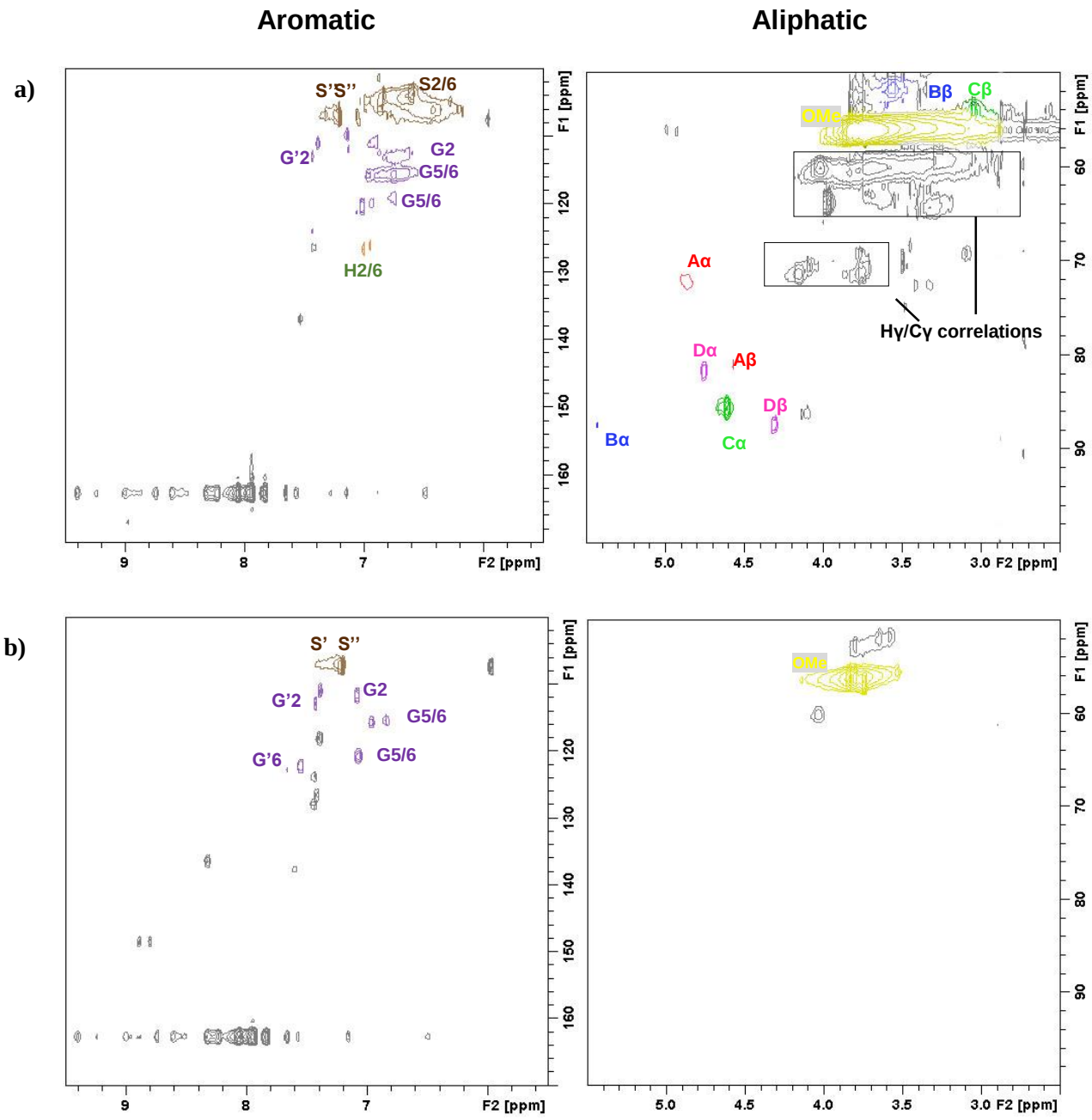

Figure 4.4 q-HSQC of NVO lignin for: a) control experiment (no catalyst) and b) catalytic oxidation using 10 wt. % [**2**] and 10 wt. % Et_3N. For all runs: solvent = EtOAc; temperature = 100 ^oC; pressure of synthetic air = 8.2 atm; reaction time = 18 h.

In order to optimize the system, we used catalyst [**2**] at shorter reaction times (4 h) using 10 wt. % [**2**] and 10 wt. % Et_3N in EtOAc. The oxidation of NVO lignin could indeed be observed at 4 h, but to a lower degree. The **S2/6** was partially oxidized to **S'** and **S''** ((**S'** + **S''**)/**S2/6** = 0.90) for 4 h and, all oxidized to **S'** and **S''** as mentioned above for 18 h, while **G'2/G** was 0.04 for 4 h and 0.70 for 18 h. Longer reaction time was thus required to achieve a higher degree of oxidation in the aromatic units. In the oxidative aliphatic region, however, the cleavage of main structural units still took place after a shorter reaction time of four hours.

Considering that catalyst [**1**] and [**2**] require the presence of a base to operate under the base-assisted redox dehydrogenation mechanism (Scheme 1.1), and *probably* under the C-C bond cleavage postulate, we used catalyst [**2**] in absence of a base (EtOAc, 10 wt. % [**2**], 18 h). As expected, q-HSQC showed that for these oxovanadium(V) catalysts, the oxidation of NVO lignin can only occur in the presence of a base (*e.g.* Et_3N).

In the catalytic oxidation of NVO lignin using [**1**] or [**2**] (EtOAc or *n*-butyl acetate) the major structural units **A**, **B**, **C** and **D** (the oxygenated aliphatic region ranging from 3.0 to 6.0 ppm) were also broken down. This was inferred from the disappearance of the corresponding H_α/C_α correlations – the methoxy group excepted – in comparison to the q-HSQC spectra of control experiments using 10 wt. % base as additive (Figure 4.4).

On the other hand, the copper catalyst [**4b**] resulted in the breakdown of **A**, **B**, **C** and **D** in addition to **S2/6** being oxidized to mostly **S'** and **S''.** The ratio of **S2/6** to **S'/S''** increased to 0.73 from 0.26 of the control experiment (no catalyst). However, paramagnetic interferences from residual copper (II) species hinder further investigation on this catalyst. Similarly to the copper catalyst [**4b**], the nature of the Chornet method (the *super*-stoichiometric amount of sodium hydroxide and the addition of paramagnetic species) prevented us obtaining a noise-free and resolved q-HSQC (Figure 4.5). Filtration resulted in a non-representative sample of the oxidized NVO lignin. However, the GPC traces showed that the molecular weight was not decreased in both the Chornet control experiment (only base) and the Chornet method (base and metals) (Figure 4.6).

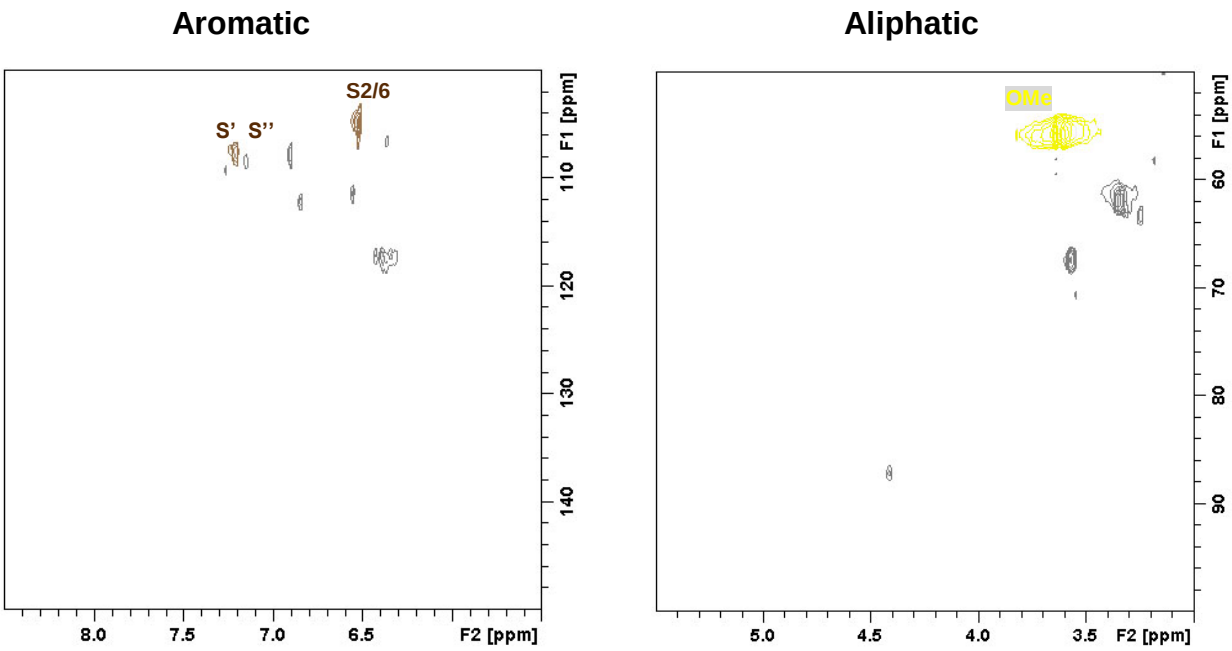

Figure 4.5 q-HSQC of NVO lignin for the Chornet method (135 wt. % NaOH, 5 wt. % $CuSO_4$ and 0.5 wt. % $FeCl_3$). For all runs: solvent = THF; temperature = 100 ^oC; pressure of synthetic air = 8.2 atm; reaction time = 18 h.

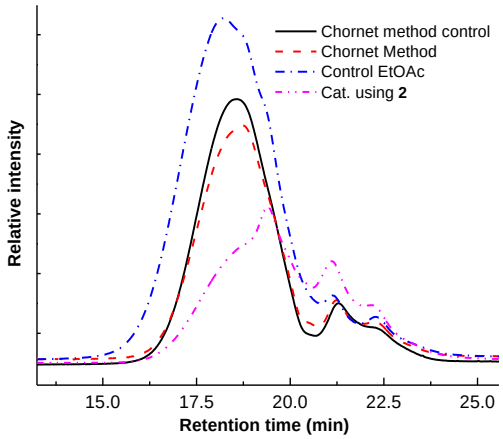

Figure 4.6 GPC data of catalytic oxidation of NVO lignin using, the Chornet method (THF, 135 wt. % NaOH, 5 wt. % $CuSO_4$ and 0.5 wt. % $FeCl_3$), Chornet control experiment (THF and 135 wt. % NaOH) and catalyst [**2**] (EtOAc, 10 wt. % [**2**], 10 wt. % Et_3N). For all runs: temperature = 100 ^oC; pressure of synthetic air = 8.2 atm; reaction time = 18 h. (THF solvent, elution rate: 1 mL/min, 254.4 nm).

Catalyst [**3**] was only able to oxidize the β-O-4 structural unit **A** in the oxygenated aliphatic region (Figure 4.7). Correlation corresponding to **H2/6** in aromatic region disappeared while other structural units remained roughly intact. This is in agreement with the C-O bond cleavage mechanism proposed for this catalyst.[31,37]

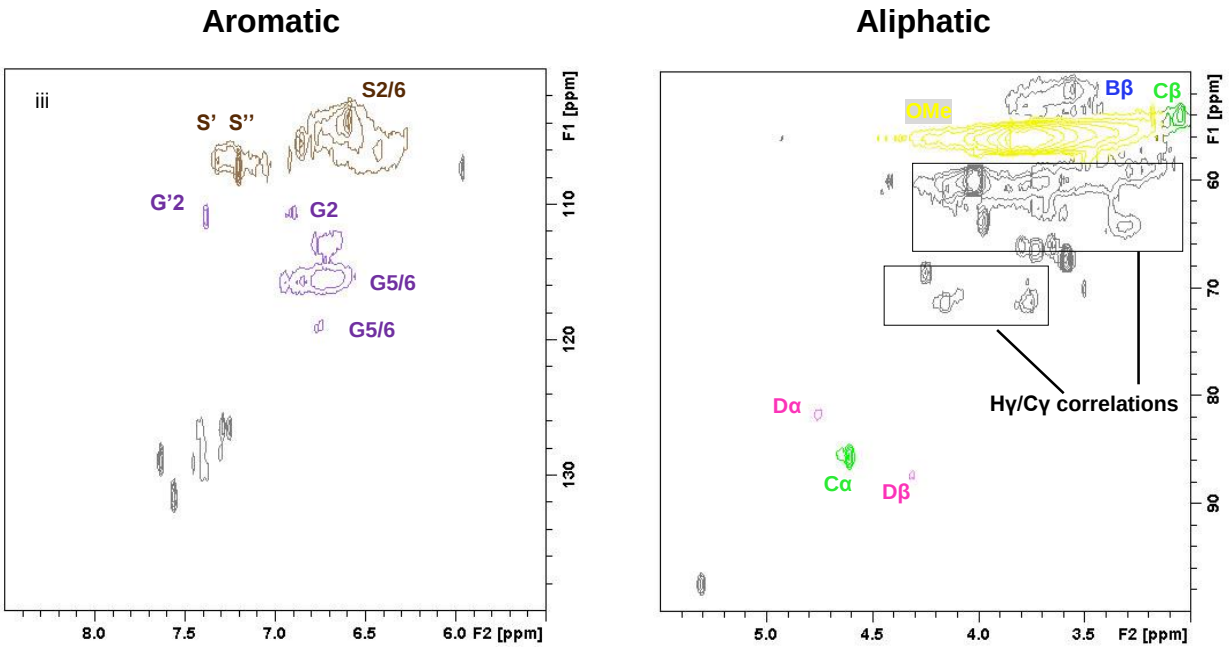

Figure 4.7 q-HSQC of the reaction of NVO lignin using catalyst [**3**]; 10 wt. % [**3**]. For all runs: solvent = 8:1 (v/v) EtOAc/THF; temperature = 80 ºC; sealed vial under atmospheric pressure of air; reaction time = 24 h.

Catalyst [**5**] cleaved the major structural units **A**, **B**, **C** and **D** at the same time increased the oxidized syringyl **S** and guaiacyl **G** units ((**S''** + **S'**)/**S2/6** to 0.82 from 0.76) (Figure 4.8). Nevertheless, the control experiment (without 4-acetamido-TEMPO) showed that the depolymerization of NVO lignin could still occur reasonably at these conditions. Contrary to what previous reports showed,[33] we did not observe the oxidized **A'** units under these conditions.

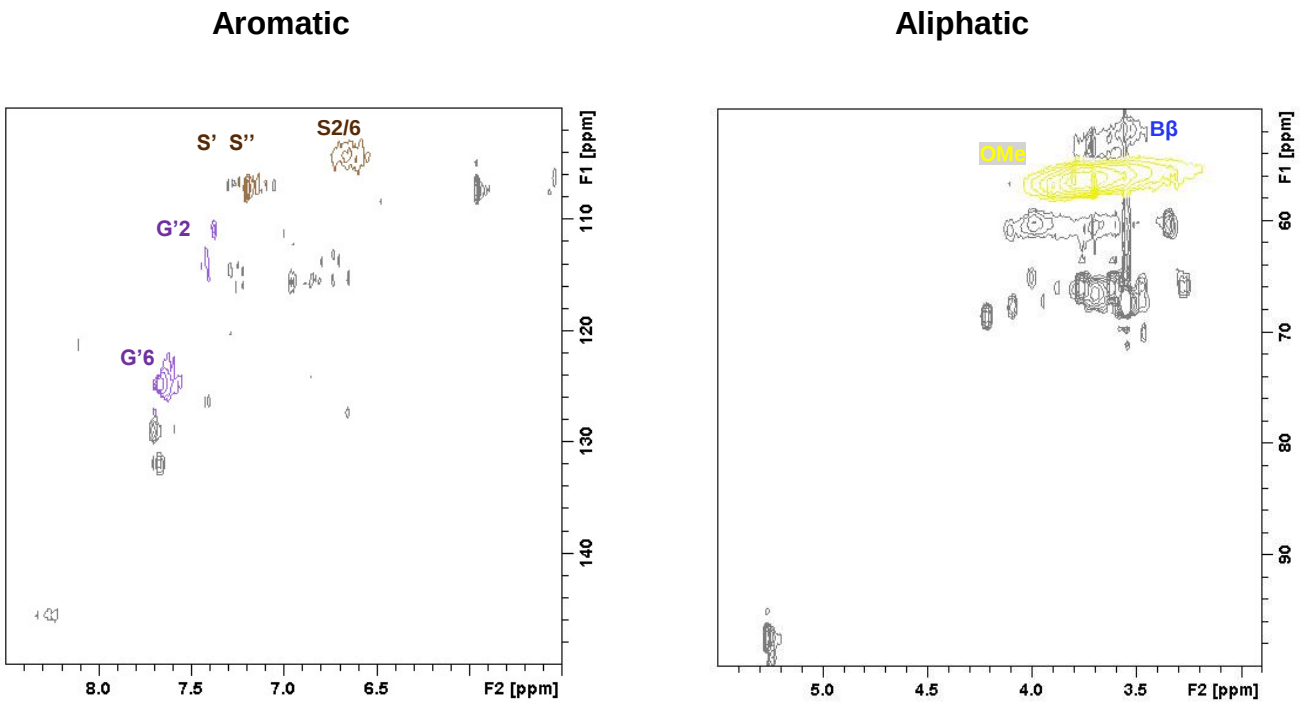

Figure 4.8 q-HSQC of the reaction of NVO lignin with the metal-free system [**5**]; 5 wt. % 4-acetamido-TEMPO, 10 wt. % HNO_3 (70%), 10 wt. % HCl (37%). For all runs: solvent = 19:1 (v/v) CH_3CN/H_2O; temperature = 65 ^oC; pressure of synthetic air = 8.2 atm; reaction time = 24 h.

Catalyst [**15**] was not able to oxidize NVO lignin (Figure 4.9), all of the major structural units in the oxygenated aliphatic region still remained intact and the aromatic region remained similar to NVO lignin spectrum. The ratio of (**S''** + **S'**)/**S2/6** and **G'2**/**G2** were found to be almost identical to the original NVO lignin: (**S''** + **S'**)/**S2/6** = 0.09 and, **G'2**/**G2** = 0.02.

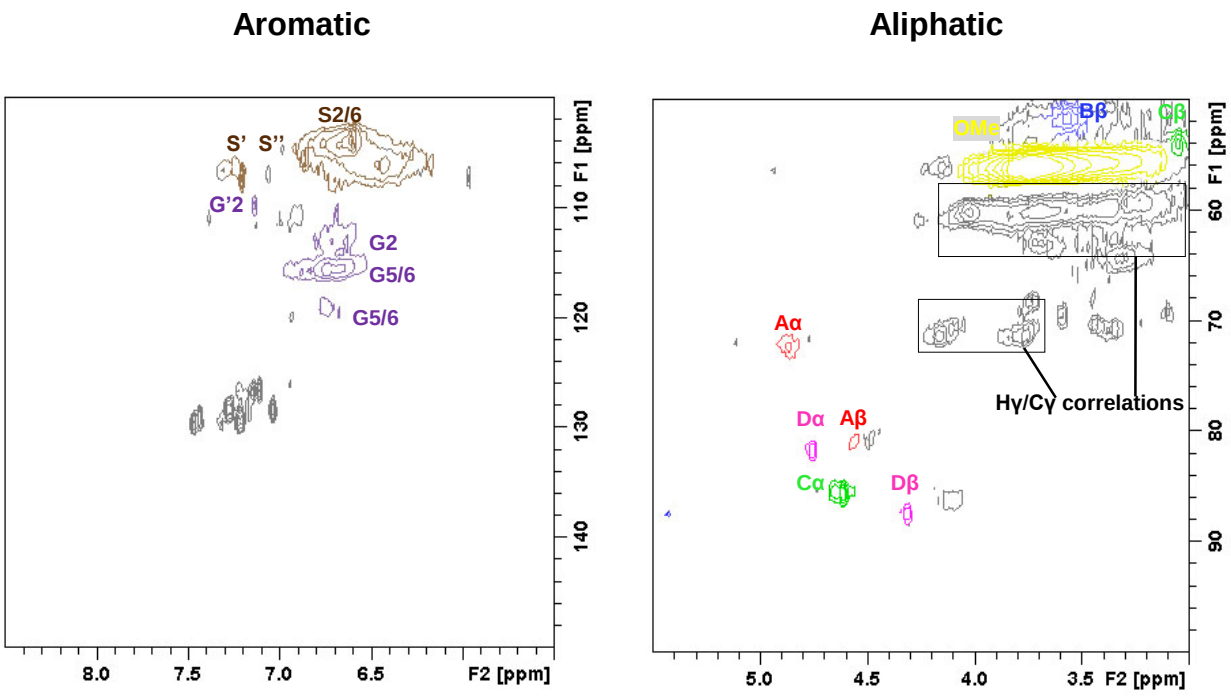

Figure 4.9 q-HSQC of the reaction of NVO lignin using 10 wt. % [**15**] and 100 wt. % pyridine. For all runs: solvent = 1:1 (v/v) MeOH/DMSO; temperature = 100 ^{o}C; pressure of synthetic air = 8.2 atm; reaction time = 18 h.

Chapter 5 – Conclusions and Future Direction

In conclusion, both molybdenum and hypervalent iodine systems developed herein are more efficient for oxidation of β-1 **A** and β-O-4 **C** model compounds than previously reported catalysts. Specifically, for the β-1 model compound **A**, the Cp*MoO_2Cl [**8**]/SPC/Adogen®464 system in benzonitrile was able to generate methyl benzoate as the major product in almost full conversion, whereas in CD_3CN the ketone product, benzoin methyl ether, dominates. The hydrogen peroxide system Cp*MoO_2Cl [**8**]/H_2O_2 system was found to be the most efficient for benzaldehyde formation amongst the molybdenum catalysts studied. From the preliminary mechanistic studies of Cp*MoO_2Cl [**8**]/H_2O_2 system, the presence of hydrogen peroxide was shown to be crucial for obtaining C_α-C_β bond cleavage products, benzaldehyde and methyl benzoate. Benzoin methyl ether may be the intermediate for this oxidative cleavage of substrate **A**. Amongst all the metallosalen complexes studied herein, Jacobsen's reagent/TBHP was the most effective catalyst for oxidation of substrate **A .**

Lewis-acid additives in molybdenum-based catalytic systems have no significant effect on improving the catalytic efficiency/selectivity of oxidation of lignin model compounds. Interestingly, Meinwald rearrangement products were observed when a catalytic amount of Lewis acid was used along with the model substrate **A**, forming 1-methoxy-2,2-diphenylethene and another aldehyde product - α-phenyl benzeneacetaldehyde. On the other hand, hypervalent iodine/Lewis acid systems were able to produce benzaldehyde as the major product with almost full conversion; of these reactions, iodosonitrobenzene/$Yb(OTf)_3$ provided the best selectivity for benzaldehyde (90%). The best reactivity/selectivity was achieved with iodosobenzene/Lewis acid.

The aforementioned catalytic systems are generally inactive for other linkage model compounds, such as β-O-4 **B**, β-5 **D** and 5-5' **E**, except for β-O-4 **C**. β-O-4 substrate **C** can be transformed to the ketone 2-phenoxyacetophenone with the SPC/Adogen®464 system. The peroxide-based systems performed poorly for the other linkage models, other than substrate **A**. The hypervalent iodine catalytic systems surpass the existing copper and vanadium systems in selectivity and reactivity for oxidation of

model compound **C**. Conversion of 77% with 70% of benzaldehyde was achieved with this system.

In chapter 4, oxidation of lignin extracts, NVO lignin, was investigated with copper and vanadium catalytic systems. Vanadium [**1**] and [**2**] system require a base for the said oxidative transformation on account of the base-assisted redox deprotonation mechanism. Amongst these, vanadium catalyst [**2**] was found to be the most active according to q-HSQC and GPC.

In summary, the hypervalent iodine outperformed the aforementioned copper and vanadium catalytic systems for monomeric model substrates in reactivity (shorter reaction time) and selectivity (for benzaldehyde) and can be a promising “green” catalytic system for oxidative lignin depolymerization. Along with the future research on its reactivity/selectivity for the oxidation of the dimeric substrate **F** and **G**, the optimized system for the real lignin extract can be developed. The analysis of its reactivity and selectivity on the real lignin could then be examined with 2D-NMR and GPC techniques as described in chapter 4.

Appendix A. X-ray data

Table 1 X-ray Crystal Data and Refinement Parameters for $CpMo(CO)_3$(1-ethynyl-3,5 bis-(CF_3)bz) [**10b**].

Empirical formula	C18 H8 F6 Mo O3
Formula weight	482.18
Temperature	200(2) K
Wavelength	0.71073 Å
Crystal system	Triclinic
Space group	P -1
Unit cell dimensions	a = 8.1393(2) Å b =11.2409(3) Å c = 11.3036(3) Å α= 108.0742(14)°. β= 110.5585(14)°. γ= 94.0559(14)°.
Volume	901.60(4) $Å^3$
Z	2
Density (calculated)	1.776 Mg/m^3
Absorption coefficient	0.803 mm^{-1}
F(000)	472
Crystal size	0.300 x 0.120 x 0.020 mm^3
Theta range for data collection	1.946 to 28.336°.
Index ranges	-10<=h<=10, -14<=k<=14, -15<=l<=13
Reflections collected	10071
Independent reflections	4379 [R(int) = 0.0197]
Completeness to theta = 25.242°	98.8 %
Absorption correction	Semi-empirical from equivalents
Max. and min. transmission	0.7457 and 0.6860
Refinement method	Full-matrix least-squares on F^2
Data / restraints / parameters	4379 / 348 / 307
Goodness-of-fit on F^2	0.928
Final R indices [I>2sigma(I)]	R1 = 0.0246, wR2 = 0.0622
R indices (all data)	R1 = 0.0301, wR2 = 0.0653
Extinction coefficient	n/a
Largest diff. peak and hole	0.471 and -0.315 $e.Å^{-3}$

Table 2 Bond lengths [Å] and angles [°] for $CpMo(CO)_3$(1-ethynyl-3,5 bis-(CF_3)bz) [**10b**].

Mo(1)-C(18)	2.001(2)
Mo(1)-C(16)	2.001(2)
Mo(1)-C(17)	2.003(2)
Mo(1)-C(6)	2.1382(19)
Mo(1)-C(4)	2.296(2)
Mo(1)-C(3)	2.298(2)
Mo(1)-C(5)	2.335(2)
Mo(1)-C(2)	2.3442(19)
Mo(1)-C(1)	2.365(2)
F(1)-C(14)	1.327(4)
F(2)-C(14)	1.313(4)
F(3)-C(14)	1.344(4)
F(1')-C(14)	1.345(10)
F(2')-C(14)	1.294(9)
F(3')-C(14)	1.304(11)
F(4)-C(15)	1.325(5)
F(5)-C(15)	1.252(4)
F(6)-C(15)	1.358(5)
F(4')-C(15)	1.344(6)
F(5')-C(15)	1.293(6)
F(6')-C(15)	1.247(5)
O(1)-C(16)	1.134(3)
O(2)-C(17)	1.140(2)
O(3)-C(18)	1.133(3)
C(1)-C(2)	1.408(3)
C(1)-C(5)	1.413(3)
C(2)-C(3)	1.412(3)
C(3)-C(4)	1.424(4)
C(4)-C(5)	1.404(4)
C(6)-C(7)	1.206(3)
C(7)-C(8)	1.430(3)
C(8)-C(9)	1.396(3)
C(8)-C(13)	1.396(3)

C(9)-C(10)	1.386(3)
C(10)-C(11)	1.378(3)
C(10)-C(14)	1.498(3)
C(11)-C(12)	1.389(3)
C(12)-C(13)	1.380(3)
C(12)-C(15)	1.498(3)

C(18)-Mo(1)-C(16)	110.41(9)
C(18)-Mo(1)-C(17)	77.91(9)
C(16)-Mo(1)-C(17)	79.38(8)
C(18)-Mo(1)-C(6)	73.90(8)
C(16)-Mo(1)-C(6)	73.65(8)
C(17)-Mo(1)-C(6)	130.50(8)
C(18)-Mo(1)-C(4)	104.59(9)
C(16)-Mo(1)-C(4)	141.08(9)
C(17)-Mo(1)-C(4)	92.07(9)
C(6)-Mo(1)-C(4)	133.93(9)
C(18)-Mo(1)-C(3)	139.02(9)
C(16)-Mo(1)-C(3)	105.43(9)
C(17)-Mo(1)-C(3)	90.04(8)
C(6)-Mo(1)-C(3)	136.69(8)
C(4)-Mo(1)-C(3)	36.10(9)
C(18)-Mo(1)-C(5)	95.47(9)
C(16)-Mo(1)-C(5)	149.01(8)
C(17)-Mo(1)-C(5)	124.03(9)
C(6)-Mo(1)-C(5)	98.67(9)
C(4)-Mo(1)-C(5)	35.29(10)
C(3)-Mo(1)-C(5)	59.36(9)
C(18)-Mo(1)-C(2)	153.34(9)
C(16)-Mo(1)-C(2)	92.80(8)
C(17)-Mo(1)-C(2)	120.64(8)
C(6)-Mo(1)-C(2)	101.62(8)
C(4)-Mo(1)-C(2)	59.07(8)
C(3)-Mo(1)-C(2)	35.41(8)
C(5)-Mo(1)-C(2)	58.71(8)
C(18)-Mo(1)-C(1)	119.61(9)

C(16)-Mo(1)-C(1)	114.33(8)
C(17)-Mo(1)-C(1)	147.50(8)
C(6)-Mo(1)-C(1)	81.95(8)
C(4)-Mo(1)-C(1)	58.28(8)
C(3)-Mo(1)-C(1)	58.45(8)
C(5)-Mo(1)-C(1)	34.98(8)
C(2)-Mo(1)-C(1)	34.78(8)
C(2)-C(1)-C(5)	108.8(2)
C(2)-C(1)-Mo(1)	71.79(11)
C(5)-C(1)-Mo(1)	71.33(12)
C(1)-C(2)-C(3)	107.7(2)
C(1)-C(2)-Mo(1)	73.43(11)
C(3)-C(2)-Mo(1)	70.49(11)
C(2)-C(3)-C(4)	107.6(2)
C(2)-C(3)-Mo(1)	74.10(12)
C(4)-C(3)-Mo(1)	71.90(12)
C(5)-C(4)-C(3)	108.4(2)
C(5)-C(4)-Mo(1)	73.85(13)
C(3)-C(4)-Mo(1)	72.00(12)
C(4)-C(5)-C(1)	107.4(2)
C(4)-C(5)-Mo(1)	70.86(13)
C(1)-C(5)-Mo(1)	73.69(12)
C(7)-C(6)-Mo(1)	177.71(18)
C(6)-C(7)-C(8)	175.0(2)
C(9)-C(8)-C(13)	118.15(17)
C(9)-C(8)-C(7)	122.07(18)
C(13)-C(8)-C(7)	119.76(18)
C(10)-C(9)-C(8)	120.53(17)
C(11)-C(10)-C(9)	121.12(17)
C(11)-C(10)-C(14)	119.64(18)
C(9)-C(10)-C(14)	119.24(18)
C(10)-C(11)-C(12)	118.50(18)
C(13)-C(12)-C(11)	121.10(19)
C(13)-C(12)-C(15)	119.11(19)
C(11)-C(12)-C(15)	119.79(19)
C(12)-C(13)-C(8)	120.60(18)

F(2')-C(14)-F(3')	108.4(9)
F(2)-C(14)-F(1)	108.0(4)
F(2)-C(14)-F(3)	106.8(3)
F(1)-C(14)-F(3)	104.3(3)
F(2')-C(14)-F(1')	106.1(8)
F(3')-C(14)-F(1')	102.5(10)
F(2')-C(14)-C(10)	113.9(7)
F(3')-C(14)-C(10)	114.7(11)
F(2)-C(14)-C(10)	113.6(3)
F(1)-C(14)-C(10)	111.0(4)
F(3)-C(14)-C(10)	112.6(3)
F(1')-C(14)-C(10)	110.4(9)
F(6')-C(15)-F(5')	110.2(5)
F(5)-C(15)-F(4)	109.6(5)
F(6')-C(15)-F(4')	105.3(5)
F(5')-C(15)-F(4')	105.7(6)
F(5)-C(15)-F(6)	104.5(5)
F(4)-C(15)-F(6)	101.7(4)
F(6')-C(15)-C(12)	113.6(3)
F(5)-C(15)-C(12)	116.5(3)
F(5')-C(15)-C(12)	110.8(4)
F(4)-C(15)-C(12)	111.9(4)
F(4')-C(15)-C(12)	110.8(4)
F(6)-C(15)-C(12)	111.5(3)
O(1)-C(16)-Mo(1)	176.27(18)
O(2)-C(17)-Mo(1)	178.60(19)
O(3)-C(18)-Mo(1)	178.2(2)

Symmetry transformations used to generate equivalent atoms:

Table 3 Crystal Structure Data for [Mo(O)(μ-O)(Mesnacnac)]$_2$ [**9**].

Empirical formula	C23 H29 Mo N2 O2
Formula weight	461.42
Temperature	200(2) K
Wavelength	0.71073 Å
Crystal system	Monoclinic
Space group	C 2
Unit cell dimensions	a = 20.1159(5) Å α= 90°. b = 8.8781(2) Å β= 121.9634(10)°. c = 14.5012(4) Å γ = 90°.
Volume	2197.14(10) Å^3
Z	4
Density (calculated)	1.395 Mg/m^3
Absorption coefficient	0.617 mm^{-1}
F(000)	956
Crystal size	0.180 x 0.140 x 0.110 mm^3
Theta range for data collection	1.655 to 28.335°.
Index ranges	-26<=h<=26, -11<=k<=11, -19<=l<=17
Reflections collected	12316
Independent reflections	5070 [R(int) = 0.0120]
Completeness to theta = 25.242°	98.9 %
Absorption correction	Semi-empirical from equivalents
Max. and min. transmission	0.935 and 0.897
Refinement method	Full-matrix least-squares on F^2
Data / restraints / parameters	5070 / 1 / 254
Goodness-of-fit on F^2	1.038
Final R indices [I>2sigma(I)]	R1 = 0.0197, wR2 = 0.0547
R indices (all data)	R1 = 0.0202, wR2 = 0.0552
Absolute structure parameter	0.38(3)
Extinction coefficient	n/a
Largest diff. peak and hole	0.366 and -0.395 e.Å^{-3}

Table 4 Bond lengths [Å] and angles [°] for [Mo(O)(μ-O)(Mesnacnac)]$_2$ [**9**].

Mo(1)-O(1)	1.686(2)
Mo(1)-O(2)	1.9066(17)
Mo(1)-O(2)#1	1.9647(18)
Mo(1)-N(2)	2.100(2)
Mo(1)-N(1)	2.142(2)
Mo(1)-Mo(1)#1	2.5620(3)
O(2)-Mo(1)#1	1.9646(18)
N(1)-C(1)	1.325(3)
N(1)-C(6)	1.450(3)
N(2)-C(3)	1.342(3)
N(2)-C(15)	1.445(3)
C(1)-C(2)	1.396(4)
C(1)-C(4)	1.522(4)
C(2)-C(3)	1.390(4)
C(3)-C(5)	1.508(4)
C(6)-C(11)	1.391(4)
C(6)-C(7)	1.394(4)
C(7)-C(8)	1.400(5)
C(7)-C(12)	1.509(5)
C(8)-C(9)	1.387(7)
C(9)-C(10)	1.373(7)
C(9)-C(13)	1.520(3)
C(10)-C(11)	1.387(5)
C(11)-C(14)	1.498(5)
C(15)-C(16)	1.394(4)
C(15)-C(20)	1.404(4)
C(16)-C(17)	1.398(4)
C(16)-C(21)	1.505(6)
C(17)-C(18)	1.382(6)
C(18)-C(19)	1.375(5)
C(18)-C(22)	1.510(5)
C(19)-C(20)	1.399(4)
C(20)-C(23)	1.497(4)

O(1)-Mo(1)-O(2)	119.51(9)
O(1)-Mo(1)-O(2)#1	106.14(9)
O(2)-Mo(1)-O(2)#1	90.25(8)
O(1)-Mo(1)-N(2)	110.15(9)
O(2)-Mo(1)-N(2)	129.74(8)
O(2)#1-Mo(1)-N(2)	82.98(8)
O(1)-Mo(1)-N(1)	95.25(8)
O(2)-Mo(1)-N(1)	83.20(7)
O(2)#1-Mo(1)-N(1)	158.07(8)
N(2)-Mo(1)-N(1)	85.21(8)
O(1)-Mo(1)-Mo(1)#1	102.92(7)
O(2)-Mo(1)-Mo(1)#1	49.54(5)
O(2)#1-Mo(1)-Mo(1)#1	47.60(5)
N(2)-Mo(1)-Mo(1)#1	126.69(6)
N(1)-Mo(1)-Mo(1)#1	132.40(6)
Mo(1)-O(2)-Mo(1)#1	82.86(7)
C(1)-N(1)-C(6)	116.7(2)
C(1)-N(1)-Mo(1)	122.47(17)
C(6)-N(1)-Mo(1)	120.07(16)
C(3)-N(2)-C(15)	115.9(2)
C(3)-N(2)-Mo(1)	123.07(17)
C(15)-N(2)-Mo(1)	120.98(16)
N(1)-C(1)-C(2)	123.8(2)
N(1)-C(1)-C(4)	119.9(2)
C(2)-C(1)-C(4)	116.3(2)
C(3)-C(2)-C(1)	126.9(2)
N(2)-C(3)-C(2)	124.3(2)
N(2)-C(3)-C(5)	119.6(2)
C(2)-C(3)-C(5)	116.1(2)
C(11)-C(6)-C(7)	120.5(2)
C(11)-C(6)-N(1)	119.3(3)
C(7)-C(6)-N(1)	120.1(3)
C(6)-C(7)-C(8)	118.7(3)
C(6)-C(7)-C(12)	122.1(3)
C(8)-C(7)-C(12)	119.1(3)
C(9)-C(8)-C(7)	121.3(4)

C(10)-C(9)-C(8)	118.2(2)
C(10)-C(9)-C(13)	122.0(5)
C(8)-C(9)-C(13)	119.8(5)
C(9)-C(10)-C(11)	122.5(4)
C(10)-C(11)-C(6)	118.7(3)
C(10)-C(11)-C(14)	120.5(3)
C(6)-C(11)-C(14)	120.8(3)
C(16)-C(15)-C(20)	121.6(3)
C(16)-C(15)-N(2)	120.9(3)
C(20)-C(15)-N(2)	117.4(2)
C(17)-C(16)-C(15)	117.6(3)
C(17)-C(16)-C(21)	121.4(3)
C(15)-C(16)-C(21)	121.0(3)
C(18)-C(17)-C(16)	122.2(3)
C(17)-C(18)-C(19)	118.7(3)
C(17)-C(18)-C(22)	121.3(4)
C(19)-C(18)-C(22)	120.0(4)
C(18)-C(19)-C(20)	122.0(4)
C(15)-C(20)-C(19)	117.8(3)
C(15)-C(20)-C(23)	121.0(3)
C(19)-C(20)-C(23)	121.2(3)

Symmetry transformations used to generate equivalent atoms:

#1 -x+1,y,-z+1

Appendix B. Infrared spectra

Figure B1 FT-IR of possible in-situ generation of [Cp*Mo(*u*-O)O(O)]$_2$.

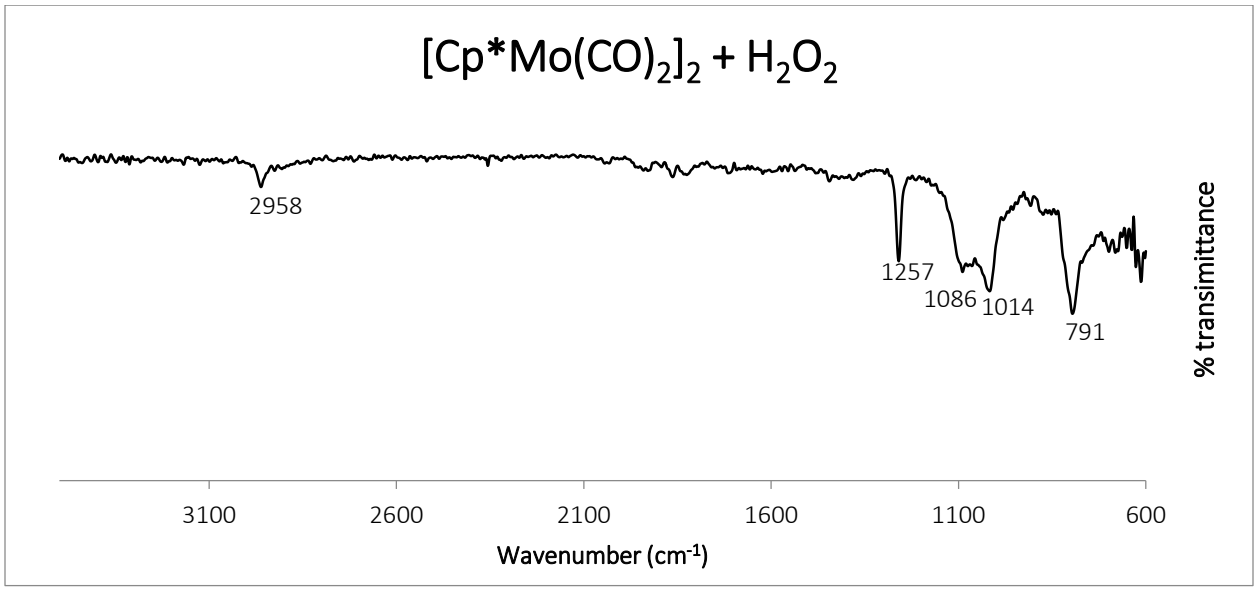

Figure B2 FT-IR of Cp*Mo(=O)(η^2-O$_2$)Cl from Roesky's method.[66]

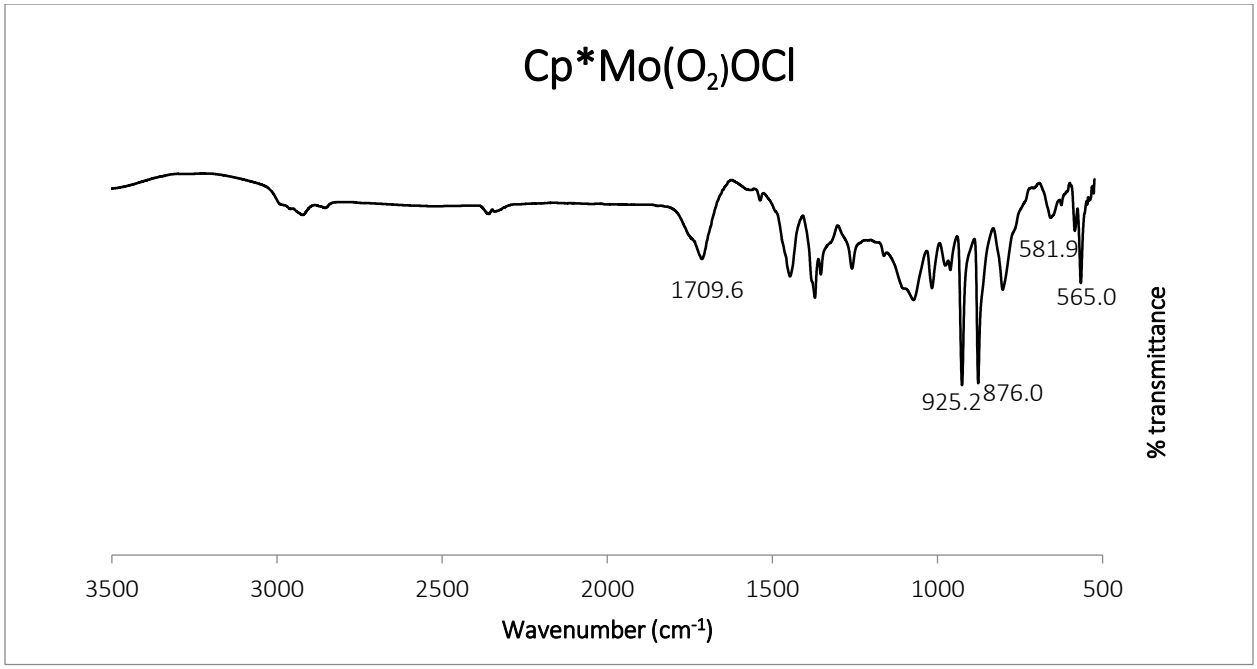

Figure B3 FT-IR of Cp*Mo(=O)$_2$Cl from Bottomley method.[46]

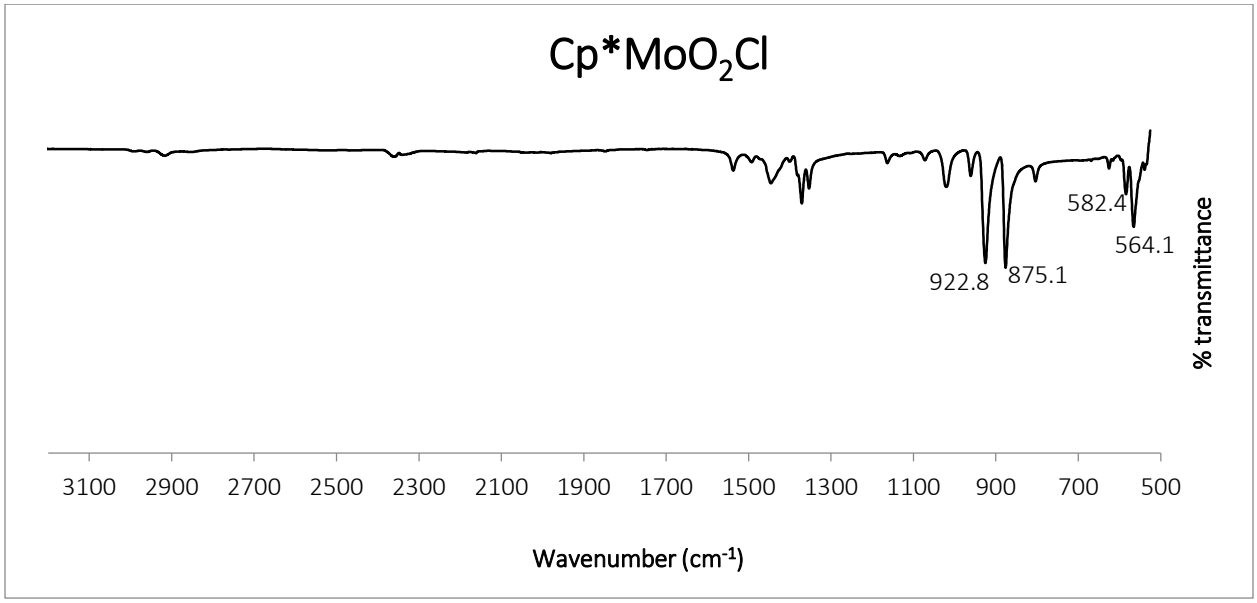

Appendix C. NMR spectra

Figure C1 Isolated benzoic acid from the white precipitate of SPC/Adogen®464 system generated from oxidation of substrate **A.**

^{1}H-NMR (300 MHz, $CDCl_3$):

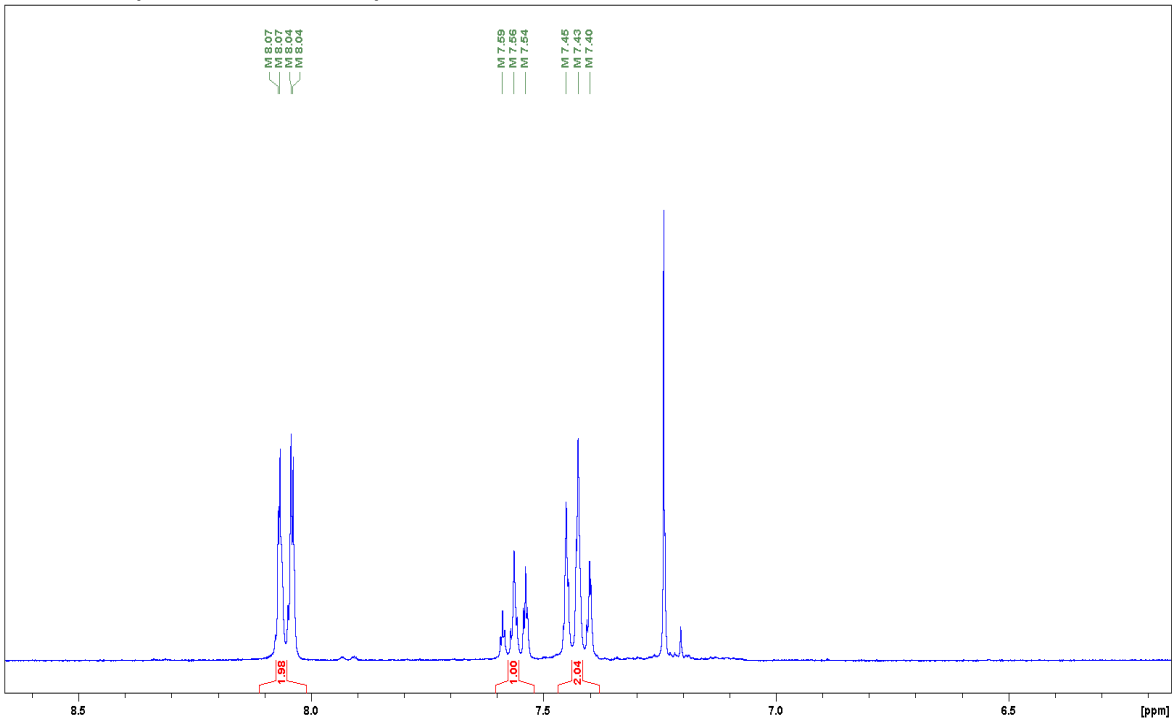

^{13}C[^{1}H]-NMR (100 MHz, $CDCl_3$):

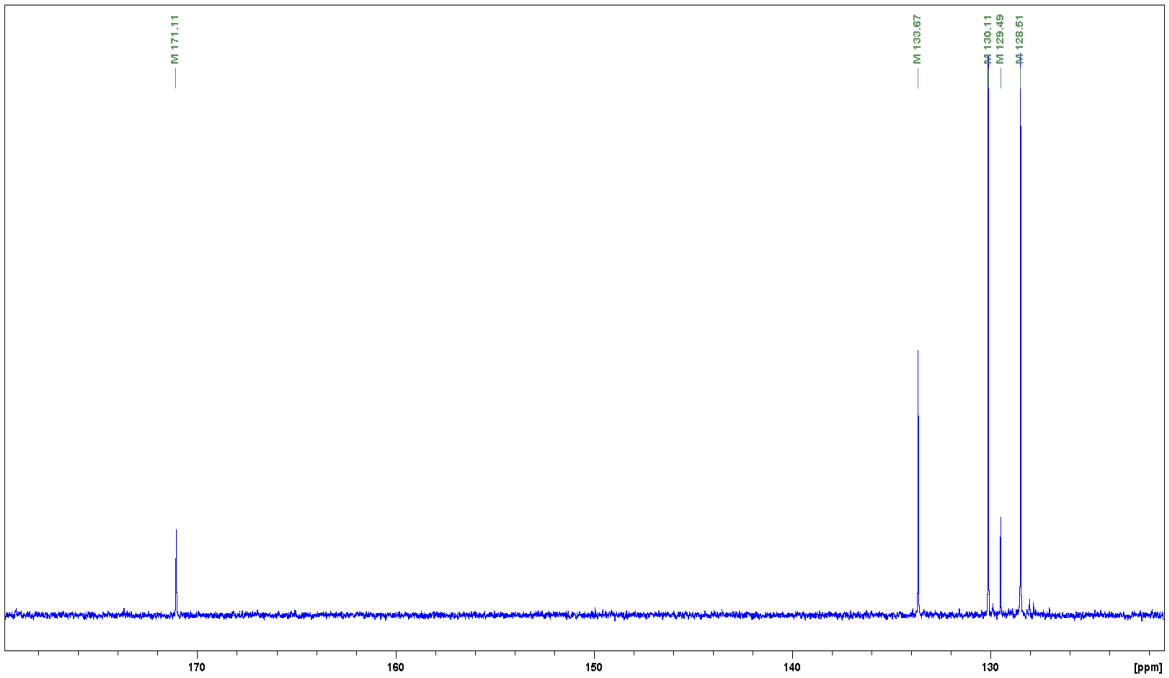

Appendix C2 Reaction of substrate **A** with catalytic amount of $AlCl_3$ in CD_3CN.

^{1}H-NMR (300 MHz, CD_3CN):

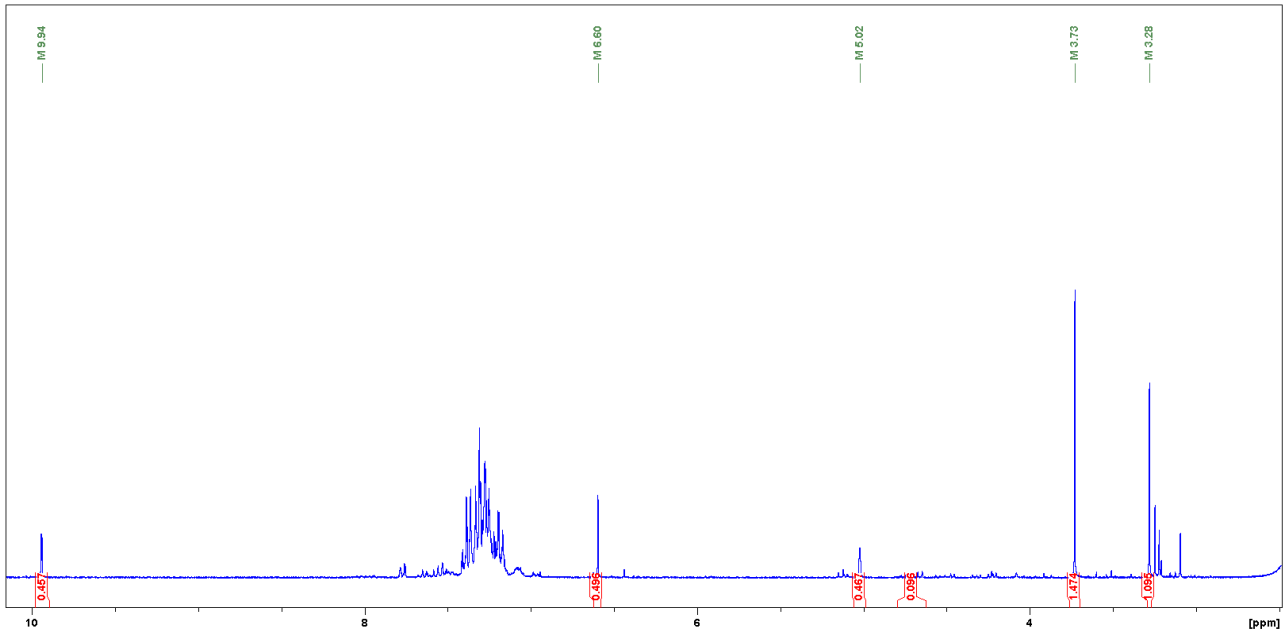

^{13}C[^{1}H]-NMR (100 MHz, CD_3CN):

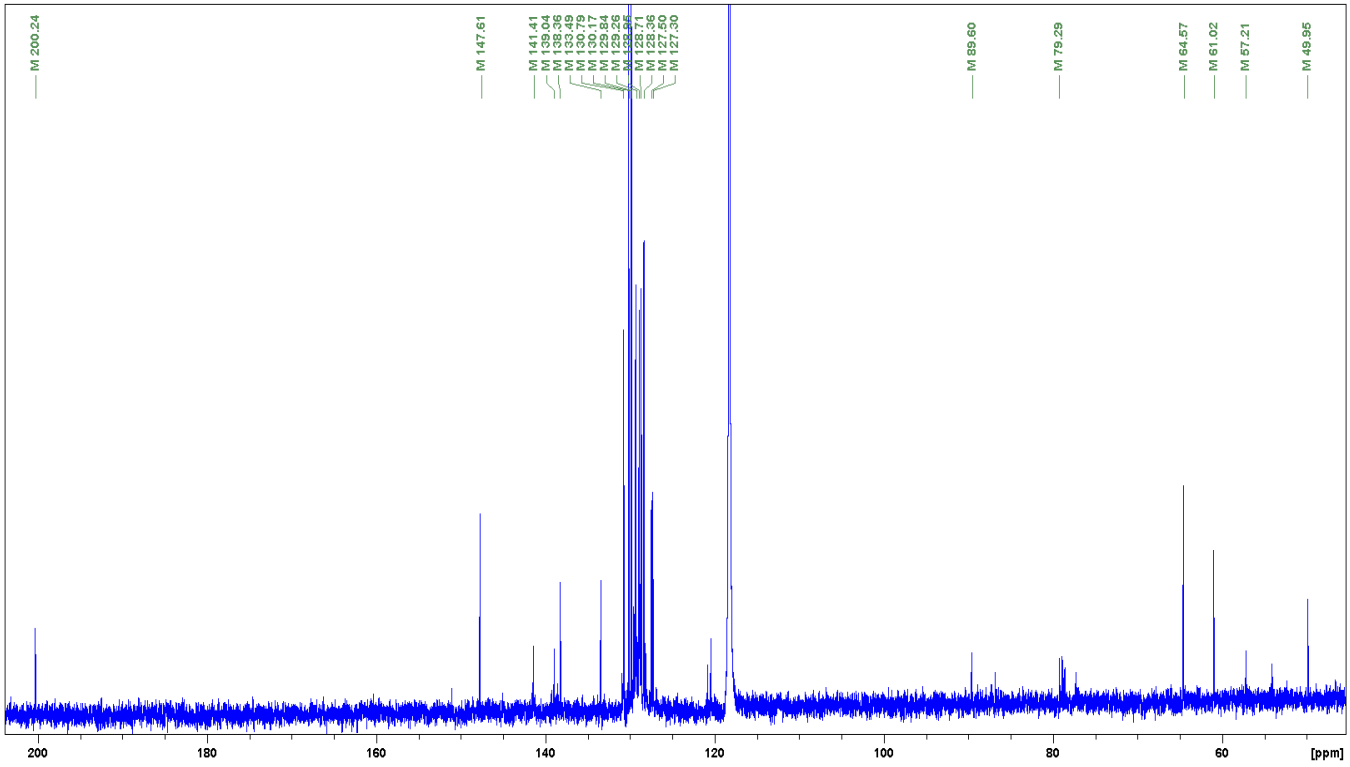

Appendix C3 Reaction of stilbene oxide with $AlCl_3$ (0.1 equiv.) in CD_3CN.

^{1}H-NMR (300 MHz, CD_3CN):

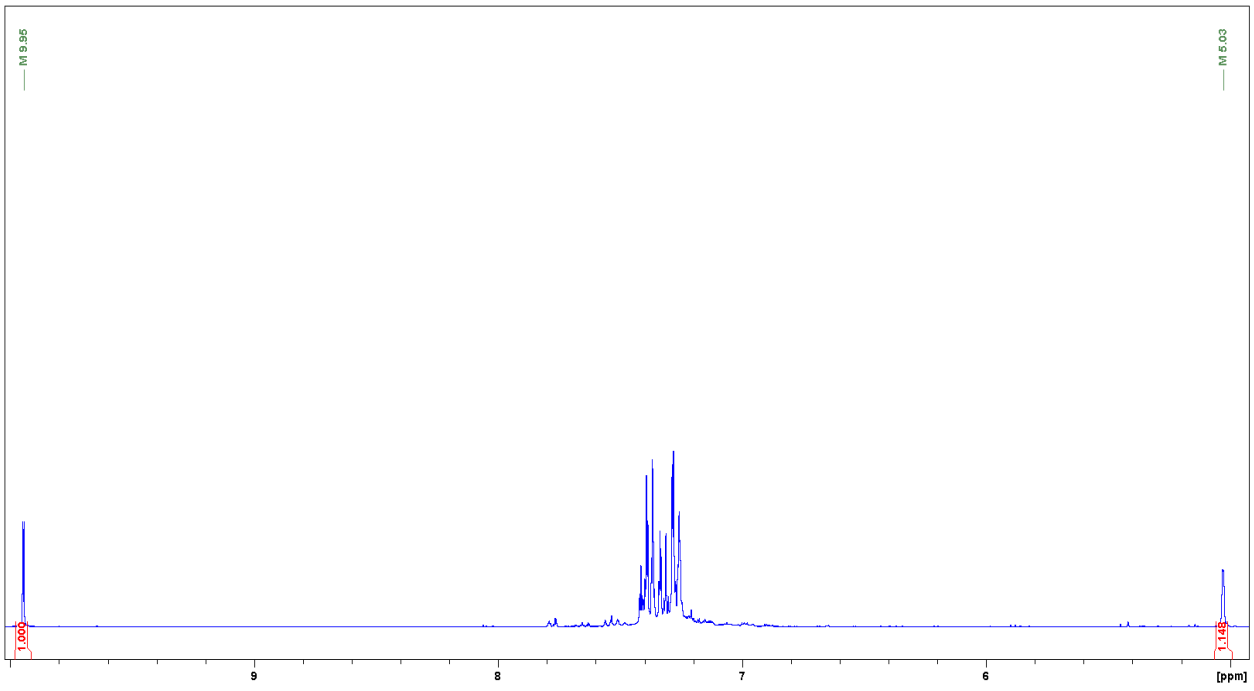

Appendix C4 Reaction of stilbene oxide with $AlCl_3$ (0.1 equiv.) and MeOH (1 equiv.) in CD_3CN.

^{1}H-NMR (300 MHz, $CDCl_3$):

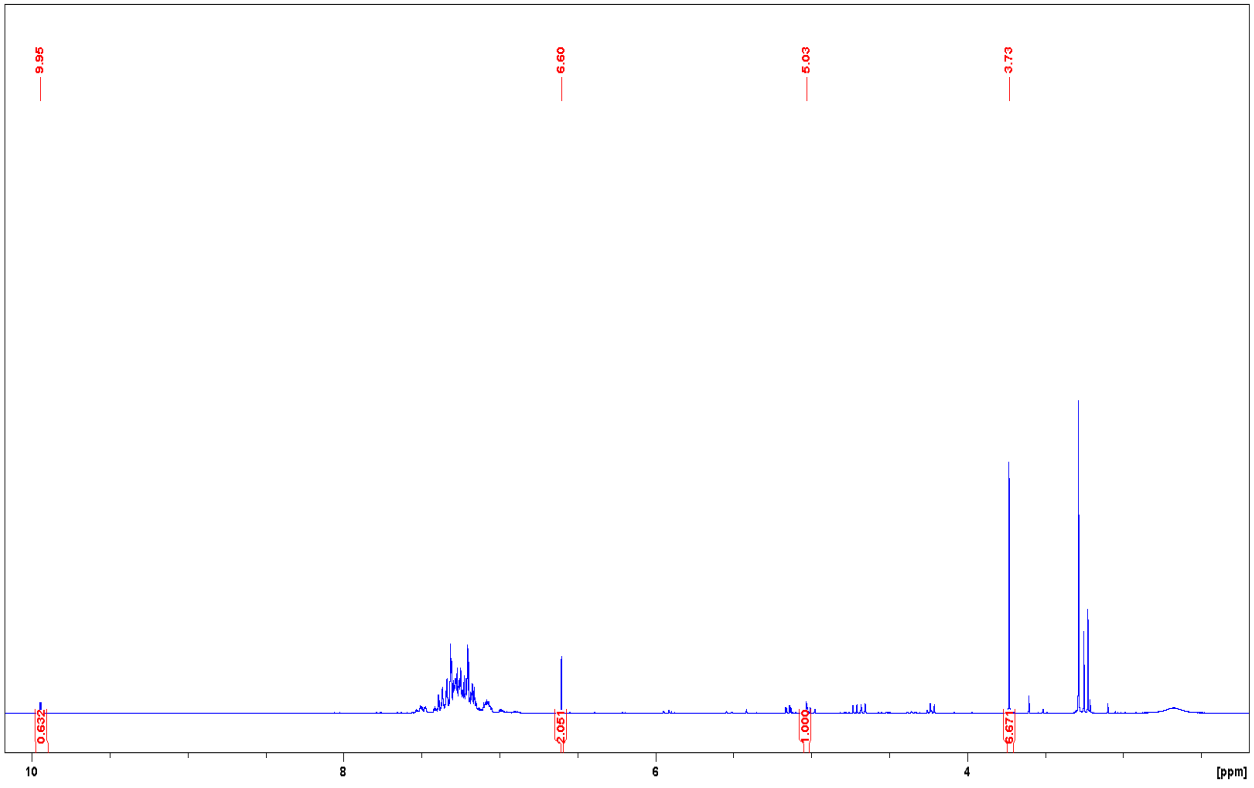

Appendix C5 Representative NMR spectrum of oxidation of model substrate **A** with iodine complex [**20a**]/Yb(OTf)$_3$ system in $CDCl_3$ (after 17 hours):

^{1}H-NMR (300 MHz, $CDCl_3$):

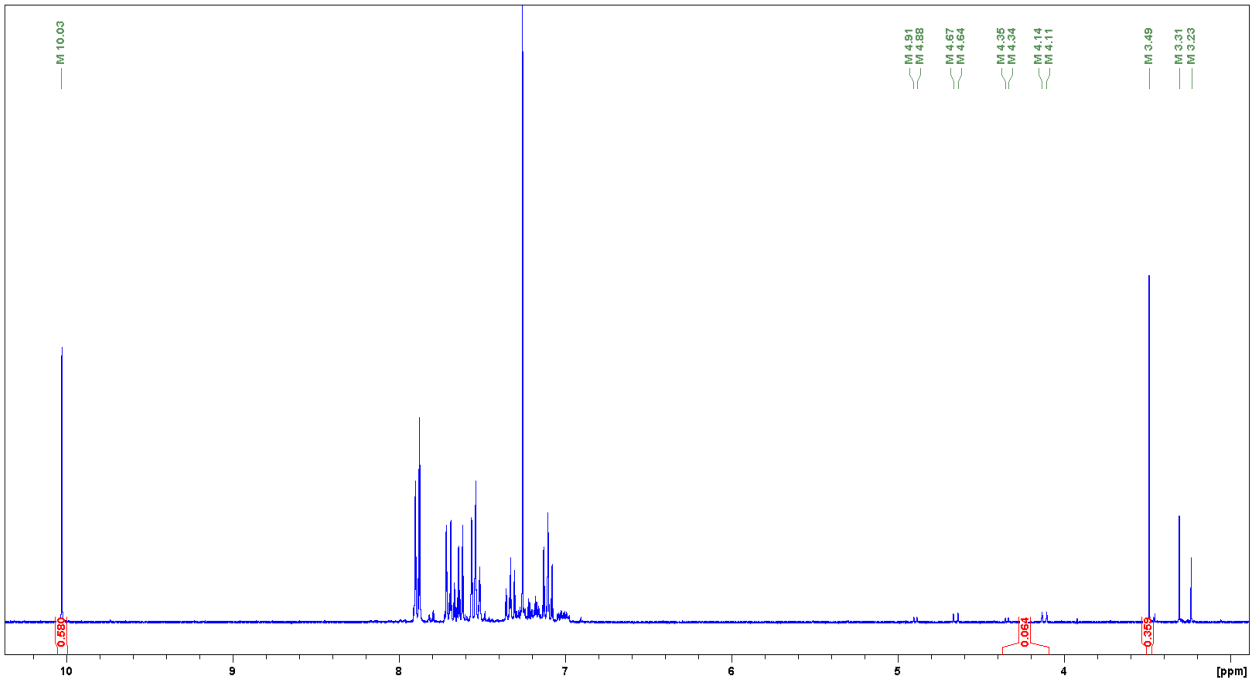

Appendix C6 Representative GC-MS chromatogram of oxidation of model substrate **A** with iodine complex [**20b**]/Yb(OTf)$_3$ system in CD_3CN (after 17 hours):

GC-MS:

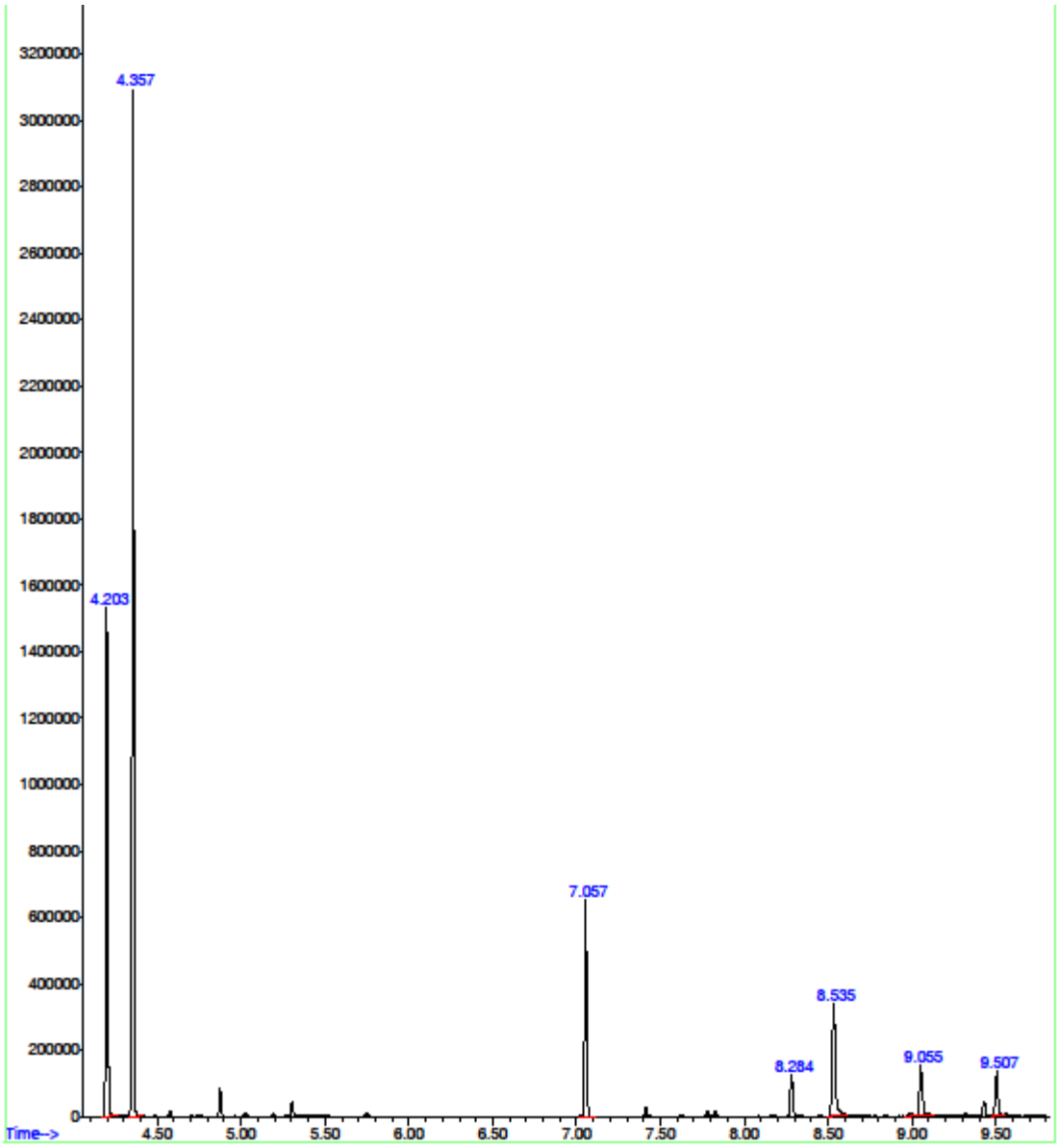

Benzaldehyde = 4.203 min; iodoperfluorobenzene = 4.357 min; 1,3,5-tri-*tert*-butylbenzene (TTB internal standard) = 7.057 min; α-phenyl benzeneacetaldehyde = 8.535 min; benzil = 9.507 min; starting material = 8.284 and 9.055 min (its decomposition product).

References

(1) Zakzeski, J.; Bruijnincx, P. C. A.; Jongerius, A. L.; Weckhuysen, B. M. *Chem. Rev.* **2010**, *110*, 3552.
(2) Joffres, B.; Laurenti, D.; Charon, N.; Daudin, A.; Quignard, A.; Geantet, C. *Oil Gas Sci. Technol. – Rev. IFP Energies nouvelles* **2013**, *68*, 753.
(3) Stewart, D. *Ind. Crop. Prod.* **2008**, *27*, 202.
(4) Yu, Y.-X.; Xu, Y.; Wang, T.-J.; Ma, L.-L.; Zhang, Q.; Zhang, X.-H.; Zhang, X. *J. Fuel Chem. Technol.* **2013**, *41*, 443.
(5) Rowe, D. J. In *Chemistry and Technology of Flavors and Fragrances*; Blackwell Publishing Ltd.: 2004, p 56.
(6) Pandey, M. P.; Kim, C. S. *Chem. Eng. Technol.* **2011**, *34*, 29.
(7) Wu, G.; Heitz, M.; Chornet, E. *Ind. Eng. Chem. Res.* **1994**, *33*, 718.
(8) Sklarz, B. *Quart. Rev. Chem. Soc.* **1967**, *21*, 3.
(9) Yang, L.; Li, Y.; Savage, P. E. *Ind. Eng. Chem. Res.* **2014**, *53*, 2633.
(10) Huo, W.; Li, W.; Zhang, M.; Fan, W.; Chang, H.-m.; Jameel, H. *Catal. Lett.* **2014**, *144*, 1159.
(11) Labat, G.; Meunier, B. *J. Org. Chem.* **1989**, *54*, 5008.
(12) Shimada, M.; Habe, T.; Umezawa, T.; Higuchi, T.; Okamoto, T. *Biochem. Biophys. Res. Commun.* **1984**, *122*, 1247.
(13) Zhu, W.; Ford, W. T. *J. Mol. Catal.* **1993**, *78*, 367.
(14) Robinson, M. J.; Wright, L. J.; Suckling, I. D. *J. Wood Chem. Techonol.* **2000**, *20*, 357.
(15) Bozell, J. J.; Hames, B. R.; Dimmel, D. R. *J. Org. Chem.* **1995**, *60*, 2398.
(16) Drago, R. S.; Corden, B. B.; Barnes, C. W. *J. Am. Chem. Soc.* **1986**, *108*, 2453.
(17) Sippola, V.; Krause, O.; Vuorinen, T. *J. Wood Chem. Techonol.* **2004**, *24*, 323.
(18) Kervinen, K.; Allmendinger, M.; Leskela, M.; Repo, T.; Rieger, B. *Phys. Chem. Chem. Phys.* **2003**, *5*, 4450.
(19) Kervinen, K.; Korpi, H.; Gerbrand Mesu, J.; Soulimani, F.; Repo, T.; Rieger, B.; Leskelä, M.; Weckhuysen, B. M. *Eur. J. Inorg. Chem.* **2005**, *2005*, 2591.
(20) Canevali, C.; Orlandi, M.; Pardi, L.; Rindone, B.; Scotti, R.; Sipila, J.; Morazzoni, F. *J. Chem. Soc., Dalton Trans.* **2002**, 3007.
(21) Zhao, Y.; Xu, Q.; Pan, T.; Zuo, Y.; Fu, Y.; Guo, Q.-X. *Appl. Catal., A* **2013**, *467*, 504.
(22) Cui, F.; Wijesekera, T.; Dolphin, D.; Farrell, R.; Skerker, P. *J. Biotechnol.* **1993**, *30*, 15.
(23) Stärk, K.; Taccardi, N.; Bösmann, A.; Wasserscheid, P. *ChemSusChem.* **2010**, *3*, 719.
(24) Binder, J. B.; Gray, M. J.; White, J. F.; Zhang, Z. C.; Holladay, J. E. *Biomass and Bioenergy* **2009**, *33*, 1122.
(25) Hanson, S. K.; Baker, R. T.; Gordon, J. C.; Scott, B. L.; Thorn, D. L. *Inorg. Chem* **2010**, *49*, 5611.
(26) Hanson, S. K.; Baker, R. T.; Gordon, J. C.; Scott, B. L.; Silks, L. A. P.; Thorn, D. L. *J. Am. Chem. Soc.* **2010**, *132*, 17804.

(27) Wigington, B. N.; Drummond, M. L.; Cundari, T. R.; Thorn, D. L.; Hanson, S. K.; Scott, S. L. *Chem. Eur. J.* **2012**, *18*, 14981
(28) Sedai, B.; Díaz-Urrutia, C.; Baker, R. T.; Wu, R.; Silks, L. A. P.; Hanson, S. K. *ACS Catal.* **2013**, *3*, 3111.
(29) Korpi, H.; Figiel, P. J.; Lankinen, E.; Ryan, P.; Leskelä, M.; Repo, T. *Eur. J. Inorg. Chem.* **2007**, *2007*, 2465.
(30) Hanson, S. K.; Wu, R.; Silks, L. A. P. *Angew. Chem. Int. Ed.* **2012**, *51*, 3410.
(31) Son, S.; Toste, F. D. *Angew. Chem. Int. Ed.* **2010**, *49*, 3791
(32) Sedai, B.; Baker, R. T. *Adv. Synth. Catal.* **2014, In press**.
(33) Rahimi, A.; Azarpira, A.; Kim, H.; Ralph, J.; Stahl, S. S. *J. Am. Chem. Soc.* **2013**, *135*, 6415.
(34) Hoover, J. M.; Ryland, B. L.; Stahl, S. S. *J. Am. Chem. Soc.* **2013**, *135*, 2357.
(35) Diaz-Urrutia, C.; Sedai, B.; Baker, R. T.; Hanson, S. K. *Curr. Org. Chem.* **In press**.
(36) Cho, D. W.; Parthasarathi, R.; Pimentel, A. S.; Maestas, G. D.; Park, H. J.; Yoon, U. C.; Dunaway-Mariano, D.; Gnanakaran, S.; Langan, P.; Mariano, P. S. *J. Org. Chem.* **2010**, *75*, 6549.
(37) Chan, J. M. W.; Bauer, S.; Sorek, H.; Sreekumar, S.; Wang, K.; Toste, F. D. *ACS Catal.* **2013**, *3*, 1369.
(38) Diaz-Urrutia, C. C., W.-C.; Crites, C.-O.; Baker, R. T. *Energy Environ. Sci* **2014, Submitted**.
(39) Sheldon, R. A. In *Organic Peroxygen Chemistry*; Hermann, W. A., Ed.; Springer: 1993, p 21.
(40) Arends, I. W. C. E.; Sheldon, R. A. In *Modern Oxidation Methods*; Wiley-VCH Verlag GmbH & Co. KGaA: 2004, p 83.
(41) Adam, W.; Malisch, W.; Roschmann, K. J.; Saha-Möller, C. R.; Schenk, W. A. *J. Organomet. Chem.* **2002**, *661*, 3.
(42) Deng, L.; Ziegler, T. *Organometallics* **1997**, *16*, 716.
(43) Hille, R.; Hall, J.; Basu, P. *Chem. Rev.* **2014**, *114*, 3963.
(44) Holm, R. H. *Coord. Chem. Rev.* **1990**, *100*, 183.
(45) Arzoumanian, H. *Coord. Chem. Rev.* **1998**, *178–180, Part 1*, 191.
(46) Abernethy, C. D.; Bottomley, F.; Chen, J.; Kemp, M. F.; Mallais, T. C.; Womiloju, O. O.; Thyagarajar, S.; Theopold, K. H. In *Inorg. Synth.*; John Wiley & Sons, Inc.: 1998, p 207.
(47) Bottomley, F.; Boyle, P. D.; Chen, J. *Organometallics* **1994**, *13*, 370.
(48) Bruce, M. I.; Humphrey, M. G.; Matisons, J. G.; Roy, S. K.; Swincer, A. G. *Aust. J. Chem.* **1984**, *37*, 1955.
(49) Biradar, A. V.; Dongare, M. K.; Umbarkar, S. B. *Tetrahedron Lett.* **2009**, *50*, 2885.
(50) Piper, T. S.; Wilkinson, G. *J. Inorg. Nucl. Chem.* **1956**, *3*, 104.
(51) Chiu, H.-T.; Chen, Y.-P.; Chuang, S.-H.; Jen, J.-S.; Lee, G.-H.; Peng, S.-M. *Chem. Commun.* **1996**, 139.
(52) Chen, H.; White, P. S.; Gagné, M. R. *Organometallics* **1998**, *17*, 5358.

(53) J. Coles, S.; B. Hursthouse, M.; G. Kelly, D.; J. Toner, A.; M. Walker, N. *J. Chem. Soc., Dalton Trans.* **1998**, 3489.
(54) Martinez, L. E.; Leighton, J. L.; Carsten, D. H.; Jacobsen, E. N. *J. Am. Chem. Soc.* **1995**, *117*, 5897.
(55) Clarke, E. F. M., E. M.; Gilheany, D. G. *ARKIVOC (Gainesville, FL, U. S.)* **2005**, *1*, 30.
(56) Gibson, V. C.; Kee, T. P.; Shaw, A. *Polyhedron* **1990**, *9*, 2293.
(57) Dilworth, J. R.; McAuliffe, C. A.; Sayle, B. J. *J. Chem. Soc., Dalton Trans.* **1977**, 849.
(58) Kandanarachchi, P. H.; Autrey, T.; Franz, J. A. *J. Org. Chem.* **2002**, *67*, 7937.
(59) Nichols, J. M.; Bishop, L. M.; Bergman, R. G.; Ellman, J. A. *J. Am. Chem. Soc.* **2010**, *132*, 12554.
(60) Kim Yong, S.; Chang, H.-m.; Kadla John, F. In *Holzforschung* 2008; Vol. 62, p 38.
(61) Voitl, T.; Rudolf von Rohr, P. *ChemSusChem* **2008**, *1*, 763.
(62) King, R. B.; Bisnette, M. B. *J. Organomet. Chem.* **1967**, *8*, 287.
(63) Maignien, S.; Aït-Mohand, S.; Muzart, J. *Synlett.* **1996**, *1996*, 439.
(64) Payne, G. B.; Deming, P. H.; Williams, P. H. *J. Org. Chem.* **1961**, *26*, 659.
(65) Trost, M. K.; Bergman, R. G. *Organometallics* **1991**, *10*, 1172.
(66) Chakraborty, D.; Bhattacharjee, M.; Krätzner, R.; Siefken, R.; Roesky, H. W.; Usón, I.; Schmidt, H.-G. *Organometallics* **1998**, *18*, 106.
(67) Al-Ajlouni, A. M.; Veljanovski, D.; Capapé, A.; Zhao, J.; Herdtweck, E.; Calhorda, M. J.; Kühn, F. E. *Organometallics* **2008**, *28*, 639.
(68) Wang, C.; Xi, Z. *Chem. Soc. Rev.* **2007**, *36*, 1395.
(69) Yiu, S.-M.; Man, W.-L.; Lau, T.-C. *J. Am. Chem. Soc.* **2008**, *130*, 10821.
(70) Lai, S.; Lee, D. G. *Tetrahedron.* **2002**, *58*, 9879.
(71) Cotton, F. A. W., G.; Murillo, C. A.; Bochmann, M. *Advanced Inorganic Chemistry*; Wiley: New York, 1999.
(72) Firouzabadi, H.; Mohammadpoor-Baltork, I. *Bull. Chem. Soc. Jpn.* **1995**, *68*, 2319.
(73) Wang, Z. In *Comprehensive Organic Name Reactions and Reagents*; John Wiley & Sons, Inc.: 2010.
(74) Procopio, A.; Dalpozzo, R.; De Nino, A.; Nardi, M.; Sindona, G.; Tagarelli, A. *Synlett.* **2004**, *2004*, 2633.
(75) Rodriguez, I.; Climent, M. J.; Iborra, S.; Fornés, V.; Corma, A. *J. Catal.* **2000**, *192*, 441.
(76) Adam, W.; Saha-Möller, C. R.; Ganeshpure, P. A. *Chem. Rev.* **2001**, *101*, 3499.
(77) Zhdankin, V. V.; Stang, P. J. *Chem. Rev.* **2008**, *108*, 5299.
(78) Dess, D. B.; Martin, J. C. *J. Am. Chem. Soc.* **1991**, *113*, 7277.
(79) Tohma, H.; Kita, Y. *Adv. Synth. Catal.* **2004**, *346*, 111.
(80) Zhdankin, V. V. *J. Org. Chem.* **2011**, *76*, 1185.
(81) Carmalt, C. J.; Crossley, J. G.; Knight, J. G.; Lightfoot, P.; Martin, A.; Muldowney, M. P.; Norman, N. C.; Orpen, A. G. *Chem. Comm.* **1994**, 2367.

(82) Ochiai, M. *Reactivities, Properties and Structures*; Springer: Berlin, 2003; Vol. 224.
(83) Vatele, J.-M. *Synlett* **2006**, *2006*, 2055.
(84) Yokoo, T.; Matsumoto, K.; Oshima, K.; Utimoto, K. *Chem. Lett.* **1993**, *22*, 571.
(85) Tohma, H.; Maegawa, T.; Takizawa, S.; Kita, Y. *Adv. Synth. Catal.* **2002**, *344*, 328.
(86) Moriarty, R. M.; Rani, N.; Condeiu, C.; Duncan, M. P.; Prakash, O. *Synth. Comm.* **1997**, *27*, 3273.
(87) Smegal, J. A.; Hill, C. L. *J. Am. Chem. Soc.* **1983**, *105*, 3515.
(88) Schulze, A.; Giannis, A. *Synthesis* **2006**, *2006*, 257.
(89) Uyanik, M.; Akakura, M.; Ishihara, K. *J. Am. Chem. Soc.* **2008**, *131*, 251.
(90) Thottumkara, A. P.; Bowsher, M. S.; Vinod, T. K. *Org. Lett.* **2005**, *7*, 2933.
(91) Page, P. C. B.; Appleby, L. F.; Buckley, B. R.; Allin, S. M.; McKenzie, M. J. *Synlett.* **2007**, *2007*, 1565.
(92) Do, H.-Q.; Daugulis, O. *Org. Lett.* **2008**, *11*, 421.
(93) Sharefkin, J. G.; Saltzman, H. *Org. Synth.* **1963**, *43*, 60.
(94) Zagulyaeva, A. A.; Yusubov, M. S.; Zhdankin, V. V. *J. Org. Chem.* **2010**, *75*, 2119.
(95) Helber, J.; Frohn, H.-J.; Klose, A.; Scholten, T. *ARKIVOC (Gainesville, FL, U. S.)* **2003**, 71.
(96) King, M. V. *The Journal of Organic Chemistry* **1961**, *26*, 3323.
(97) Adam, W.; Gelalcha, F. G.; Saha-Möller, C. R.; Stegmann, V. R. *J. Org. Chem.* **2000**, *65*, 1915.
(98) Sedai, B.; Díaz-Urrutia, C.; Baker, R. T.; Wu, R.; Silks, L. A. P.; Hanson, S. K. *ACS Catal.* **2011**, *1*, 794.
(99) Heikkinen, S.; Toikka, M. M.; Karhunen, P. T.; Kilpeläinen, I. A. *J. Am. Chem. Soc.* **2003**, *125*, 4362.
(100) Hanson, S. K.; Wu, R.; Silks, L. A. P. *Org. Lett.* **2011**, *13*, 1908.